



Doctoral Thesis

**Enhancing the AUV long-term
deployment: Non-holonomic AUV
autonomous docking using acoustics in a
funnel-shaped docking station**

JOAN ESTEBA MASJUAN

2023



Doctoral Thesis

**Enhancing the AUV long-term
deployment: Non-holonomic AUV
autonomous docking using acoustics in a
funnel-shaped docking station**

JOAN ESTEBA MASJUAN

2023

Doctoral Program in Technology

Supervised by:

PERE RIDAO RODRÍGUEZ
NARCÍS PALOMERAS ROVIRA

Thesis submitted to the University of Girona
in fulfillment of the requirements for the degree of

DOCTOR OF PHILOSOPHY

*Amb la voluntad adequada,
l'impossible deixa de ser-ho.*

AGRAÏMENTS

En aquest document pretenc exposar una part del que ha significat la meva estada en el Centre d'Investigació en Robòtica Submarina ([CIRS](#)). Han sigut uns anys d'aprenentatge i de descobriment d'un món molt distanci al que la meva trajectòria professional m'havia portat. Molt em temo, que no seré capaç de que la tesi reflecteixi més d'un petit percentatge de la col·laboració que hem tingut durant els darrers anys, potser molt centrada en les publicacions i obviant el que hem continuat construint junts.

Des del primer moment se m'ha permés formar part d'un equip que arrossega una trajectòria de més de vint anys acumulant coneixements i experiència. Sentint-me un privilegiat per poder seguir aportant en el que tants abans que jo van construir. No és menor el fet de disposar de les facilitats que he tingut el plaer de tenir durant la meva estada: dos plataformes robotitzades en desenvolupament, unes instal·lacions privilegiades amb piscina per fer proves, una embarcació per poder portar les proves un pas més endavant i una xarxa de contactes que permeten fer possible les idees. Tot això acompanyat d'un finançament que ha permés l'èxit d'aquest projecte. Estic segur que no seré capaç de ser just en la redacció d'aquests agraïments, degut al llistat de personal que ha fet possible arribar a obtenir el llistat anteriorment i que no he tingut el plaer de conèixer.

Aquesta tesi és el fruit d'un treball d'equip, on per circumstàncies sóc jo el protagonista, però en cap cas ha sigut una tasca individual. En primera instància és imperatiu destacar la figura d'en Pere, un somiador que guia el futur de l'equip. Ell va ser qui va originar la idea que durant tant de temps hem anat desenvolupant, anticipant necessitats i mostrant una fe quasi cega davant l'escepticisme general; fet que sospito, explica l'èxit del nostre centre. La seva passió per la feina i la voluntat d'entendre són simplement exemplars, sens cap dubte han sigut una font d'inspiració durant aquests anys. En Narcís, fidel seguidor d'en Pere, ha sigut una altre figura destacada en aquest procés. Combinant la càrrega docent del centre amb la recerca, a tot past ha tingut la porta oberta per mi, fet que sempre agrairé. Per sistema ha trobat una estona per dedicar-me i poder comentar les idees i detalls no només de la tesi, sino del dia a dia del centre. Tal i com les publicacions mostren, el meu fidel acompanyant en aquest viatge ha sigut en Patryk, el qual mereix sense cap dubte el títol de co-tutor honorífic de la tesi. Junts ens hem complementat d'una forma inèdita per tal de fer realitat totes les idees que hem tingut al llarg d'aquests anys. Més que un company, un amic, hem passat moltes hores junts aprenent l'un de l'altre, on sempre hem fet broma que ha sigut el meu "sparring" per adquirir un bon nivell d'anglès i que gràcies en part a mi, espero que acabi seguint capaç de parlar en català.

Enllaçat amb en Patryk, m'agradaria distingir l'equip que estem a l'oficina en el moment de redacció d'aquest document. Em considero un privilegiat d'haver pogut formar part i participar activament en la creació i consolidació de l'equip, que tants èxits ha aconseguit

en aquests anys. Hem creat una relació de confiança que ens ha permés especialitzar-nos, desencadenant que tots junts poguessim arribar més lluny. Per ordre d'antiguitat, en Roger el nostre especialista en "software". Sempre ha mostrat una actitud impecable envers els companys, ajudant i guiant quan ha sigut necessari i solucionant tots els problemes que se li han presentat, fet que no és menor.

En Miguel, amb una actitud més pausada i metòdica, ha tingut un projecte clar des d'un inici i l'ha anat seguint sens falta fins a acabar-lo. Amb una ambició de futur distant a la meva, ha sigut un plaer poder contrastar opinions i projectes.

L'Eduardo, el meu fidel amic, ha demostrat sempre un compromís i una dedicació admirables. Acompanyant i ajudant desinteressadament sempre que ha pogut, ha transmés aquesta manera de fer en l'ensenyament, aconseguint uns destacables resultats amb els estudiants.

En Hayat, marcant el camí de la dedicació, no només és una company amb un talent tècnic destacable sinó també un constructor de projectes. Entén com ningú la importància de les relacions humanes en la feina, aconseguint uns resultats provablement no vistos abans en el nostre centre.

I finalment en Pau, qui tot i tenir una capacitat d'aprenentatge tècnic inquietable, el més destacable és la seva visió. Una persona capaç d'entendre el present i el futur, desengranjar els problemes i solucionar-los, és la personificació d'un enginyer. Ha sigut sens dubte un plaer haver pogut compartir aquests mesos amb algú que realment entén.

M'agradaria fer especialment èmfasis en la figura d'en Lluís, des del meu punt de vista el pilar fonamental del centre. Amb un professionalisme exquisit, és la persona encarregada que tot el que fem el dia a dia es faci realitat. Des de disseny i fabricació electrònica, passant per la mecànica i fins i tot essent el capità de l'embarcació. Possiblement la persona amb més experiència en missions del centre.

També m'agradaria destacar la guia i ensenyances que m'han transmés els anteriors integrants de l'equip, destacant la figura d'en Guillem, qui em va introduir a l'entorn de l'Sparus II. Com també tot l'equip d'IQUA Robotics, els quals ha sigut un plaer compartir les instal·lacions del centre i sempre han tingut la porta oberta per respondre dubtes i debatre les solucions tècniques. En la mateixa línia, agrair també les diferents companyies que han treballat amb nosaltres aquests anys i han fet possible la materialització dels nostres projectes, per la seva flexibilitat i confiança.

Finalitzant, destacar la resta de companys en el camí, principalment en Ricard qui ha demostrat una actitud impecable i al qui espero tindrà un bon futur. Els companys del centre: en Rafael, en Nuno, en Marc, en Valerio, la Virginia, la Marta, en Ferran, en Jordi, en Roger Feliu, la Khadidja, la Sana, en Freixonet, en Cufí, l'Albert, en Forest. Els companys d'administració: la Noèlia, la Mònica, la Mireia, l'Eva, l'Olga, la Sussana, l'Anna, l'Imma, en David. Els estudiants del màster que han col·laborat amb nosaltres: l'Alaaeddine, l'Amina, l'Ahmad, l'Enrique, en Bruk, en Vsevolod, en Muhammad, en Jad, l'Ulugbek, en Miguel Malagón, l'Oscar.

Ja per acabar, agrair també a la gent del meu entorn no professional. En Ferran i l'Eduard, els meus companys inseparables durant aquests últims anys, acompanyats d'en Robert i en Salvi. Els amics del grau: en David, l'Alberto, l'Aida, l'Haytam, en Francesc, en Bardalet, en Xavi, en Quim, l'Ariadna, en Ricard, l'Ernest. Els companys i amics de l'equip de rugbi, de l'airsoft i del club de tir. I finalment la meva família qui sempre ha cregut i apostat per mi, permetent-me créixer al ritme que ho he fet.

ACKNOWLEDGMENTS

In this document, I intend to show a part of what my stay in the CIRS has meant. They have been years of learning and discovering a world far removed from the one my professional career has taken me to. I am afraid that I will not be able to make this thesis reflect more than a small percentage of the collaboration we have had over the last few years, perhaps focusing too much on publications and ignoring what we have continued to build together.

From the very first moment, I have been allowed to be part of a team that has been accumulating knowledge and experience for more than twenty years. I feel privileged to be able to continue contributing to what so many before me have built. It is no less important to have the facilities that I have had the pleasure of using during my stay: two robotic platforms under development, privileged facilities with a water tank for testing, a boat to be able to take the tests a step further, and a network of contacts that make the ideas possible. All this is accompanied by funding that has allowed the success of this project. I am sure that I will not be able to be fair in writing these acknowledgments, due to the list of staff who have made it possible to obtain the above list and who I have not had the pleasure of meeting.

This thesis is the result of a team effort, in which I am the protagonist, but it has never been an individual task. First of all, it is imperative to highlight the figure of Pere, a dreamer who guides the team's future. It was he who originated the idea that we have been developing for so long, anticipating needs and showing almost blind faith at the general skepticism; a fact that I suspect, explains the success of our center. His passion for his work and his willingness to understand are simply exemplary and have undoubtedly been a source of inspiration over the years. Narcís, a faithful follower of Pere, has been another outstanding figure in this process. Combining teaching at the university with research, he has always had an open door for me, a fact that I will always be grateful for. He has always found time to spend with me and to be able to comment on the ideas and details not only of the thesis but also of the day-to-day life of the center. As the publications show, my faithful companion on this journey has been Patryk, who undoubtedly deserves the title of honorary co-author of the thesis. Together we have complemented each other in an unprecedented way in order to make all the ideas we have had over the years a reality. More than a colleague, a friend, we have spent many hours together learning from each other, where we have always made jokes that have been my "sparring" to acquire a good level of English and that thanks in part to me, I hope he will end up being able to speak Catalan.

In connection with Patryk, I would like to distinguish the team that we are in the office at the time of writing this document. I consider myself privileged to have been able to take part and actively participate in the creation and consolidation of the team, which has been so successful in recent years. We have created a relationship of trust that has allowed us to specialize, a fact that has allowed us to go further together. In order of seniority, Roger is

our software specialist. He has always shown an impeccable attitude towards his colleagues, helping and guiding when necessary and solving all the problems that have arisen, a fact that is not minor.

Miguel, with a slower and more methodical attitude, has had a clear project from the start and has followed it through to its completion. With an ambition for the future far removed from my own, it has been a pleasure to be able to compare opinions and projects.

Eduardo, my faithful friend, has always shown admirable commitment and dedication. Accompanying and helping disinterestedly whenever he could, he has transmitted this way of doing things in teaching, achieving outstanding results with the students.

Hayat, marking the path of dedication, is not only a colleague with outstanding technical talent but also a builder of projects. He understands like no other the importance of human relationships in the workplace, achieving results that have probably never been seen before in our center.

And finally, Pau, who despite having an unquestionable technical learning ability, the most remarkable thing is his vision. A person capable of understanding the present and the future, and also capable of unraveling problems and solving them, he is the epitome of an engineer. It has undoubtedly been a pleasure to have been able to share these months with someone who really understands.

I want to place special emphasis on the figure of Lluís, from my point of view the fundamental pillar of the center. With exquisite professionalism, he is the person in charge of making everything we do on a daily basis a reality. From electronic design and manufacturing to the mechanics and even being the captain of the boat. Possibly the person with the most experience in the field of our center.

I would also like to highlight the guidance and teachings that the previous members of the team have given me, especially Guillem, who introduced me to the environment of Sparus II. As well as the whole IQUA Robotics team, who have been a pleasure to share the center's facilities and have always had an open door to answer questions and discuss technical solutions. In the same vein, I would also like to thank the different companies that have worked with us over the years and have made it possible for our projects to materialize, thanks to their flexibility and trust.

Finishing, I would like to highlight the other companions along the way, especially Ricard, who has shown an impeccable attitude and who I hope will have a good future. The companions of the center: Rafael, Nuno, Marc, Valerio, Virginia, Marta, Ferran, Jordi, Roger Feliu, Khadidja, Sana, Freixenet, Cufí, Albert, Forest. The administrative colleagues: Noèlia, Mònica, Mireia, Eva, Olga, Sussana, Anna, Imma, David. The Master's students who have collaborated with us: Alaaeddine, Amina, Ahmad, Enrique, Bruk, Vsevolod, Muhammad, Jad, Ulugbek, Miguel Malagón, Oscar.

Finally, I would also like to thank the people in my non-professional environment. Ferran and Eduard, my inseparable companions during these last years, together with Robert and Salvi. My friends from the bachelor's degree: David, Alberto, Aida, Haytam, Francesc, Bardalet, Xavi, Quim, Ariadna, Ricard, Ernest. My mates and friends from the rugby team, the airsoft team, and the shooting club. And finally, my family, who have always believed in me and supported me, allowed me to grow as fast as I had.

LIST OF PUBLICATIONS

Publications in the compendium

The presented thesis is a compendium of the following research articles:

- **Joan Esteba**, Patryk Cieslak, Narcis Palomeras, and Pere Ridao. “Docking of Non-holonomic AUVs in Presence of Ocean Currents: a Comparative Survey”. In: *IEEE Access* 9 (2021), pages 86607–86631. doi: [10.1109/ACCESS.2021.3083883](https://doi.org/10.1109/ACCESS.2021.3083883)

Quality index: JCR2021 Engineering, Electrical & Electronic, Impact Factor: 3.476, Q2 (105/276).

Contributions: This publication reviews the state-of-the-art approaches present in the literature for docking a non-holonomic Autonomous Underwater Vehicle (**AUV**) in a funnel-shaped Docking Station (**DS**) in the presence of ocean currents, comparing them in a common framework. The goal of this publication is to analyze the solutions presented in the literature and create a novel framework to compare them and understand their strengths and weaknesses, with the final objective to select the appropriate one or to conclude the need to design a novel one.

Author contributions: The author of this thesis was responsible for surveying the different algorithms, creating a metric to evaluate them, creating a simulation framework to compare them in the same conditions, applying each algorithm in the framework, simulating them to generate the data, analyzing the data, and writing the article.

- **Joan Esteba**, Patryk Cieslak, Narcís Palomeras, and Pere Ridao. “Managed Surge Controller : A Docking Algorithm for a Non-Holonomic AUV (Sparus II) in the Presence of Ocean Currents for a Funnel-Shaped Docking Station”. In: *Sensors* 23 (2023). doi: [10.3390/s23010241](https://doi.org/10.3390/s23010241)

Quality index: JCR2021 Engineering, Electrical & Electronic, Impact Factor: 3.847, Q2 (92/276).

Contributions: This article presented a novel controller for a non-holonomic **AUV** with two horizontal thrusters, focused on the docking maneuver in a funnel-shaped **DS** with ocean currents. Demonstrating it theoretically and simulating it in the same framework where the rest of the algorithms were compared in the previous publication.

Author contributions: The author of this thesis developed the concept of the novel controller, developing the mathematical demonstration, testing it in kinematics and dynamics, simulating and comparing it with the rest, analysing the results, and writing the article.

- **Joan Esteba**, Patryk Cieslak, Narcís Palomeras, and Pere Ridao. “Sparus Docking Station: A Current Aware Docking Station For a Non-holonomic AUV”. in: *Journal of Field Robotics* ()

Quality index: JCR2021 Robotics, Impact Factor: 6.385, Q2 (8/30).

Contributions: This work presents an experimental autonomous docking application for a non-holonomic **AUV** in a funnel-shaped **DS**. Developing, building, and coding a new prototype of **DS**. Integrating an acoustic sensor for the localization of the **AUV**. Applying the controller developed in the previous publication. And testing the application in two different scenarios in the sea.

Author contributions: The author of this thesis is the main developer of the full application.

With respect to the **DS**, the author had a protagonist role in all the processes. Starting from conceptual design in collaboration with the team, the mechanical design, the manufacturing process in collaboration with several suppliers, the assembly, and the mechanical tests. In collaboration with the team, the author participated in electronic design, and software development.

With respect to the acoustic sensor integration, the author had also notable participation. In collaboration with the team, the driver of the sensor was developed. Leading, preparing, buying, and building all the material needed, and developing the main task of the experiments: the first working tests were performed in the water tank, transitioning to the sea in several steps. To finally integrate it into the navigation of the **AUV**, developing a series of methodic sea tests to ensure the robustness of the system.

Regarding the controller application, the author integrated it into the **AUV**, and tested it in the field, leading the experiments and preparing all the necessities.

Finally, the author had the leading role in the experiments developed for testing the final application, hiring all the needed companies, managing the team, preparing all the material, and managing the **AUV**. Also, the author is the main writer of the article.

ACRONYMS

AUV	Autonomous Underwater Vehicle
CAD	Computer-Aided Design
CNC	Computerized Numerical Control
DoF	Degree of Freedom
DS	Docking Station
DVL	Doppler Velocity Log
GPS	Global Positioning System
HROV	Hybrid Remotely Operated Vehicle
I-AUV	Intervention AUV
IMR	Inspection Maintenance and Repair
LTD	Long Term Deployment
ROS	Robot Operation System
ROV	Remotely Operated Vehicle
TRL	Technology Readiness Level
USBL	Ultra-Short BaseLine

Institutions

CIRS	Centre d'Investigació en Robòtica Submarina
UdG	Universitat de Girona
ViCOROB	Institut de Recerca en Visió per Computador i Robòtica

CONTENTS

Abstract	1
Resum	3
Resumen	5
1 Introduction	7
1.1 Motivation	8
1.2 Objectives	10
1.3 Context	11
1.4 Document structure	13
2 Survey, study, and comparison of the docking algorithms	15
3 Development of the docking strategy	41
4 Experimental implementation	69
5 Results and discussion	95
5.1 Summary of the completed work	96
5.2 Ocean current observer	97
5.2.1 Context and motivation	97
5.2.2 Oportunity	98
5.2.3 Concept	98
6 Conclusions and Future Work	103
6.1 Contributions of this thesis	104
6.2 Future work	104
Appendix A Sparus Docking Station	107
A.1 Context	108
A.2 Concept	108
A.2.1 Tripod	108
A.2.2 Funnel	109
A.3 Experimental expirience	112

Appendix B Girona Docking Station	115
B.1 Context	116
B.2 Concept	116
B.2.1 Girona AUV coupling accessory	116
B.2.2 Body structure	117
B.2.3 Interface structure	117
B.3 Future work	118

LIST OF FIGURES

1.1	AUV application examples developed by the Universitat de Girona (UdG) team.	8
1.2	Conceptual Docking Stations for the Universitat de Girona (UdG)'s AUVs.	9
1.3	Photography of the Sparus II AUV from the top.	10
1.4	AUVs developed by Institut de Recerca en Visió per Computador i Robòtica (ViCOROB).	12
1.5	Infrastructure for experiments.	12
5.1	Example of the result of a survey developed with the Sparus II AUV, using a forward-looking sonar [18], processed with SounTiles [19] with the collaboration of IQUA Robotics. The survey was performed in Viana do Castelo (Portugal), in the context of the ATLANTIS research project [14].	98
5.2	Representation of the horizontal (left) and the vertical (right) ocean current observation, when the steady state is achieved.	99
5.3	Conceptual path representation for the development of a survey with a forward-looking sonar.	100
A.1	Sparus Docking Station conceptual general view.	107
A.2	Representation of the main elements of the tripod of the Sparus Docking Station.	110
A.3	Sparus Docking Station funnel representation. 1) Acoustic modem from BluePrint Subsea, 2) camera, 3) WiFi antenna, 4) latching motor, 5) inductive charger from INESC TEC, 6) visual modem from Hydromea, 7) Doppler Velocity Log (DVL) from LinkQuest.	111
A.4	Sparus Docking Station frontal and back view representation.	111
A.5	Representation of the modular center of mass adjustment of the funnel of the DS. In green is represented the main axis of the DS, and zoomed in blue is presented the modular weight system.	112
A.6	Photographies of the Sparus Docking Station in different scenarios.	113
A.7	Photographies of the Sparus Docking Station deployment in Viana do Castelo.	113
B.1	Girona Docking Station conceptual general view.	115
B.2	Conceptual representation of two of the Universitat de Girona (UdG) research projects that involves the Girona Docking Station.	116
B.3	Conceptual representation of the Girona AUV adaptation for docking, with the coupling accessory assembled.	117
B.4	Main structure of the Girona Docking Station representation.	118

B.5	Conceptual representation of the contact part of the DS with the AUV. On the left is an image from a top view, and on the right is an image from a lateral view. In green is represented the funnel and in blue is the axis alienation.	118
B.6	Photography of the Girona Docking Station.	119

ABSTRACT

UNDERWATER robotics has undergone significant development in recent years. It has been applied to a wide range of sectors, such as the mapping of areas of interest, the collection of scientific data, or the Inspection Maintenance and Repair (IMR) tasks for the energy sector (oil and gas, renewable energies, etc.). Nowadays, Remotely Operated Vehicles play a leading role in these fields and are gradually being replaced by Autonomous Underwater Vehicles (AUVs).

In the coming years, the market will need AUVs deployed for long term in strategic locations, such as offshore wind farms. To achieve this goal, a key factor is the development of Docking Station (DS) where robots can be stationed, charge their batteries, and have a stable channel for fast communication. With this in mind, this thesis focuses on the development of new technologies for the Long Term Deployment (LTD) of non-holonomic AUVs at sites of interest.

The work began with a review of the state of the art. Next, a new metric for scoring docking success was proposed and used for the comparison of different strategies. Then, a new docking algorithm that takes into account the ocean current was proposed, simulated, and compared to methods in the literature; with promising results. At this point, a new funnel-based DS, which can be self-aligned with the ocean current to simplify the docking process, was designed and implemented. Finally, the proposed DS and docking algorithm were validated at sea using Sparus II AUV equipped with an inverse Ultra-Short BaseLine (USBL) system for the DS localization. The results demonstrate the validity of the proposal and pave the way for applications requiring the LTD of AUVs.

RESUM

A robòtica submarina ha experimentat un desenvolupament notable al llarg dels últims anys. Essent aplicada a una àmplia gamma de sectors com pot ser el mapeig de zones d'interès, l'obtenció de dades per altres científics o el sector energètic; des del petroli fins a les energies renovables. A dia d'avui els robots teleoperats (**ROV**) són protagonistes en aquests camps i progressivament s'està evolucionant cap als robots autònoms (**AUV**). Aquests darrers, estan començant a ser utilitzats per certes aplicacions i es preveu que en un futur podran substituir en gran mesura els primers.

Per tal de poder consolidar la tecnologia dels **AUVs**, els robots no només han de ser capaços de desenvolupar una aplicació concreta, sinó que també és imperatiu desenvolupar la tecnologia relacionada a la seva logística. La nostra visió indica que en els propers anys, el mercat necessitarà flotes permanent de robots autònoms situats en ubicacions estratègiques, com podria ser una estació eòlica marina. Per tal d'aconseguir aquest fi, un factor clau és el desenvolupament de plataformes logístiques (**DS**) on els robots puguin ser guardats, protegits, carregats de bateria i disposin d'un canal estable de comunicació ràpida. Detectada tal necessitat, aquesta tesi s'ha centrat en el desenvolupament d'una aplicació pràctica d'estació subaquàtica per un dels robots del nostre centre: l'Sparus II.

El treball es va iniciar amb un estudi de l'estat de l'art. A continuació, es va proposar una nova mètrica per puntuar l'èxit d'acoblament i es va utilitzar per comparar diferents estratègies publicades a la literatura. Seguidament, es va proposar un nou algoritme d'acoblament que considera les corrents marines, simulant-lo i comparant-lo amb les estratègies anteriorment mencionades, obtinguen resultats prometedors. Arribats a aquest punt, es va dissenyar i implementar un nova **DS** basada en la tipologia d'embut, que es pot autoalinear amb la corrent marina per poder simplificar el procès d'acoblament. Finalment, la **DS** y l'algoritme d'acoblament es van validar experimentalment en el mar, utilitzant el Sparus II **AUV** equipat amb un sistema invers de **USBL** per a la localització de la **DS**. Els resultats demostren la validesa de la proposta i aplanen el camí per a aplicacions que requereixin el desplegament a llarg plaç de **AUVs**.

RESUMEN

La robótica submarina ha experimentado un notable desarrollo en los últimos años. Se ha aplicado a sectores muy diversos, como la cartografía de zonas de interés, la obtención de datos para otros científicos o el sector energético; desde el petróleo hasta las energías renovables. Hoy en día, los robots teleoperados (**ROV**) desempeñan un papel protagonista en estos campos y están evolucionando progresivamente hacia los robots autónomos (**AUV**). Estos últimos se están empezando a utilizar para determinadas aplicaciones y se prevé que en el futuro puedan sustituir a los primeros en la mayoría de las aplicaciones.

Para poder consolidar la tecnología robótica, los robots no sólo deben ser capaces de desarrollar una aplicación específica, sino que también es imprescindible desarrollar la tecnología relacionada con su logística. Nuestra visión indica que, en los próximos años, el mercado necesitará flotas permanentes de robots autónomos en lugares estratégicos, como un parque eólico marino. Para lograr este objetivo, un factor clave es el desarrollo de plataformas logísticas (**DS**) donde los robots puedan almacenarse, protegerse, cargar sus baterías y disponer de un canal estable para una comunicación rápida. Detectada esta necesidad, esta tesis se ha centrado en el desarrollo de una aplicación práctica de una estación submarina para uno de los robots de nuestro centro de investigación: el Sparus II.

El trabajo comenzó con una revisión del estado del arte. A continuación, se propuso una nueva métrica para puntuar el éxito del acoplamiento y se utilizó para comparar diferentes estrategias. Posteriormente, se propuso un nuevo algoritmo de acoplamiento que tiene en cuenta las corrientes marinas, se simuló y se comparó con métodos de la literatura, con resultados prometedores. En este punto, se diseñó e implementó una nueva **DS** basada en la tipología de embudo, que puede autoalinearse con la corriente marina para simplificar el proceso de atraque. Finalmente, la **DS** y el algoritmo de acoplamiento fueron validados en el mar utilizando el Sparus II **AUV** equipado con un sistema inverso de **USBL** para la localización de la **DS**. Los resultados demuestran la validez de la propuesta y allanan el camino para aplicaciones que requieran el despliegue a largo plazo de **AUVs**.

1

INTRODUCTION

THIS chapter summarizes the motivation behind the development of this PhD thesis. First, Section 1.1 presents a brief overview of the challenges and the need for autonomous docking systems. Next, Section 1.2 states the objectives of the thesis and Section 1.3 describes the context in which this work has been developed. Finally, Section 1.4 concludes with a summary of the organization of this document.

1.1 Motivation

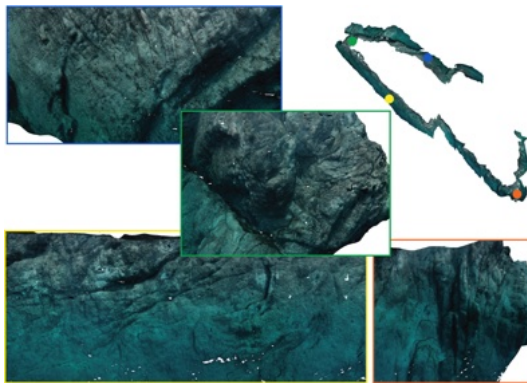
Underwater robotics is an interesting field and is developing rapidly for several reasons. First of all, the ocean represents an important part of our planet; the number of resources and opportunities has virtually no limits. Also, usually when humans use to automatize one process used to be for its efficiency. In an underwater context is not only that; but the environment is unsafe or even impossible to operate with humans, so the use of a robot is mandatory. Finally, during the last few years, offshore infrastructures have grown significantly, mostly due to the oil industry, and in the present and future probably due to wind farms.

All these arguments justify the strong development of underwater robotic technology during the last thirty years, which started with Remotely Operated Vehicles (**ROVs**) applications [4, 5] and are now passing the baton to autonomous robots.

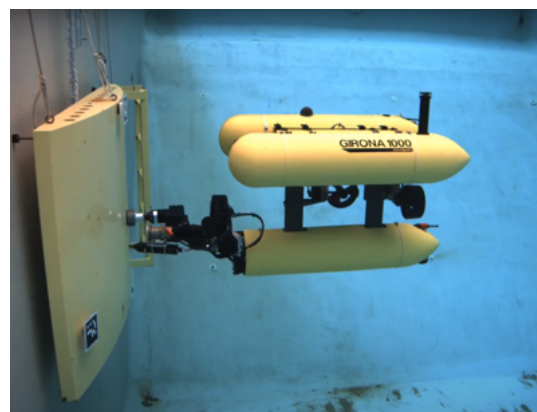
Today, the Autonomous Underwater Vehicles (**AUVs**) are beginning to be capable of performing an extensive number of tasks, which can be useful in a variety of scenarios. Examples are underwater autonomous mapping (see Fig. 1.1a) [6] and autonomous manipulation (see Fig. 1.1b), being able to perform tasks that are currently performed by divers or **ROVs** [7]. From the author's point of view, it is clear that in the future the need of having permanent autonomous robotic fleets in strategic locations will be imperative.

Long term deployment Parallel to the development of the robot application itself that performs a specific task, the development of technologies related to robotic logistics is mandatory. From this need arises the Long Term Deployment (**LTD**) research line, which aims to focus on the development of complementary technologies that allow a robot not only to develop a specific task but also to be permanently deployed for a long period of time and to perform tasks whenever required. This line of research intends to develop in the coming years studies of materials, devices, infrastructures, and strategies with the aim of improving the deployment time of vehicles. The ultimate goal is to achieve permanently deployed robotic fleets.

Currently, **LTD** is becoming an interesting research topic, supported by several research projects such as ATLANTIS [8], OPTHIROV [9], and PLOME [10] which are currently being developed by the Universitat de Girona (**UdG**) team, in collaboration with several partners. In addition, major research institutions have made advances in the **LTD**, such as the [11], and the [12].



(a) Underwater map reconstruction after an autonomous mission of mapping.



(b) Autonomous underwater manipulation.

Figure 1.1: **AUV** application examples developed by the Universitat de Girona (**UdG**) team.

Docking Station The first key development needed for the LTD is the Docking Station (**DS**) system, see Fig. 1.2. At present, the **AUV** usually operates with a support vessel. It is usually deployed from the ship, followed by the ship during the mission, and recovered by the ship's crew; being able to develop missions of only one day (or less) duration. There are several reasons why the ship is needed right now to support the **AUVs** in the sea:

1. **Protection:** The first reason is to protect the **AUV** from the uncertainties that can happen during a mission, allowing the technical crew to react if something unexpected happens.
2. **Batteries:** The second reason is the limitation of the batteries, which allows the **AUV** to operate for a certain amount of time.
3. **Communication:** The third reason is the limited communication bandwidth, which does not allow the **AUV** to transmit the obtained data to the onshore center.
4. **Navigation:** Also in some cases, the ship is used to enhance the navigation of the **AUV** (combining Global Positioning System (**GPS**) with Ultra-Short BaseLine (**USBL**)).

The **DS** system pretends to solve these problems. Being able to be deployed in a certain place for a large period of time: right now the objective is set to one week, but in the future, it will be enhanced. First, preparing an infrastructure where the **AUV** can protect itself if the environment is not friendly. Second, providing a place where the **AUV** can recharge its batteries. Third, offering a high bandwidth communication between the **AUV** and the **DS**. And fourth, offering a constant marker that can update the position of the **AUV** if it is navigating close to the **DS**. Depending on the application, the **DS** can have its own batteries or can be connected directly to a shore-based facility for power and data transmission. Other systems, such as floating buoys with a satellite connection, can also be used to transmit data from the **AUV** to a shore-based facility.



(a) Sparus II conceptual Docking Station.

(b) Girona 1000 conceptual Docking Station.

Figure 1.2: Conceptual Docking Stations for the UdG's AUVs.



Figure 1.3: Photography of the Sparus II AUV from the top.

With this technology, a new framework of opportunities appears. From having a permanent fleet of AUV operating in a closed environment such as a wind farm. Passing to a system of DS located on a route of interest that allows the AUV to traverse it (for example for patrolling). Or having a system that can be deployed in a region of interest, exploring it for a period of a few weeks, and be recovered after reaching objectives. Or even having a maintenance system that can be deployed in a given area, develop the required tasks, and be recovered to be deployed again in another location.

Non-holonomic vehicle This thesis focuses in a particular case of DS, the ones designed for non-holonomic AUV. By definition, a non-holonomic vehicle has a constraint on the motion, not being able to reach a position in the space if a certain trajectory is not followed. A clear example of that is the Sparus II AUV (see Fig. 1.3) which has three propellers, requiring control of the vehicle's heading to control its position. The docking maneuver that has to be designed is more challenging in this type of vehicle, compared to the standard holonomic ones, and becomes more interesting if we consider the ocean currents effect.

At the time this thesis was initiated, the UdG team had already developed one proposal of DS system for the Sparus II AUV [13]. But it presented three major problems:

1. **Mechanics:** The design and manufacturing process of the DS was not appropriate for real sea scenarios. It was the first conceptual prototype.
2. **Localization:** The final localization of the DS with respect to the AUV was based on a camera system. This proved to be insufficiently robust in some scenarios.
3. **Ocean currents:** The controller developed to perform the docking maneuver was not able to cope with ocean currents. Causing system failure if the scenario was not ideal.

1.2 Objectives

With the motivations of this thesis described, we can now state that the main goal is:

To develop a robust docking station system for a non-holonomic AUV, establishing the bases for the Long Term Deployment (LTD) research line.

This general aim can be divided into the following objectives:

1. **Docking station solution:** Designing and developing a DS solution tailored to the requirements of the ATLANTIS research project [14].
 - 1.1. **State of the art:** Reviewing the existing literature on experimental DS systems already developed.
 - 1.2. **Detecting the needs:** Studying the ATLANTIS research project demands, and evaluating the requirements that the DS system has to fulfill.
 - 1.3. **Model:** Developing a Computer-Aided Design (CAD) model that can be tested and validated in simulation (using Stonefish [15]) that fulfills the demands of the project.
 - 1.4. **Prototype:** Building the DS to test the new proposal in real scenarios. Studying and applying the best materials to obtain the desired results at an acceptable price. Understanding and applying the most suitable manufacturing process available with the suppliers. Also, designing and building the electrical system to optimize battery consumption.
2. **Non-holonomic docking maneuvers:** Developing and applying the best maneuver in order to dock with a non-holonomic vehicle in presence of ocean currents.
 - 2.1. **State of the art:** Reviewing the existing literature on docking maneuvers for non-holonomic robots in a funnel-shaped DS.
 - 2.2. **Modeling:** Developing a new strategy for maneuvering the AUV, optimized for the Sparus II AUV, with a novel controller. Demonstrate its exponential stability from a mathematical point of view as well as in simulation.
 - 2.3. **Experimenting:** Applying the proposed controller to real experiments.
3. **AUV/DS relative localization system:** Studying and developing a system to localize the DS relative to the AUV.
 - 3.1. **Studing the market:** Selecting and acquiring an acoustic system for localization that fits the application requirements.
 - 3.2. **Studing the device:** Developing a study of the selected device, to assess its suitability for the system and to obtain a model of it.
 - 3.3. **Integrating the device:** Integrating the relative localization system to the already existing AUV navigation architecture.
4. **Testing the final system:** Test the complete solution integrated with the docking maneuver.

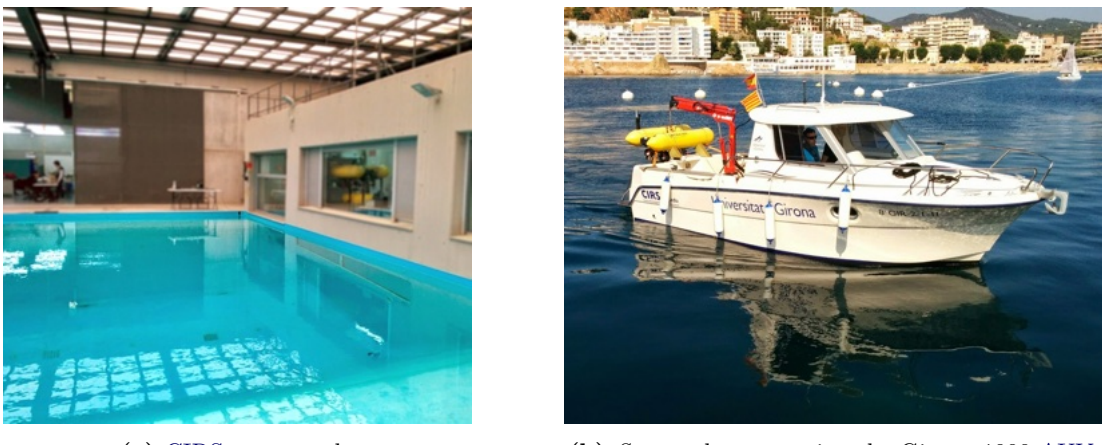
1.3 Context

The work presented in this thesis has been developed at Centre d'Investigació en Robòtica Submarina (**CIRS**), which is part of the Institut de Recerca en Visió per Computador i Robòtica (**ViCOROB**) institute of the **UdG**. Formed in 1992, this research group has become a leading team in the underwater robotics and computer vision community. One of the key elements that have allowed **ViCOROB** to have such a performance is the in-house availability of extraordinary infrastructure. On the one hand, there are two **AUVs** available as research platforms: the Sparus II [16] and the Girona 500 (and the new Girona 1000) [17]



(a) Sparus II in open sea.

(b) Girona 500 in the water tank at CIRS.

Figure 1.4: AUVs developed by ViCOROB.

(a) CIRS water tank.

(b) *Sextant* boat carrying the Girona 1000 AUV.**Figure 1.5:** Infrastructure for experiments.

(see Fig. 1.4). Sparus II can efficiently cover long distances, which makes it ideal for missions such as photogrammetric sea-bottom surveying (recall Fig. 1.1a), whereas Girona 500 can carry a heavier payload, so it is typically used for manipulation tasks (recall Fig. 1.1b). On the other hand, the laboratory counts with a freshwater tank of dimensions $16\text{m} \times 8\text{m} \times 5\text{m}$ (length \times width \times depth) and a crane-equipped boat named *Sextant* at Sant Feliu de Guíxols harbor (see Fig. 1.5).

The already developed AUVs along with the infrastructure allows for a relatively easy experimental data collection. Also, it is important to remark on the contact network built in the last years, which made it possible to contact with the different institutions that collaborated with the research projects.

In the context of this thesis, the AUV employed was Sparus II. The first tests were developed on the CIRS water tank, afterward, the test was done in Sant Feliu de Guíxols harbor (using *Sextant* as a support vessel), and finally in Viana do Castelo harbor.

This thesis was mostly financed by the doctoral grant of the UdG IFUDG2020. The experiments, equipment, and infrastructure resources used in this thesis have been mainly funded by Project ATLANTIS (ref. H2020-ICT-2019-2-871571), funded by the European Commission.

1.4 Document structure

This document is structured into the following chapters:

- **Chapter 2:** In this chapter, the work *Docking of Non-Holonomic AUVs in Presence of Ocean Currents: A Comparative Survey* is presented. First, a general introduction to the context and the challenges of the DS systems is made. Then, a state of the art of experimental docking station systems that are already in the literature is presented. Continuing, with the presentation of a novel frame to compare and evaluate docking methods. Finalizing with the summary, testing, and comparison of the strategies to dock with a non-holonomic vehicle to a funnel-shaped DS.
- **Chapter 3:** In this chapter, the author presents the work *Managed Surge Controller: A Docking Algorithm for a Non-Holonomic AUV (Sparus II) in the Presence of Ocean Currents for a Funnel-Shaped Docking Station*. After reaching, in the previous chapter, the conclusion that the already published maneuvers were not suitable for the demands of the Sparus II AUV; the authors decided to develop a new docking strategy. In this chapter, the new strategy is presented and demonstrated in a theoretical frame. This strategy includes a controller that utilizes the mechanical design and characteristics of the Sparus II AUV in order to optimize the docking maneuver. This controller is developed and theoretically demonstrated, and tested in simulation using kinematics and dynamics (via Stonefish [15]). Finally, the new strategy is compared with the ones analyzed in the previous chapter.
- **Chapter 4:** This chapter presents the work *Sparus Docking Station: A Current Aware Docking Station For a Non-holonomic AUV*. After developing the theoretical framework in the previous chapters, experimental results in the context of a real LTD scenario are presented. This chapter starts with the presentation of the state of the art of the funnel-shaped DS from the literature. Presents the LTD system proposed by the UdG for the Sparus II AUV. Including an upgrade of the Sparus II AUV for LTD, a novel funnel-shaped DS, the presentation of the docking strategy, and the navigation system. Showing the final results, achieving successful robust autonomous docking in two different sea locations.
- **Chapter 5:** This chapter summarizes and discusses the results obtained during this thesis, as well as other developments related to this thesis that has not been yet published.
- **Chapter 6:** Finally, the last chapter presents the conclusions and some proposals for future work.

2

SURVEY, STUDY, AND COMPARISON OF THE DOCKING ALGORITHMS

In this chapter the state-of-the-art approaches present in the literature for docking a non-holonomic AUV in a funnel-shaped DS in the presence of ocean currents is reviewed, comparing them in a common framework. The goal of this publication is to analyze the solutions presented in the literature and create a novel framework to compare them and understand their strengths and weaknesses, with the final objective to select the appropriate one or to conclude the need to design a novel one.

Title: Docking of Non-holonomic AUVs in Presence of Ocean Currents: a Comparative Survey

Authors: **Joan Esteba**, Patryk Cieslak, Narcis Palomeras, and Pere Ridao

Journal: IEEE Access

Volume: 9, Pages: 86607–86631, Published: 2021

DOI: [10.1109/ACCESS.2021.3083883](https://doi.org/10.1109/ACCESS.2021.3083883)

Quality index: JCR2021 Engineering, Electrical & Electronic, Impact Factor: 3.476, Q2 (105/276)

Received April 30, 2021, accepted May 16, 2021, date of publication May 26, 2021, date of current version June 22, 2021.

Digital Object Identifier 10.1109/ACCESS.2021.3083883

Docking of Non-Holonomic AUVs in Presence of Ocean Currents: A Comparative Survey

JOAN ESTEBA^{ID}, PATRYK CIEŚLAK^{ID}, NARCÍS PALOMERAS^{ID}, (Member, IEEE),
AND PERE RIDAO^{ID}, (Member, IEEE)

Computer Vision and Robotics Research Institute (VICOROB), University of Girona, 17003 Girona, Spain

Corresponding author: Joan Esteba (joan.esteba@udg.edu)

This work was supported by the European Union's Horizon 2020 Research and Innovation Program through the ATLANTIS "The Atlantic Testing Platform for Maritime Robotics: New Frontiers for Inspection and Maintenance of Offshore Energy Infrastructures" Project under Grant 871571.

ABSTRACT This paper presents a comparative study of docking algorithms intended for non-holonomic autonomous underwater vehicles, docking in funnel-shaped docking stations, operating under the influence of ocean currents. While descriptive surveys have been already reported in the literature, our goal is to compare the most relevant algorithms through realistic Monte Carlo simulations to provide an insight into their performance. To this aim, a new numerical performance indicator is proposed, which, based on the geometry of the manoeuvre, is able to characterize a successful or unsuccessful docking, providing a metric for comparison. The experimental study is carried out using hardware-in-the-loop simulation by means of the Stonefish simulator, including the dynamic/hydrodynamic model of the Sparus II AUV, models of all internal and external sensors, and the collision geometry representing the docking station.

INDEX TERMS Docking, AUV, ocean currents, non-holonomic.

I. INTRODUCTION

In recent years, underwater robotic technologies have been used in several economic sectors, like oil and gas industry, offshore wind energy generation, scientific research, etc. Nowadays, it is common to use Remotely Operated Vehicles (ROV) to perform tasks such as manipulation and deployment of structures [1], visual inspection and non-destructive testing, core sampling, etc. Moreover, Autonomous Underwater Vehicles (AUV) are being consolidated in this field and starting to be considered a mature technology [2], [3]. This fact encourages the development of complementary technologies to solve some of their current limitations: limited communications bandwidth when the vehicle is submerged (i.e., when relying only on acoustic channels) and highly limited autonomy, resulting from the weight of batteries. These are two of the main concerns that AUVs have to address when facing missions that require persistent autonomy. To mitigate these issues, a concept has been proposed by several researchers, to endow AUVs with the capacity to persistently operate over an area: the use of docking stations (DS). A DS provides the AUV with a protected environment, allows

it to recharge its batteries, and can include high-bandwidth communication channels, to transfer huge amounts of data. In the literature, several examples of DS systems can be found ([4]–[9]). Each DS concept was tailored to a specific AUV and used its own perception and docking strategy. Several descriptive surveys about docking can be already found in the literature: [10]–[12].

In a previous work, [13] the University of Girona developed a prototype of a DS consisting of a fixed funnel equipped with an acoustic transponder and a set of light beacons. The experience obtained while validating this design showed us that the control strategy used to dock was insufficient to deal with severe ocean currents. Furthermore, reliance on a vision system presented problems in very turbid water scenarios. Building from this previous experience, this article compares several docking algorithms, already established in the literature, and how they behave in the presence of ocean currents. All methods have been adapted to use a non-holonomic AUV, a fixed funnel DS, and an ultra-short baseline (USBL) system to localize the DS with respect to the AUV. Extensive tests, based on dynamic simulations [14], have been performed to find the methods' strengths and weaknesses.

The paper is organized as follows: Section II explores the state of the art of docking system designs and docking

The associate editor coordinating the review of this manuscript and approving it for publication was Tao Liu^{ID}.

algorithms developed for non-holonomic AUV, able to deal with ocean currents. Section III describes selected methods and how they have been adapted to the proposed setup. Section IV presents the tools used to develop and evaluate the experiments, and Section V introduces the simulation setup. Obtained results are shown in Section VI, discussed in Section VII, and the conclusions are presented in Section VIII.

II. STATE OF THE ART

A thorough review of the literature on autonomous docking was carried out, focusing especially on those methods that take into account the presence of ocean currents. Starting with the references of one of the most comprehensive surveys in the field [11], all cited articles that meet our criteria were reviewed and added to the list. This exercise was repeated for all the articles in the list that were not previously reviewed. After several iterations, more than one hundred eighty publications were reviewed.

Docking systems can be classified from many different points of view. One possible classification is to differentiate holonomic and non-holonomic robots. A holonomic AUV can control all its degrees of freedom, which makes it easier to complete the docking maneuver even in the presence of ocean currents. Examples of docking of holonomic robots include systems based only on acoustics [15], or approaches that combine acoustics with vision [16], [17]. In [18] a system where the AUV reaches another vehicle using vision is presented, while [19] presents a system where an AUV docks on a submarine, with a mechanical system guided by acoustic, electromagnetic, and optical sensors. In [20] and [21] solutions based on sonar and vision technology are presented. [22] introduces an adaptive DS which is automatically leveled to maintain horizontal orientation.

The non-holonomic AUVs have a limitation on their control that makes the docking maneuver more challenging, especially in presence of ocean currents. The docking concepts for non-holonomic robots can be classified considering the capture mechanism used: pole docking, landing docking, net docking, and funnel docking.

The pole docking system consists of a vertical pole where the AUV attaches. It allows the vehicle to reach the DS from any direction (see Fig. 1), simplifying the way to deal with ocean currents. To allow the AUV to attach to the pole, some modifications to the AUV are required, for example, adding a mechanical V-shaped structure on its front. One of the drawbacks of pole systems is that they usually offer neither protection nor connection (i.e., neither power nor data link) between the AUV and the DS. Therefore, some other mechanism is needed to deliver this functionality. Examples of the pole docking concept are presented in [7], and in [23] where the acoustics (i.e., USBL system) are used to detect the DS position, in [24] where vision (i.e., camera system using markers) is used to detect the DS, or in [25] where both acoustics and vision are used to localize the DS (i.e., USBL

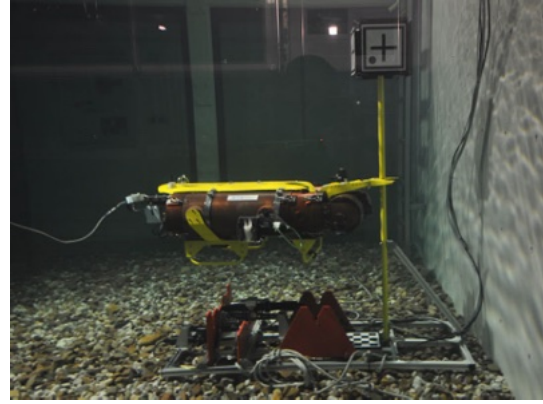


FIGURE 1. Example of pole docking [24].



FIGURE 2. Example of landing docking [28].

system combined with a camera). There are also commercial applications for pole docking like the one reported in [26].

The concept of landing-based docking is similar to the concept of a jet landing on an aircraft carrier. It consists of a mechanical structure where the AUV lands and is attached with a mechanical appendix installed on the AUV. An example of this system appears in [27]. A similar concept is presented in [28] (see Fig. 2) where the AUV has a T-shaped appendage that docks to a V-shaped structure. The problem with this system is that it forces the AUV to approach the DS from a specific direction, which can be problematic in the presence of ocean currents.

The net docking system is presented in [29]. This concept is designed to be a launch and recovery system but is not intended for permanent deployment (see Fig. 3). It consists of a net with an acoustic sensor located in its center, the AUV attaches to the net using a hook added to its nose. Like pole docking, the AUV can choose the direction of the approach, but with the advantage of having the optimal sensor placement (i.e., a USBL can be placed exactly at the position where the AUV should arrive).



FIGURE 3. Example of net docking [29].



FIGURE 4. Example of funnel docking [4].

The funnel docking system is probably the most popular one (see Fig. 4). The mechanical structure of the DS has a shape of a funnel to help the AUV to enter it. The main advantages of this concept are that it allows long-term deployment (i.e., it can offer protection, charging, and data transmission), and there is no need to add mechanical parts to the AUV; for these reasons, this article is focused on funnel-shaped docking systems. Examples where funnel docking is used are reported in [4], [8], [9], [30], and [31]. Like the landing docking system, this configuration has a potential problem with ocean currents because the AUV is required to achieve a particular orientation to enter the DS.

Several strategies to deal with ocean currents with a non-holonomic AUV, when using a funnel-shaped DS, have been published. In [4] the AUV assumes a crab angle to compensate for the ocean currents. In [5], a DS able to control the funnel orientation is presented, to improve the crab angle solution. In [32] a fuzzy controller is applied to perform the docking maneuver. In [31], the AUV heads towards the

DS with a crab angle and when it almost reaches the DS, it suddenly changes the heading to be parallel to the DS axis. In [33] and [34] it is proposed to follow a path with some offset, with respect to the DS axis, and use the ocean current to correct this error, in order to enter parallel to the DS.

III. METHODOLOGIES

Seven methods, described in the literature, have been implemented and compared in this article. A unified setup has been defined, including a funnel-shaped DS, a non-holonomic AUV, and a USBL to detect the DS position with respect to the AUV. The methods have been slightly adapted when necessary to make them compatible with the proposed setup. All the methods generate only a heading reference and a surge velocity reference for the AUV, assuming that a low-level controller will transform them into thruster setpoints [35]. The problem is tackled as a 2D problem (i.e., xy plane) assuming that the z component (i.e., depth or altitude with respect to the bottom) is known and can be independently controlled for an AUV, like the one proposed in Section IV-A1.

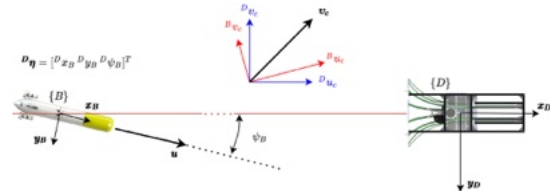


FIGURE 5. Basic variables representation.

In the following subsection, the studied docking algorithms are described.

In Fig. 5 the basic variables involved in the process are described. Two different reference frames are presented, the {D} frame located at the position of the DS, and the {B} frame at the position of the AUV. The ocean current vector (\mathbf{v}_c) is represented for both systems. In the {D} frame the pose of the DS is represented as $\mathbf{P}_D = [{}^Dx_D \ {}^Dy_D \ {}^Dz_D]^T = [0 \ 0 \ 0]^T$. The AUV is represented in the {D} frame as three components: $\mathbf{P}_\eta = [{}^Dx_B \ {}^Dy_B \ {}^D\psi_B]^T$. The simulated robot, a Sparus II AUV, has direct control on the desired surge velocity (i.e., velocity with respect to the ground: u) and on the vehicle heading with respect to the {D} frame (i.e., ${}^D\psi_B$).

A. PURE PURSUIT CONTROLLER

This method is based on the pure pursuit controller [36]. Despite having been used by several authors [5], [28], [37] it is not designed to deal with ocean currents. However, it has been included in this article as a baseline to which the others are compared. The method is based on following a linear path, centered on the DS (see Fig. 6). At each time step, the AUV computes the heading reference ψ_d that moves the AUV from its current position (\mathbf{P}_η) to reach a look-ahead point \mathbf{P}_p , on the path, in front of the robot. The look-ahead distance Δx

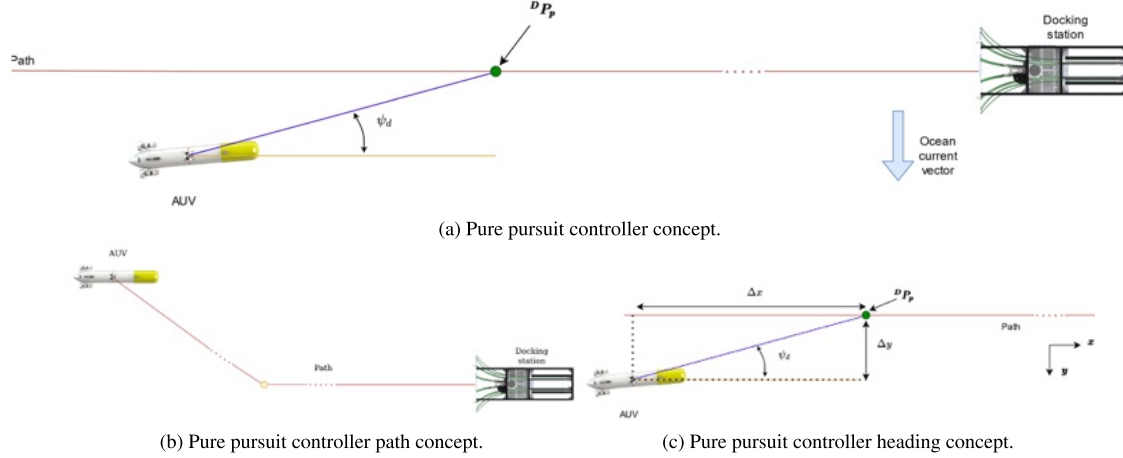


FIGURE 6. Pure pursuit controller representation.

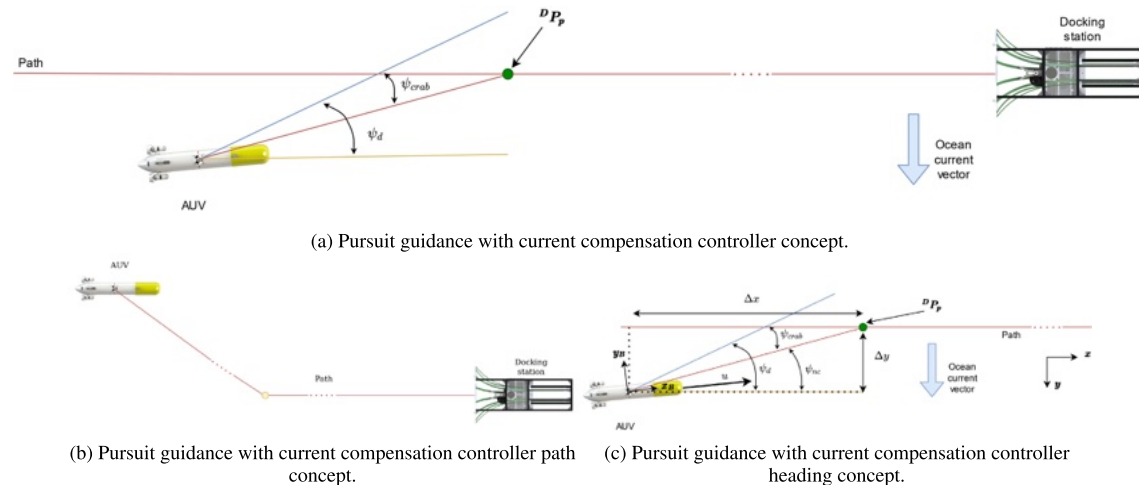


FIGURE 7. Pursuit guidance with current compensation controller representation.

is defined on the x axis of the $\{D\}$ frame and must be tuned:

$$\mathbf{D}\mathbf{P}_p = [{}^Dx_p \ 0]^T, \quad (1)$$

$$\Delta x = {}^Dx_p - {}^Dx_B, \quad \Delta y = {}^Dy_B. \quad (2)$$

The desired heading of the AUV to reach $\mathbf{D}\mathbf{P}_p$ is calculated following (see Fig. 6c):

$$\psi_d = \text{atan}2(\Delta y, \Delta x). \quad (3)$$

The AUV surge velocity (u) is considered constant and set to the desired docking velocity (u_{dock}). The pure pursuit method guarantees the AUV docking velocity but not its heading.

B. PURSUIT GUIDANCE WITH CURRENT COMPENSATION CONTROLLER

The *Pursuit guidance with current compensation controller* (PGCC controller) is based on the idea of applying a correction of the desired heading of the AUV (i.e., introducing a crab angle) in order to compensate for the ocean currents. This concept has been presented by different authors: [5], [38]. The method (see Fig. 7) computes the reference heading for the AUV, adding a corrective crab angle to the default heading that matches the path bearing.

The desired heading and the linear velocity of the AUV are calculated to compensate for the ocean currents. First, the ocean current vector is estimated with respect to the robot's local frame $\{B\}$. Then, the through-water surge



FIGURE 8. Cross-track controller representation.

velocity of the AUV is calculated:

$${}^B u_{B,w} = u_{dock} - {}^B u_c. \quad (4)$$

Knowing the velocity with respect to the water ${}^B u_{B,w}$ and knowing the y component of the ocean current on the $\{B\}$ frame ${}^B v_c$, the crab angle ψ_{crab} can be calculated as follows:

$$\psi_{crab} = \text{atan2}(-{}^B v_c, {}^B u_{B,w}), \quad (5)$$

limiting the maximum angle to 90° . As in the previous method, the controller tries to reach a point ${}^D P_p$ in front of the vehicle, computed using (1). To reach it, a heading is defined, without considering the ocean currents:

$$\psi_{nc} = \text{atan2}(\Delta y, \Delta x). \quad (6)$$

The desired heading ψ_d is defined as the sum of both ψ_{crab} and ψ_{nc} , see Fig. 7c:

$$\psi_d = \psi_{nc} + \psi_{crab}. \quad (7)$$

The AUV surge velocity u is considered constant and set to the desired docking velocity u_{dock} . As well as the previous method, this method guarantees the AUV docking velocity but not the heading.

C. CROSS-TRACK CONTROLLER

The strategy of this method is based on applying a correction to the AUV heading, in order to compensate for the cross-track error, that appears due to the lateral current. This method is used in [4], [39].

A path co-linear with the center-line of the DS is defined and the cross-track error e is obtained as the difference between the y component of the path (that is zero) and the position of the AUV (see Fig. 8):

$$e = {}^D y_B. \quad (8)$$

The desired heading ψ_d is obtained with a PID control law, acting over e , which uses an integral anti-windup limit, see [40]. As in the previous methods, u is considered constant and set to u_{dock} . This method guarantees the AUV docking velocity but not the heading.

D. FUZZY CONTROLLER

This method is based on [32] and [41]. It calculates the heading and the linear velocity of the robot, following the fuzzy rules presented in [41] (Fig. 9). It calculates the associated weights of the fuzzy rules according to Fig. 9b and the membership functions presented in Fig. 9c and Fig. 9d to obtain the heading (Table 1) and the linear velocity of the AUV (Table 2). For the experiment set in this paper, not all the sections are used. To better understand which ones are used, see the green sections represented in Fig. 9b and the set of the experiments presented in Section V.

Like the previous methods, this method guarantees the AUV docking velocity but not the heading.

E. TOUCHDOWN ALIGNMENT CONTROLLER

The method showed in [31] is used to fix one of the possible problems that appear when using the pure pursuit, the cross-track, the PGCC, or the fuzzy controllers, that is reaching the DS without being parallel to it. In this method, the AUV executes a cross-track controller but when it reaches a position just in front of the DS the AUV heading is abruptly changed to align it with the DS before *touchdown*.¹ In the original article direct control of the AUV rudder is used for this purpose. However, because the Sparus II AUV does not have a rudder, in this article the ${}^D \psi_B$ is suddenly modified to emulate this behavior.

The method follows two steps (see Fig. 10):

- The AUV follows the DS center-line path using a cross-track controller. A conventional PID with an integral anti-windup is used to compute the crab angle β that reduces the cross-track error to zero (as in the cross-track controller).
- Before touchdown, the crab angle must be eliminated. According to the maximum yaw rate (r_{max}), β , and u_{dock} ; the distance with respect to the DS (d_f), at which the AUV heading must be abruptly changed, must be computed. The original authors propose to use a cosine curve described by (10) to change the reference heading during the final alignment (see Fig. 10b).

¹According to Park, *touchdown* means the contact of the AUV and the docking station. The word comes from airplane flight operation.

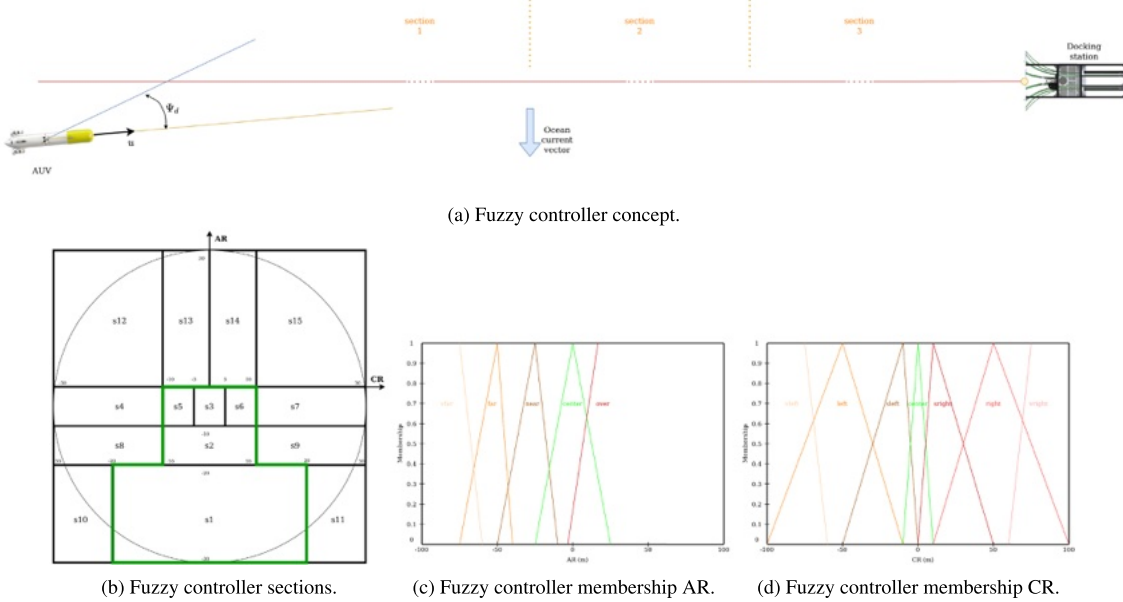


FIGURE 9. Fuzzy controller representation.

TABLE 1. Fuzzy controller ψ_d related to the section.

Heading reference related to the section		
$\psi_1 = -8 CR$	$\psi_6 = -90$	$\psi_{11} = -1.5 AR - 125$
$\psi_2 = -12 CR$	$\psi_7 = -175$	$\psi_{12} = 0.4 CR - 160$
$\psi_3 = -15 CR$	$\psi_8 = 0.4 CR + 150$	$\psi_{13} = -60$
$\psi_4 = 175 CR$	$\psi_9 = 0.4 CR - 150$	$\psi_{14} = 0.4 CR + 160$
$\psi_5 = 90$	$\psi_{10} = 1.5 AR - 125$	$\psi_{15} = 60$

TABLE 2. Fuzzy controller u_d related to the section (u_{dock} corresponds to docking entrance velocity).

Linear velocity reference related to the section		
$u_1 = u_{dock}$	$u_6 = 0.85 u_{dock}$	$u_{11} = 0.7 u_{dock}$
$u_2 = u_{dock}$	$u_7 = 0.7 u_{dock}$	$u_{12} = 0.7 u_{dock}$
$u_3 = u_{dock}$	$u_8 = 0.7 u_{dock}$	$u_{13} = 0.7 u_{dock}$
$u_4 = 0.7 u_{dock}$	$u_9 = 0.7 u_{dock}$	$u_{14} = 0.7 u_{dock}$
$u_5 = 0.85 u_{dock}$	$u_{10} = 0.7 u_{dock}$	$u_{15} = 0.7 u_{dock}$

The distance between the AUV and the DS is defined as d , keeping in mind that the position of the DS is the origin of the $\{D\}$ frame:

$$d = -{}^Dx_B. \quad (9)$$

The desired heading of the AUV in the last part of the maneuver is defined as a cosinusoidal function of the distance:

$$\psi_d = -\frac{\beta}{2} \cos\left(\pi \frac{d}{d_f}\right) + \frac{\beta}{2}. \quad (10)$$

Then, given the cosinusoidal heading the minimum distance ($d_{f,min}$) required to perform the maneuver is given by:

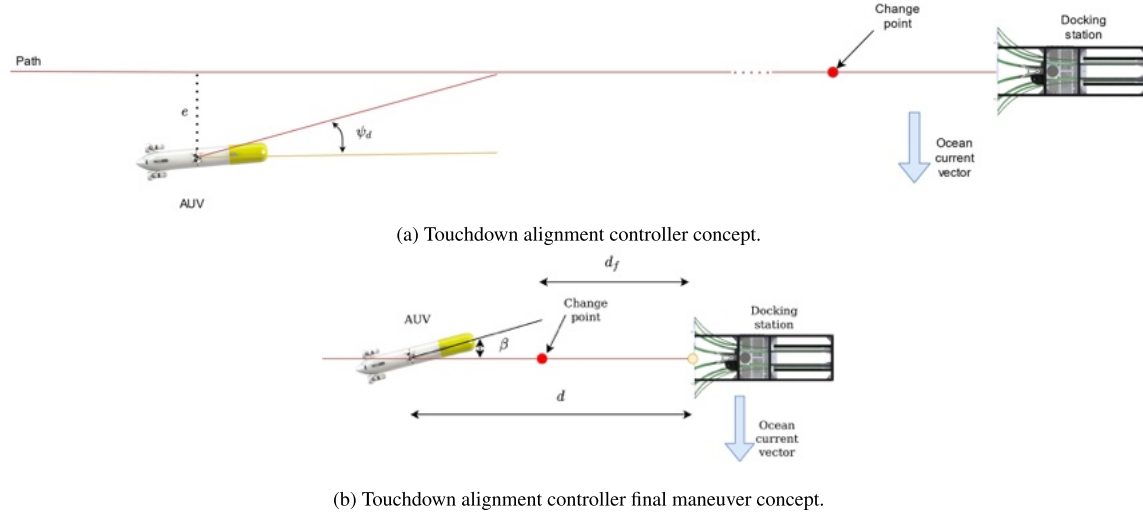
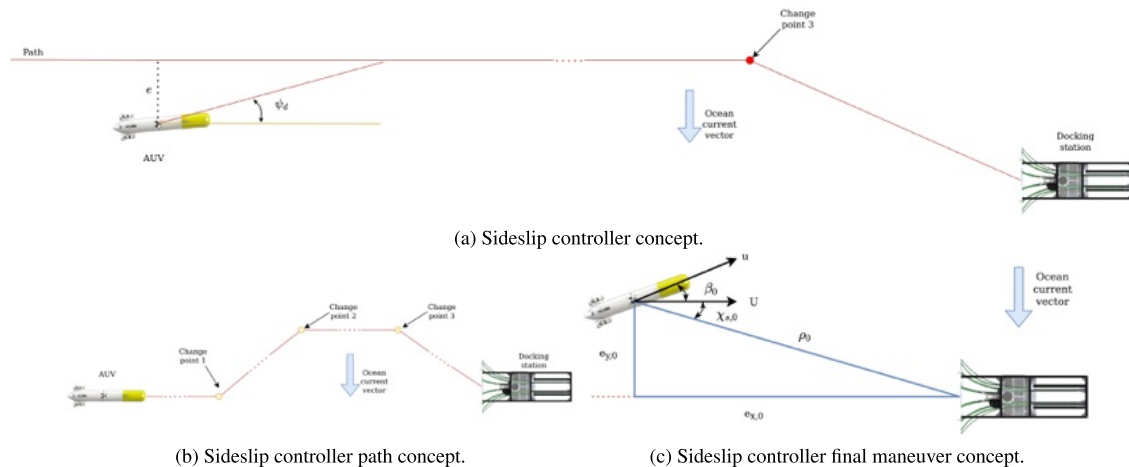
$$d_{f,min} = \left| \frac{\beta}{2} \frac{\pi}{r_{max}} u_{dock} \right|. \quad (11)$$

To have some safety margin the distance where the change point is set is defined as:

$$d_f = k d_{f,min}. \quad (12)$$

where k corresponds to a gain.

This method allows controlling both the AUV docking heading and forward velocity.

**FIGURE 10. Touchdown alignment controller representation.****FIGURE 11. Sideslip controller representation.**

F. SIDESLIP CONTROLLER

Park *et al.* [33] propose an alternative methodology to deal with the problem of reaching the DS with the desired angle. In this method, the authors create a path parallel to the DS axis at some distance from the docking station. Once the AUV reaches a specific point, a maneuver to move the robot from this path to the DS center-line, while keeping the vehicle parallel to the DS, is performed.

This methodology consists of three steps (see Fig. 11):

- First the AUV approaches the DS using the cross-track controller to compensate for the ocean current.

- When the necessary crab angle (β), to compensate the ocean currents, is achieved (*change point 1*), the vehicle accelerates keeping the same heading (i.e., ${}^D\psi_B = \beta$) until the cross-track error is around 3 m (*change point 2*) on the side from where the current is coming (see Fig. 11b).
- The vehicle follows the path parallel to the DS axis until it is around 20 m in front of the DS (*change point 3*). At this moment the AUV heading reference ψ_d is gradually changed from β to the DS angle (${}^D\psi_D = 0$) that is the desired heading, that the vehicle has to

achieve when it reaches the DS, following (13) to (21), see Fig. 11c.

$$e_x = \rho \cos(\chi_s), \quad e_{x,0} = \rho \cos(\chi_{s,0}) \quad (13)$$

$$e_y = \rho \sin(\chi_s), \quad e_{y,0} = \rho \sin(\chi_{s,0}) \quad (14)$$

$$0 \leq w_1 \leq 1, \quad 0 \leq w_2 \leq 1, \quad 0 \leq w_3 \leq 1 \quad (15)$$

$$w_1 = e_x / \max(e_x, e_{x,0}) \quad (16)$$

$$w_2 = e_y / \max(e_y, e_{y,0}) \quad (17)$$

$$w_3 = \rho / \max(\rho, \rho_0) \quad (18)$$

$$\alpha = (1 - w_2) \beta_0 + w_2 \chi_s \quad (19)$$

$$\gamma = (1 - w_1) {}^D\psi_D + w_1 \beta_0 \quad (20)$$

$$\psi_d = (1 - w_3)\alpha + w_3 \gamma \quad (21)$$

where ρ is the distance between the DS and the AUV, e_x and e_y are the x and y component of the distance between the DS and the AUV, χ_s is the angle between the DS axis and the AUV, ρ_0 , $e_{x,0}$, $e_{y,0}$, $\chi_{s,0}$ are the values of the variables explained before when the AUV starts the final approaching maneuver. This method allows controlling both the AUV docking heading and forward velocity.

G. SLIDING PATH CONTROLLER

Sans-Muntadas et al. [34] presents a strategy that, like Park et al. [33], requires planning a path. This method follows the following steps (see Fig. 12):

- The AUV approaches the DS following a path parallel to its center-line with an offset of a few meters on the side of the current (approaching path, see Fig. 12a). An Integral Line-Of-Sight (ILOS) controller is used to regulate the cross-track error to zero.
- When a certain distance from the DS is reached, the AUV switches to the sliding path. In the sliding path a control rule is set to compensate the offset of the approaching path in the y component of the $\{D\}$ frame, using the ocean currents, and aligning the AUV with the DS.

The ILOS controller [42] uses an integral function that controls the heading of the AUV, in order to minimize the cross-track error (see Fig. 12c), which is represented by the following rules:

$$\psi_d = \text{atan2}(y + \sigma y_{int}, \Delta), \quad (22)$$

$$\dot{y}_{int} = \frac{\Delta y}{(y + \sigma y_{int})^2 + \Delta^2}. \quad (23)$$

where y is the distance between Dy_B and the approaching path, y_{int} is the integral factor, σ is a gain, and Δ is a look-ahead distance (as in the Pure pursuit controller). During this approaching phase the AUV has a crab angle to compensate for the ocean currents. The distance between the center-line and the approaching path (y_a) is computed as follows (see Fig. 12a):

$$\tan(\chi_s) = {}^Dv_c/u_{dock}, \quad (24)$$

$$y_a = -l \sin(\chi_s). \quad (25)$$

where Dv_c is the lateral current, and l is the distance to the DS where the sliding path controller will be enabled.

The sliding path is a straight line that leads to the entrance of the DS. Two control laws are used to follow this path. On one side the ILOS controller drives the cross-track error to zero but does not guarantee the AUV heading to be the same as ${}^D\psi_D$. On the other side, a Speed Regulated Guidance (SRG) controller forces the AUV to be parallel to the DS and tries to adjust the AUV position with respect to the sliding path, controlling only its surge velocity, see Fig. 12d:

$$\psi_d = 0, \quad (26)$$

$$S_c = u_m \frac{2}{\pi} \tan(k_u e), \quad (27)$$

$$u_{srg} = u_{dock} - {}^Dv_c - S_c. \quad (28)$$

where u_m is the maximum velocity that the AUV could reach, k_u is a gain, and Dv_c is the ocean current velocity on the x axis in the $\{D\}$ frame. A hybrid framework is used during the sliding path to decide which controller, the ILOS or the SRG, is active. Basically, when the AUV cross-track error is above a threshold, the ILOS controller is activated. When the cross-track error is below another threshold, the SRG is enabled instead. Some hysteresis is added when defining the thresholds to avoid chattering due to sensor noise (see Fig. 12b). In order to define the different zones, first, the line that represents the sliding path is calculated:

$$a = \frac{{}^Dy_D - {}^Dy_{cp2}}{{}^Dx_D - {}^Dx_{cp2}}, \quad (29)$$

$$b = {}^Dy_D - a {}^Dx_D, \quad (30)$$

where ${}^D\mathbf{P}_{cp2}$ is the position of the *change point 2* in the $\{D\}$ frame (see Fig. 11b). The SRG guidance zone is defined as:

$$a {}^Dx_B + b - \phi_{dock}/2 \leq {}^Dy_B \leq a {}^Dx_B + b + \phi_{dock}/2, \quad (31)$$

where ϕ_{dock} is the external diameter of the funnel. The zone where the SRG control is changed to ILOS control is defined as the union of:

$${}^Dy_B > a {}^Dx_B + b + \phi_{dock}/2, \quad (32)$$

and

$${}^Dy_B < a {}^Dx_B + b - \phi_{dock}/2. \quad (33)$$

The ILOS guidance zone is defined as the union of:

$${}^Dy_B \geq a {}^Dx_B + b + \phi_{dock}/4, \quad (34)$$

and

$${}^Dy_B \leq a {}^Dx_B + b - \phi_{dock}/4. \quad (35)$$

Finally, the zone where the ILOS control is changed to SRG control is represented as:

$$a {}^Dx_B + b - \phi_{dock}/4 < {}^Dy_B < a {}^Dx_B + b + \phi_{dock}/4. \quad (36)$$

If the SRG control is applied, when the AUV reaches the DS, the rules of the control can be defined as:

$$\psi_d = 0, \quad (37)$$

$$u_d = u_{srg}. \quad (38)$$

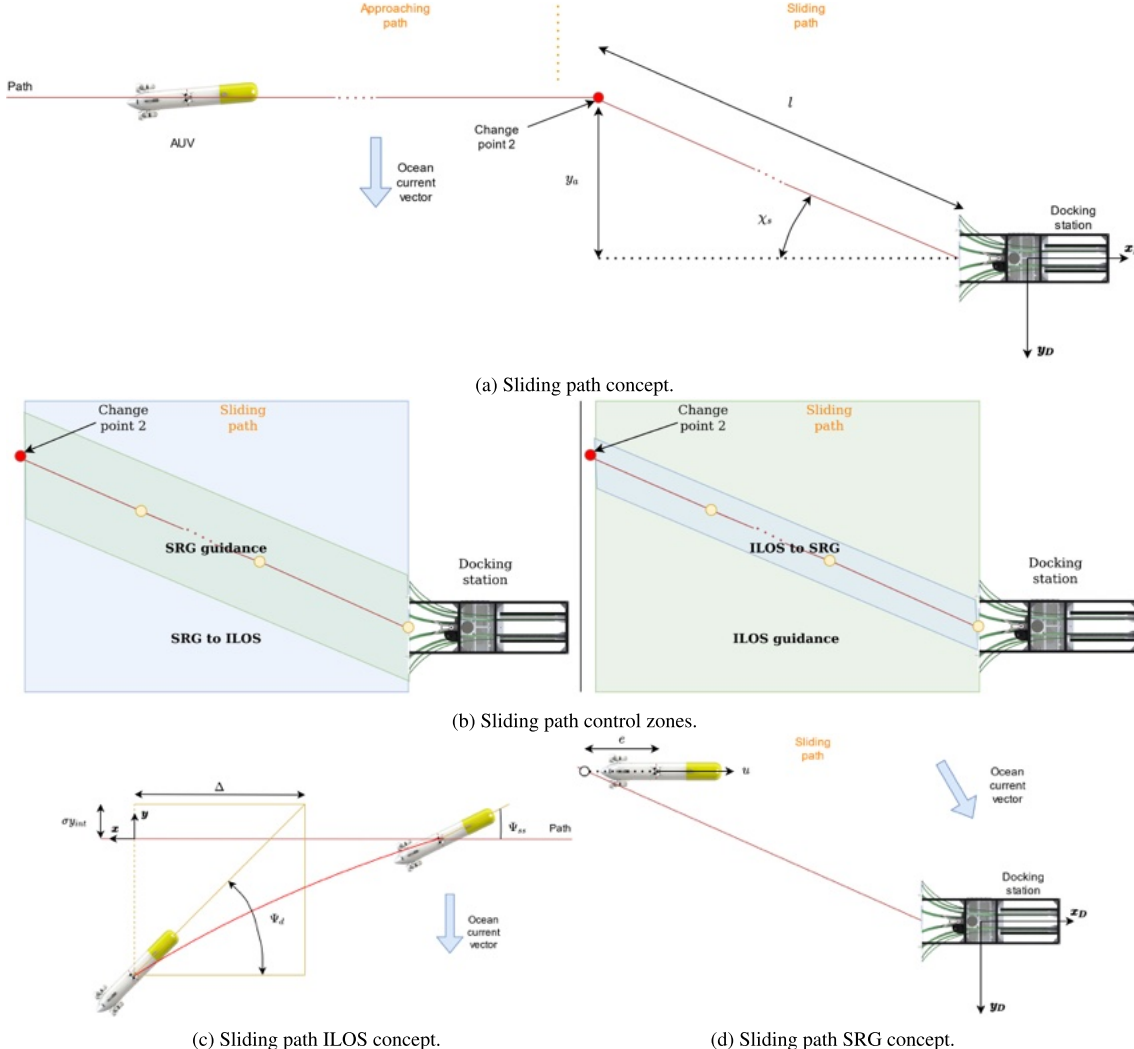


FIGURE 12. Sliding path representation.

Note that the u_{srq} defined in (28) is with respect to the water, while the one defined in (38) is with respect to the ground. This method allows for controlling the heading of the AUV but not the docking velocity.

IV. DESIGN TOOLS

This section presents the setup (i.e., AUV, DS, and localization system) used for the comparative analysis; as well as the Stonefish dynamic simulator used to carry out all the tests; and a new metric, proposed in this article, to evaluate the quality of a docking maneuver.

A. DOCKING SETUP

This section introduces the AUV, the DS, and the USBL system that have been simulated.

1) SPARUS II

The Sparus II is an AUV developed primarily for seabed surveys and offshore structure inspection by the University of Girona, and recently commercialized by Iqua Robotics SL. [43], [44]. It combines the classical concept of a torpedo-shaped vehicle with hovering capabilities (see Fig. 13). To allow for the integration of equipment, that depends on the



FIGURE 13. Photography of the sparus II.

application, the robot has a fully configurable payload area. Its software architecture is based on COLA2 [35] which is utilising the ROS open-source middleware [45]. The main specifications and features of the Sparus II can be found in Table 3. The shape of the AUV hull is optimised for navigation at medium/high velocities. The vehicle can be controlled in surge, heave, and yaw degrees of freedom independently by means of three thrusters (one vertical and two horizontal). It can reach a maximum velocity in surge of 3 kn. The vehicle is rated for up to 200 m depth. Its navigation suite includes an Inertial Measurement Unit (IMU), a Doppler Velocity Log (DVL), a GPS, and, optionally, a USBL. The latter can be used as a beacon to localize the AUV from the surface or, as inverted-USBL, to localize a target underwater, here the DS equipped with an acoustic beacon.

A Kalman filter estimates the position and velocity of the vehicle using the information from the sensors. The filter is first initialized at the surface, with the GPS, but it is also possible to apply position updates using the USBL when the vehicle is submerged. The control system is divided into two parts: a high-level controller and a low-level controller. In this article, a high-level controller for each of the docking methods, described in Section III, has been defined. The low-level controller, based on a cascade of PID and an open-loop thruster model, takes the desired velocities or heading set-points, defined by the high-level controller, and generates the thrusters' set-points.

The depth of the vehicle is controlled independently by the vertical thruster. This reason justifies that the study presented in this paper could have been simplified to the xy plane.

2) DOCKING STATION

The DS that has been simulated in all of the experiments was developed by the University of Girona [13], see Fig. 14. This DS was tailored to the Sparus II AUV and it has been designed to be as small and lightweight as possible, for easy deployment, recovery, and transportation. The structure

TABLE 3. Sparus II specifications.

Sparus II specifications	
Lenght	1.6 m
Hull diameter	230 mm
Max width	460 mm
Weight in air	52 kg
Maximum depth	200 m
Energy	1.4 kWh Li-Ion battery
Endurance	8 - 10 h
Max surge velocity	3 kn
Propulsion system	3 thrusters (magnetic coupling)
DoFs	Surge, heave, pitch, roll and yaw
Structure	Modular aluminium and acetal hull
Navigation	DVL, IMU, pressure sensor and GPS
Payload area	8 l or 7 kg in air
Payload interface	Ethernet, RS-232 / regulated 12 V and 24 V
Communications	WiFi, XBee, GSM/3G, acoustic modem
Safety	Emergency primary battery, independent pinger tracking system, flasher light, USBL and acoustic modem

is divided into two parts: the base and the docking funnel (see Fig. 15). It can handle translation misalignment of up to 40 cm and heading misalignment of up to 30°. The rails are made of flexible POM (polyoxymethylene) to absorb collisions.

3) VEHICLE-DS LOCALIZATION

An inverted-USBL (i.e., a transceiver located on the AUV and a transponder on the DS) has been simulated to obtain the position of the DS from the AUV. To simplify the visualization of all of the experiments, the DS position has been defined at the origin of the $\{D\}$ frame.

B. STONEFISH SIMULATOR

The Stonefish simulator [14] is an advanced open-source simulation tool, designed for marine robotics. It can simulate



FIGURE 14. Photography of the docking station.

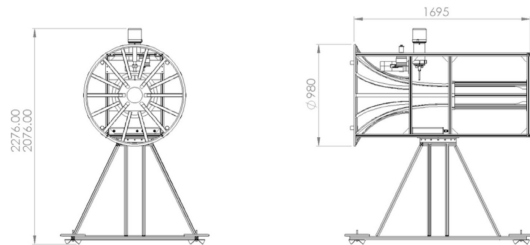


FIGURE 15. Main dimensions of the docking station (in mm).

multiple underwater and surface robots, working in a virtual ocean environment. The simulator is able to compute the full dynamics and hydrodynamics of underwater and surface robots, simulate the operation of thrusters and sensors, and to emulate the acoustic communication devices. The simulated sensors cover the full range of devices found in marine robots, e.g., DVL, pressure sensor, USBL, and all types of sonars. Moreover, it delivers the possibility to fully define an environment using geometric models or heightmap-based terrain. It can simulate ocean currents and Fast-Fourier transform (FFT) based waves. Finally, realistic rendering of the ocean surface and underwater environment, including light absorption and scattering, enables accurate simulation of underwater cameras.

The Stonefish simulator was used to recreate the docking scenario, including the complete models of the Sparus II AUV and the DS, situated at the bottom of a virtual ocean. In Fig. 16 the simulator window is presented, showing the visualisation of the docking scenario during one of the simulations.

The docking algorithms presented in Section III have been implemented as high-level controllers that run within the COLA2 robot architecture [35]. The simulator communicates with the COLA2 architecture, through a ROS-based interface, and it replaces the real vehicle in a hardware-in-the-loop (HIL) configuration. In this way all of the developments carried out using the simulator can be directly tested on the real vehicle. The parameters of all of the devices, including noise characteristics, were set up according to the manufacturers' specifications. Moreover, different types of underwater ocean



FIGURE 16. Stonefish simulation example.

current models can be defined in Stonefish. Here, a uniform current velocity field was used, with different current direction and velocity for different experiments. The simulator can also compute rigid collisions between the AUV and the DS, allowing estimation of the behaviour of the system during the entrance.

In order to realistically recreate the behavior of a physical USBL, the Stonefish uses equations reported in [46] and sets the different parameters using real data from the EvoLogics 18/34 USBL. This allows us to account for the equipment's measurement errors and noise characteristics.

The DVL characteristics match those of the Teledyne Marine WHN 600, which is the model used by the AUV Sparus II. The DVL readings are used by the AUV's navigation system to estimate its position and velocity, relative to the ground, as well as to estimate the direction and magnitude of ocean currents.

C. ENTRANCE QUALITY ANALYSIS

To evaluate the docking methods, a new technique to measure the quality of the entrance to the DS is proposed here. A geometrical analysis to obtain a representative value of the quality of the entrance is presented, based on a collision analysis where the momentum lost in the entrance maneuver is estimated.

1) COLLISION ANALYSIS

The collision analysis estimates the momentum lost on the entrance due to the collisions and friction between the robot and the DS (m_1). To do that, it compares the momentum of the AUV crossing the first section of the DS (m_{s1}) with the momentum of the AUV crossing the second section (m_{s2}), see Fig. 17. These quantities can be obtained using the velocity of the AUV at the moment of crossing each of the sections $|\vec{v}_1|$, $|\vec{v}_2|$ and the mass of the vehicle M :

$$m_{s1} = M|\vec{v}_1|, \quad m_{s2} = M|\vec{v}_2|. \quad (39)$$

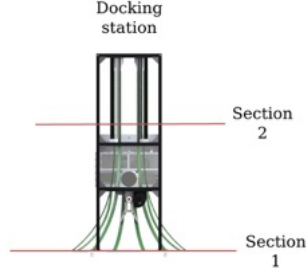


FIGURE 17. Collision analysis sections representation.

The change in momentum is mainly explained by the action of the thrusters (m_T) and the energy lost in the collisions and friction between both sections:

$$m_{s2} = m_{s1} + m_T - m_l. \quad (40)$$

The software architecture of the Sparus II allows us to record the force that the thrusters are generating at each moment in time (F_t). Integrating this force over the period between the sections, the change of momentum (impulse) caused by thrusters can be obtained:

$$m_T = \int_{t_1}^{t_2} F_t dt. \quad (41)$$

Then, the change of momentum related to the collisions and friction can be calculated as:

$$m_l = m_T + m_{s1} - m_{s2}. \quad (42)$$

This analysis has a few drawbacks: the maneuver needs to be performed before it is evaluated, the method cannot distinguish whether the AUV enters the DS or does not, and it does not provide a normalized value. For these reasons the geometrical analysis, presented in the next subsection, was developed.

2) GEOMETRICAL ANALYSIS

Let us simplify the system representing the DS with a triangle, where one side represents the DS entrance section and the opposite vertex the DS center (see Fig. 18). When the AUV reaches the *entrance section*, the position and the heading of the AUV ${}^D\eta_e$ are registered. To simplify the nomenclature ${}^D\psi_{B,e}$ will be called α . With this diagram, an optimal entrance angle (α_o) for each entrance position can be approximated:

$$\alpha_o = \text{atan}2({}^Dy_{B,e}, {}^Dx_{B,e}). \quad (43)$$

The heading of the AUV at the entrance and the optimal entrance angle can be compared as:

$$e_\alpha = \alpha - \alpha_o. \quad (44)$$

It is necessary to take into account on which side of the center-line of the DS the AUV is located, when colliding with

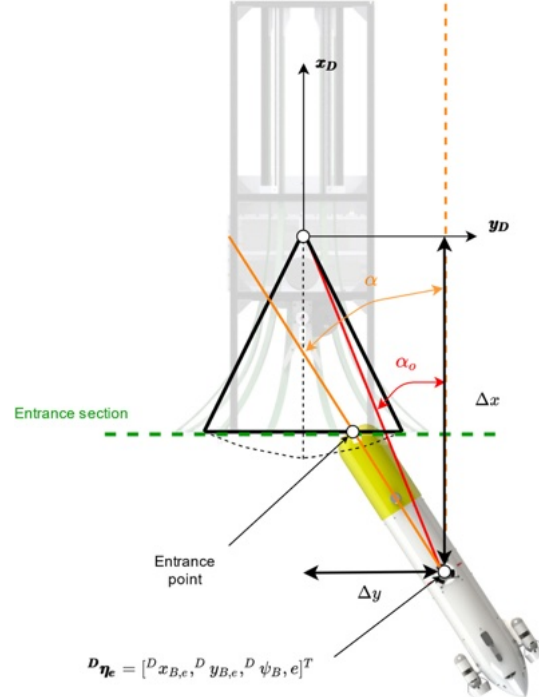


FIGURE 18. Geometrical analysis concept.

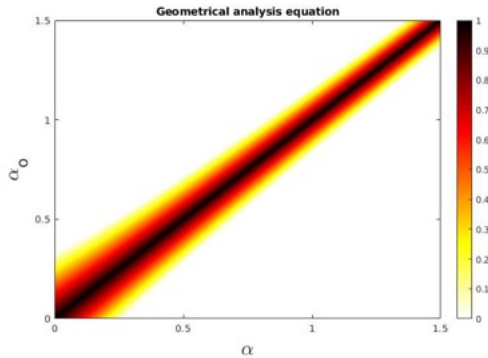


FIGURE 19. Graphical representation of the geometrical analysis equation. The value of g is represented by the 'hot' color map.

the funnel, because the same e_α value will result in different behaviours, e.g., when the vehicle approaches the funnel on its right side and $e_\alpha > 0$, the docking maneuver will be performed more smoothly and the lost momentum will be lower, than if it was approaching on the left side. To consider this fact, a weight w is assigned, following these criteria:

$$w = \begin{cases} w_1, & \text{sgn}(\Delta y) = \text{sgn}(e_\alpha) \\ w_2, & \text{otherwise.} \end{cases} \quad (45)$$

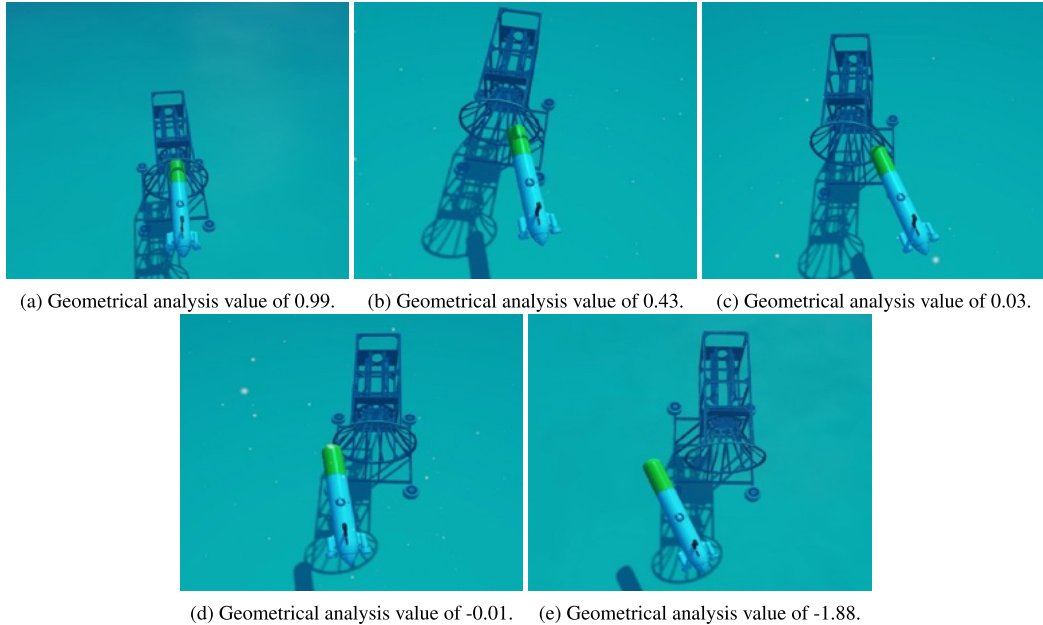


FIGURE 20. Geometrical analysis examples.

Regarding the presented concept, the geometrical analysis can be expressed with the formula:

$$g = 1 - w|e_\alpha|(1 + |\alpha_o|). \quad (46)$$

It should be noticed that this formulation consists of two terms. The first one evaluates the entrance angle against the optimal entrance angle. The second one considers the value of the optimal entrance angle itself to reward entrances in the center of the DS. These behaviours can be seen in Fig. 19. The combination of these two terms was used, in an attempt to reflect the results obtained in the collision analysis in the cases in which the AUV enters the DS. Moreover, the equation (46) was designed to have a value of $g = 1$ if the docking maneuver is ideal, a value of $0 < g \leq 1$ if the AUV enters the DS, and a value $g \leq 0$ if the AUV does not enter the DS, see Fig. 20. The weights in (45) were evaluated as $w_1 = 1$ and $w_2 = 3.05$, based on the collision analysis performed on simulated data, assuming the aforementioned properties of (46). To summarize, the value of the geometrical analysis g , allows evaluation of the quality of the docking maneuver and at the same time it retains the connection with the physical phenomena accompanying the entrance (collision and friction). It provides a normalized value that allows an intuitive understanding of the docking process. Moreover, it can be used to compute the set of preferred docking parameters (pairs of the offset from the center-line and the heading), i.e., the region of attraction of a particular docking algorithm.

V. COMPARISON BENCHMARKS

The docking algorithms presented in Section III were tested using the setup introduced in Section IV, at three levels of increasing complexity. In order to average the results, at each level, a set of fifty simulations have been made, for each specific ocean current velocity vector (\mathbf{v}_c), considered to lie on the xy plane of $\{D\}$ and sampled from a square set ranging from $(-0.4 \text{ m/s}, -0.4 \text{ m/s})$ to $(0.4 \text{ m/s}, 0.4 \text{ m/s})$, with a step of 0.1 m/s on each axis. This resulted in more than eighty five thousand simulations executed. In each simulation, the AUV starts 300 m in front of the DS, to ensure sufficient space to perform the docking maneuver ($D\eta = [-300, 0, 0]^T$).

A. LEVEL 1: PERFECT MEASUREMENTS, 1.0 m/s

At this level, the AUV knows exactly the position of the DS in the world frame as well as its own position and the velocity of the current (\mathbf{v}_c). The desired docking velocity (u_{dock}) is set to 1 m/s to guarantee that it is significantly higher than the ocean current velocity. Some of the reviewed papers assume the same conditions ([31], [33], [34]). The objective of this level is to determine the ocean current conditions which these methods can cope with, when perfect measurements about the environment are available. It is important to remember that Sparus II dynamics and hydrodynamics are fully simulated and the vehicle control is affected by them.

B. LEVEL 2: NOISY MEASUREMENTS, 1.0 m/s

At this level, the AUV detects the position of the DS using a USBL, modeled as explained in Section IV. Moreover, a DVL

is used to estimate the ocean current velocity. The desired docking velocity is set to 1 m/s. The objective of this level is to determine how inaccuracies in both the localization and ocean current estimation affect the methods reviewed.

C. LEVEL 3: NOISY MEASUREMENTS, 0.3 m/s

Because colliding with the DS at 1 m/s is not recommendable for a vehicle like the Sparus II AUV, the authors wanted to evaluate how the studied docking algorithms behave when the docking velocity was much lower, here around 0.3 m/s. This condition means that it is possible to experiment with an ocean current faster than the docking velocity, here up to 0.55 m/s. The same localization and current estimation system as in Level 2 are used.

VI. RESULTS

This section presents the results of the performed simulations. An intuitive graphical representation of the behavior of each method was created, in a form of 3D plots depicting the mean geometrical value (\bar{g}) for each v_c . Therefore, the 2D current velocity is represented on the xy plane, while the z axis represents \bar{g} , computed based on averaging fifty experiments. To further improve the readability, the *Hot* color map was used, where the black color denotes a perfect entrance while the white color a failed docking, and red and yellow being intermediate points. A single indicator, named ‘score’, can be obtained based on this representation, by integrating \bar{g} over the set of v_c for which $\bar{g} \geq 0$. This volume is then normalized by comparing it with the maximum volume, given by a theoretical perfect score distribution where $\bar{g} = 1$ for all tested values of v_c . The 2D plots presented in the Annex help to understand the behaviour of the methods in detail.

Figures 22 and 23 show the results obtained at Level 1 and Table 4 shows the average value and the standard deviation for the score obtained for each method.

The results of Level 2 can be analysed following Fig. 24, which shows the results in 3D, for more detail, Fig. 25 shows the results in the plane with the color map and Table 5 shows the geometrical volume mean and standard deviation of the different simulations.

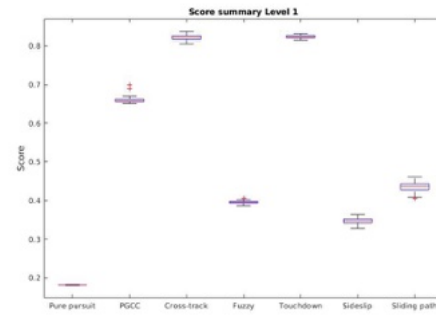
Finally, related to Level 3, in order to have a first picture of the results, see Fig. 26; for more details see Fig. 27; and for the quality number associated with each method see Table 6. As a summary, a comparison of all of the methods for each level is shown in Fig. 21.

VII. DISCUSSION

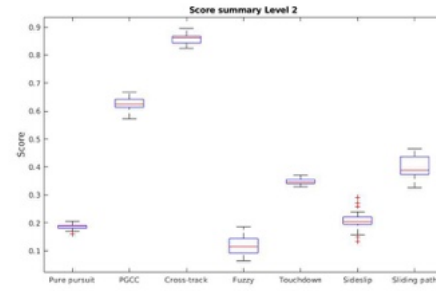
In this section, the results are discussed method by method.

A. PURE PURSUIT CONTROLLER

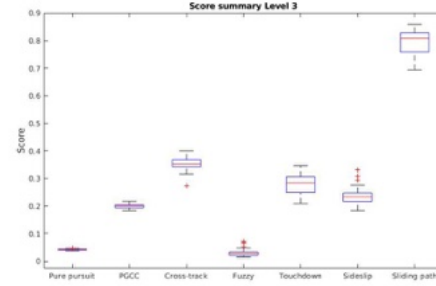
The pure pursuit controller is not designed to deal with ocean currents. It is presented here as a baseline to compare with the other methods. As already seen in [37], this controller cannot deal with lateral currents. It is not able to ensure successful docking at any level, if the lateral component of the current velocity is higher than 0.1 m/s.



(a) Score summary for the Level 1.



(b) Score summary for the Level 2.



(c) Score summary for the Level 3.

FIGURE 21. Score summary for each level.

B. PGCC CONTROLLER

The Pure Guidance with Current Compensation controller generally delivers good results. For the first two levels, it can deal with practically all the ocean current conditions, reaching a score of 0.660 at Level 1, and a score of 0.624 at Level 2. A little decline in performance is noticed moving from Level 1 to Level 2, due to the sensors’ measurement noise. The Level 3 is significantly affected by the reduction of the docking velocity, resulting in a low score of 0.148, due to low values of \bar{g} when $u_{dock} \leq {}^D u_c$. For example, in the case of $u_{dock} = {}^D u_c$ the AUV velocity with respect to the water has to be zero. Therefore, the only way to reduce the cross-track error is to set the desired heading $\psi_d = 90^\circ$. However, this

TABLE 4. Score results for the perfect measurements simulations.

Method	Score	
	mean	std
Pure pursuit controller	0.181	0.001
PGCC controller	0.660	0.005
Cross-track controller	0.822	0.007
Fuzzy controller	0.395	0.005
Touchdown alignment controller	0.824	0.004
Sideslip controller	0.347	0.009
Sliding path controller	0.436	0.013

TABLE 5. Score results for the noisy measurements simulations with a docking velocity of 1 m/s.

Method	Score	
	mean	std
Pure pursuit controller	0.186	0.009
PGCC controller	0.624	0.026
Cross-track controller	0.858	0.015
Fuzzy controller	0.119	0.033
Touchdown alignment controller	0.348	0.010
Sideslip controller	0.207	0.033
Sliding path controller	0.402	0.039

does not allow the vehicle to enter the DS. As a result, it is not possible to simultaneously eliminate the cross-track error and complete the docking.

C. CROSS-TRACK CONTROLLER

The cross-track controller generally performs well, with the best score of 0.858 at Level 2 and also a very good result at Level 1 (0.822). It exhibits the same problems as the PGCC

TABLE 6. Score results for the noisy measurements simulations with a docking velocity of 0.3 m/s.

Method	Score	
	mean	std
Pure pursuit controller	0.148	0.002
PGCC controller	0.224	0.008
Cross-track controller	0.403	0.019
Fuzzy controller	0.128	0.014
Touchdown alignment controller	0.345	0.022
Sideslip controller	0.311	0.021
Sliding path controller	0.790	0.025

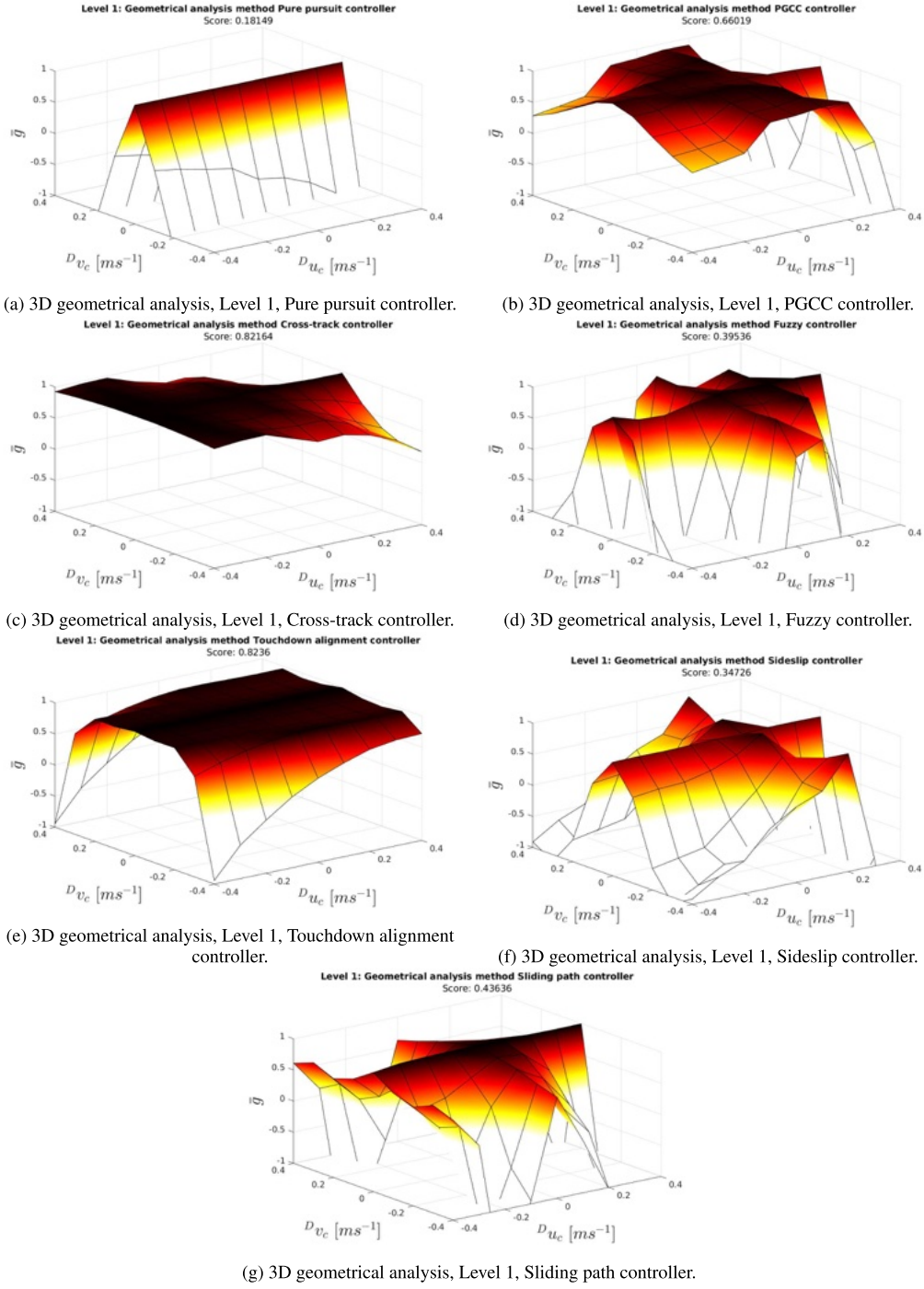
controller, when $u_{dock} \leq D u_c$. However, it still scores an acceptable value of 0.403 at Level 3.

The improvement observed between Level 1 and Level 2, occurring despite the addition of noise in the sensors, can be explained by the way the geometrical analysis works. The geometrical analysis tries to evaluate not only if the AUV enters the DS but also how it enters. When the cross-track controller, or the PGCC controller, is working perfectly, the AUV enters the DS right through its center with the necessary crab angle to counteract the lateral component of the ocean current velocity. This crab angle is penalized by the geometrical analysis if the vehicle is perfectly in the center, but it is less penalized if there is some cross-track error, as shown in Fig. 18. When noisy measurements are used, the controller is unable to reduce the cross-track error to zero, and therefore a slight improvement in the score appears.

D. FUZZY CONTROLLER

The fuzzy controller achieves acceptable results at Level 1 (0.395), however, its performance at Level 2 and Level 3 is very low (0.119 and 0.128 respectively).

This controller has different particularities. A parameter-varying proportional controller corrects the heading, in order to reduce the cross-track error (CR, following Fig. 9). The proportional gain varies according to the fuzzy rules, which take into account the cross-track error (gain-scheduling). Due to the lack of an integral part in the control law, it cannot regulate the cross-track error to zero in the steady state. In order to deal with the ocean currents, it requires a non-zero cross-track error. Therefore, in the final phase of the approach, a large proportional gain is required to increase

**FIGURE 22.** 3D representation of the geometrical analysis for the perfect measurements simulations.

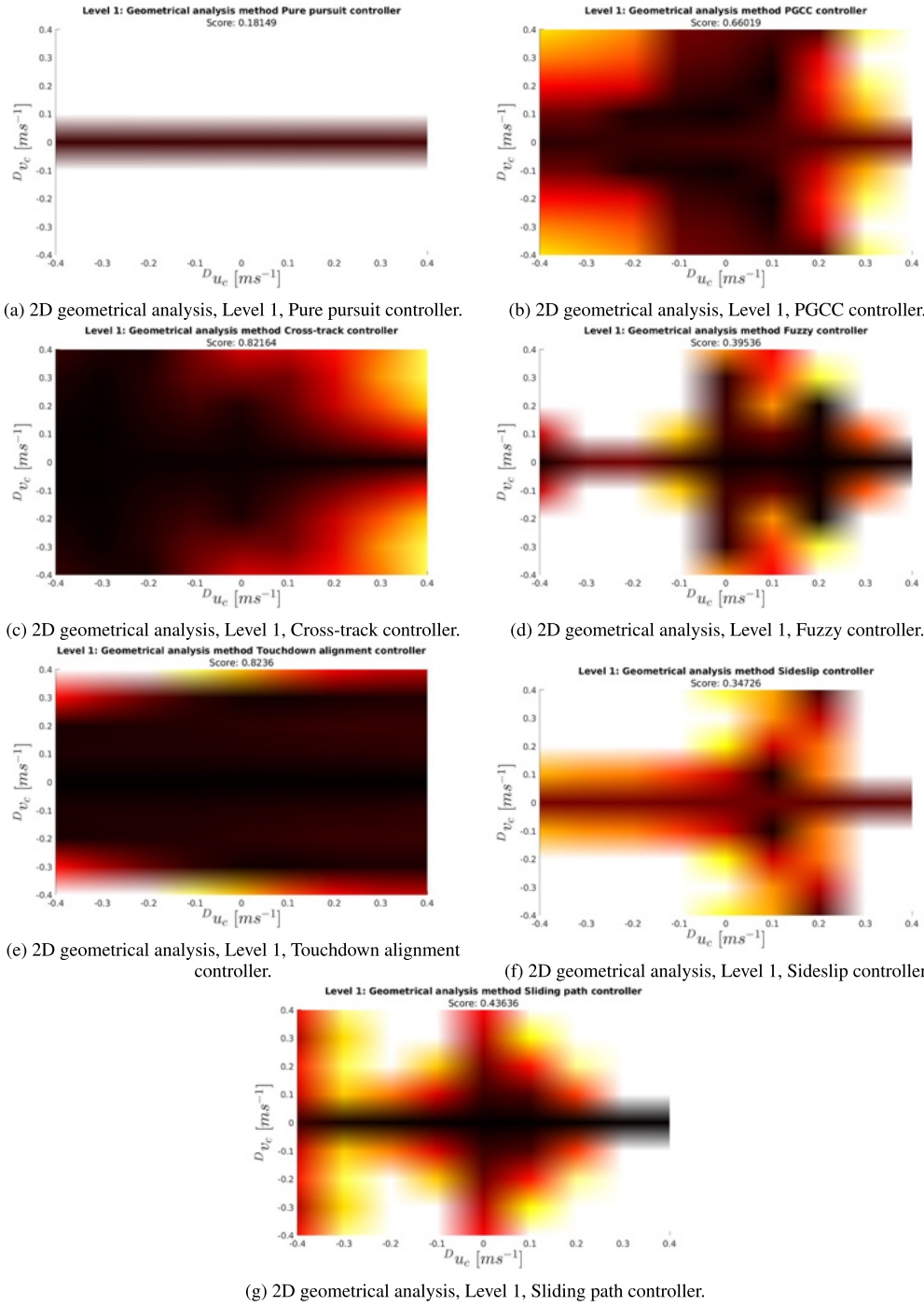


FIGURE 23. 2D representation of the geometrical analysis for the perfect measurements simulations. The value of \bar{g} is represented by the 'hot' color map, according to Fig. 19.

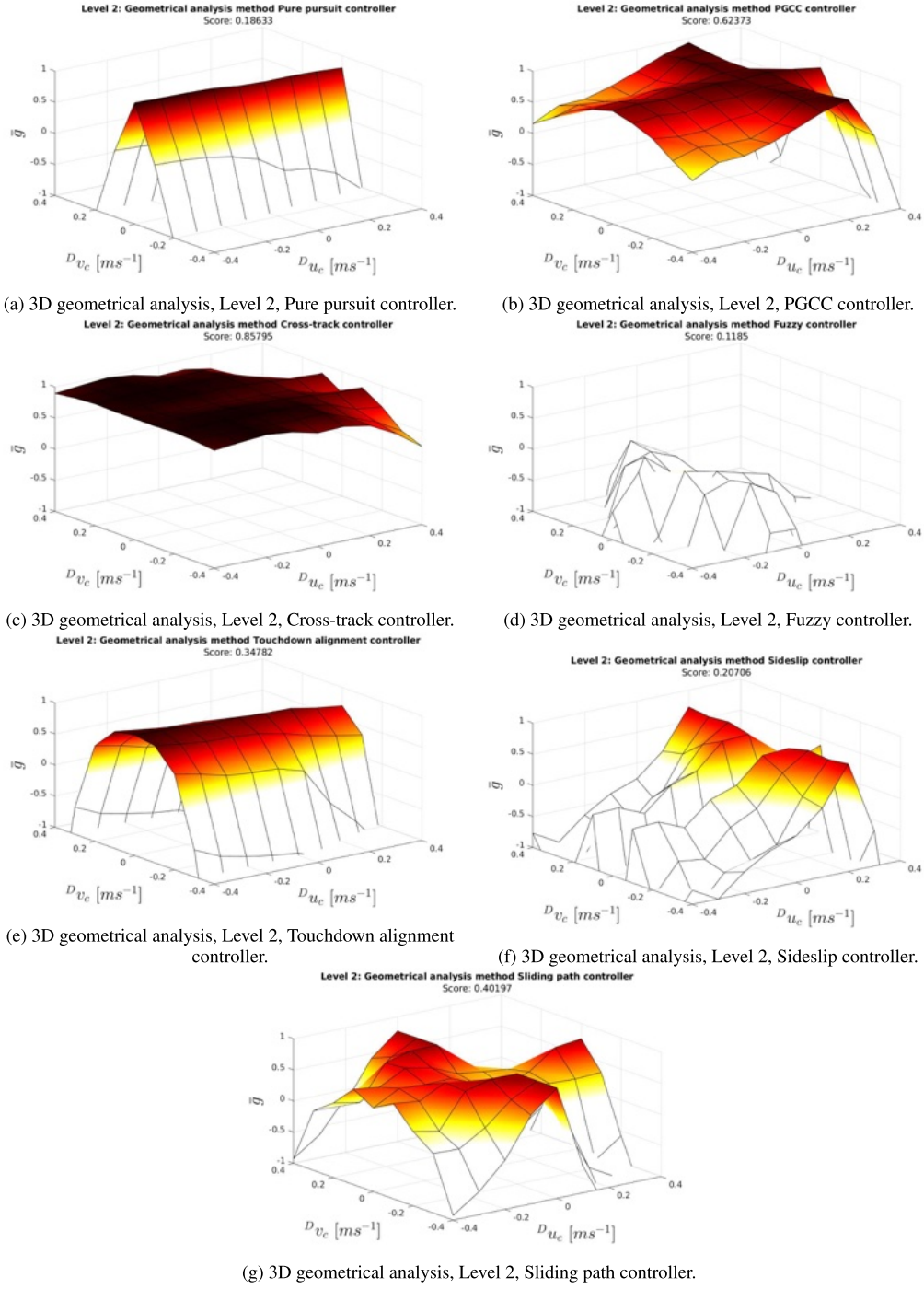


FIGURE 24. 3D representation of the geometrical analysis for the noisy measurements simulations with a docking velocity of 1 m/s.

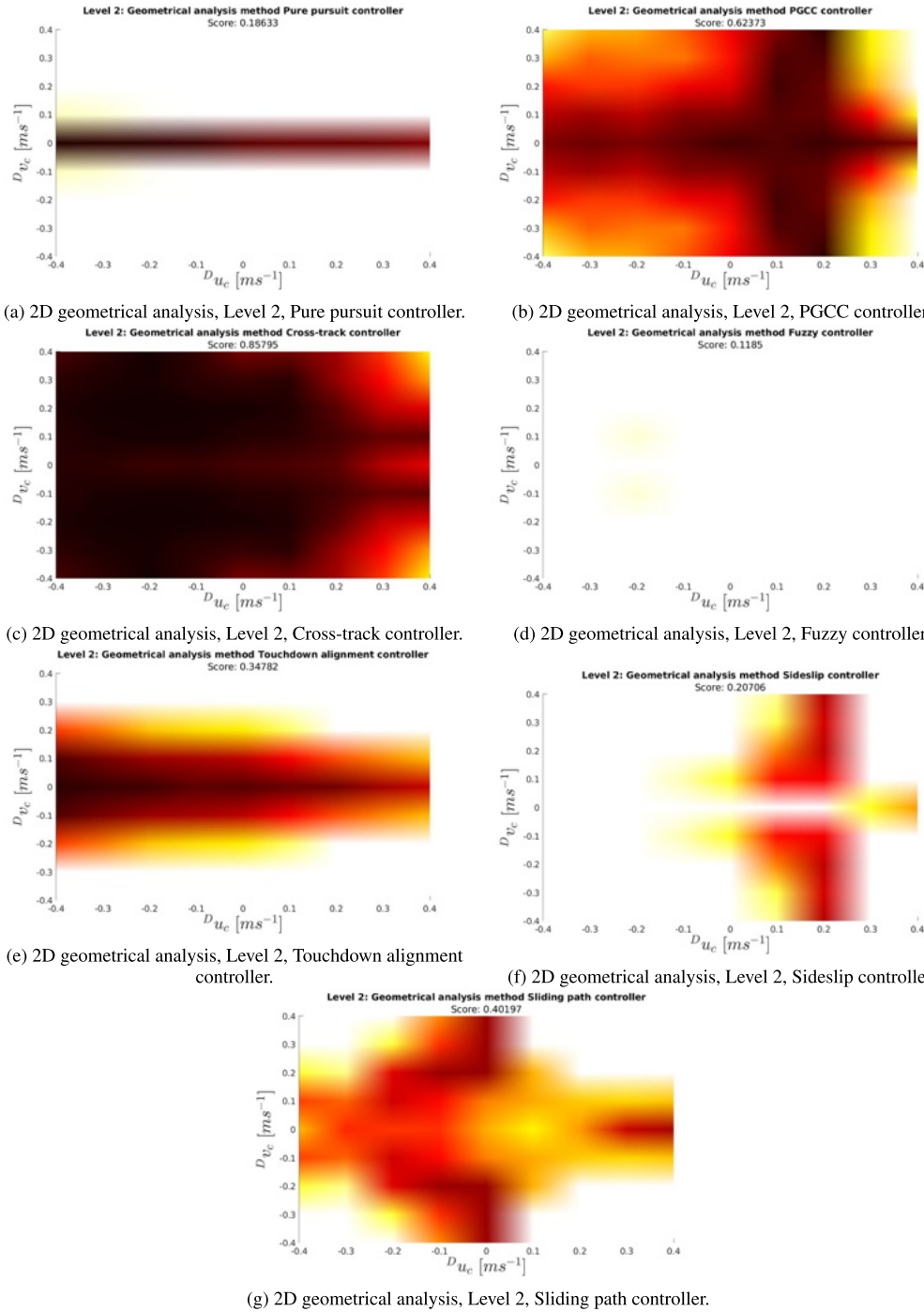


FIGURE 25. 2D representation of the geometrical analysis for the noisy measurements simulations with a docking velocity of 1 m/s. The value of \hat{g} is represented by the ‘hot’ color map, according to Fig. 19.

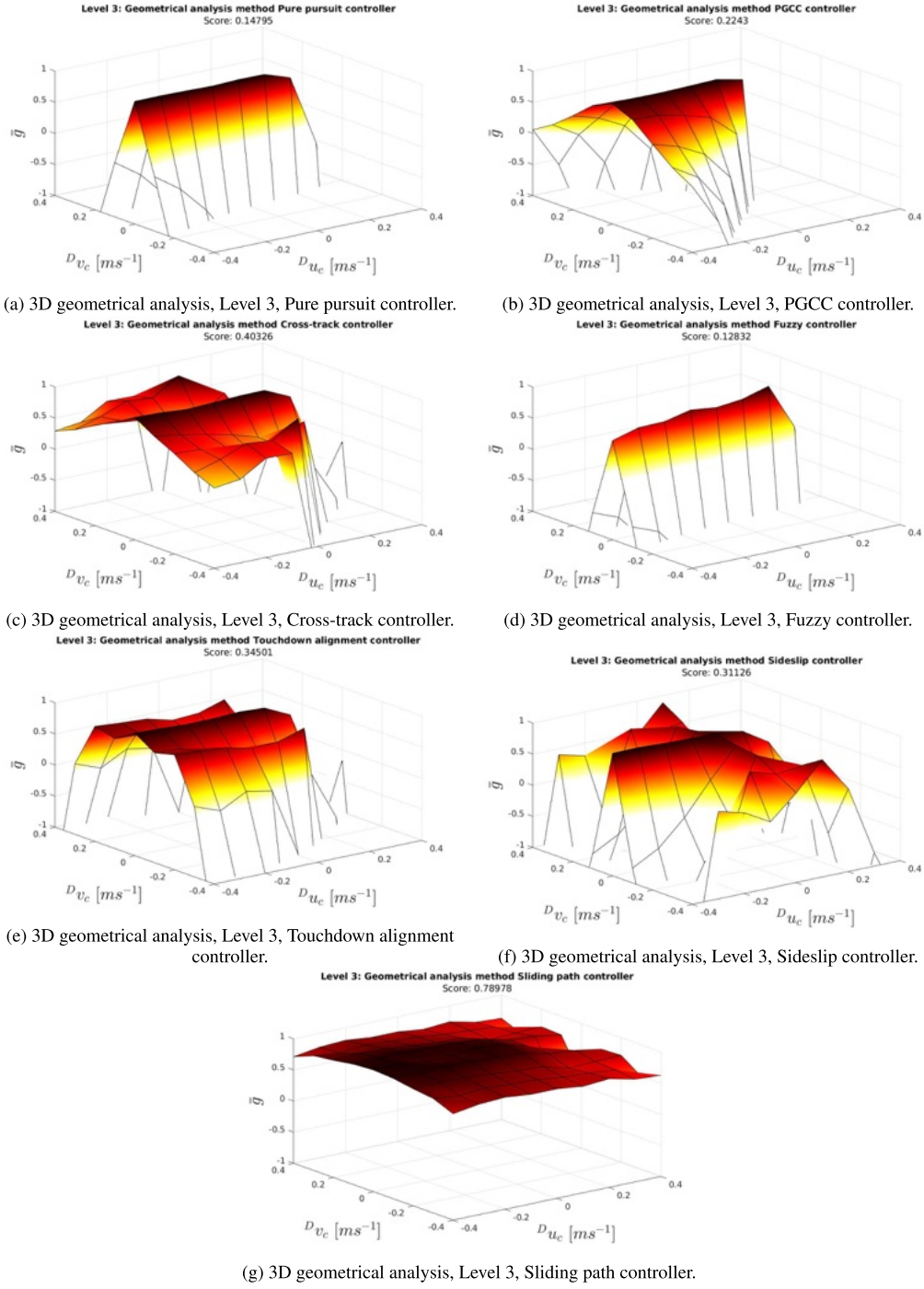


FIGURE 26. 3D representation of the geometrical analysis for the noisy measurements simulations with a docking velocity of 0.3 m/s.

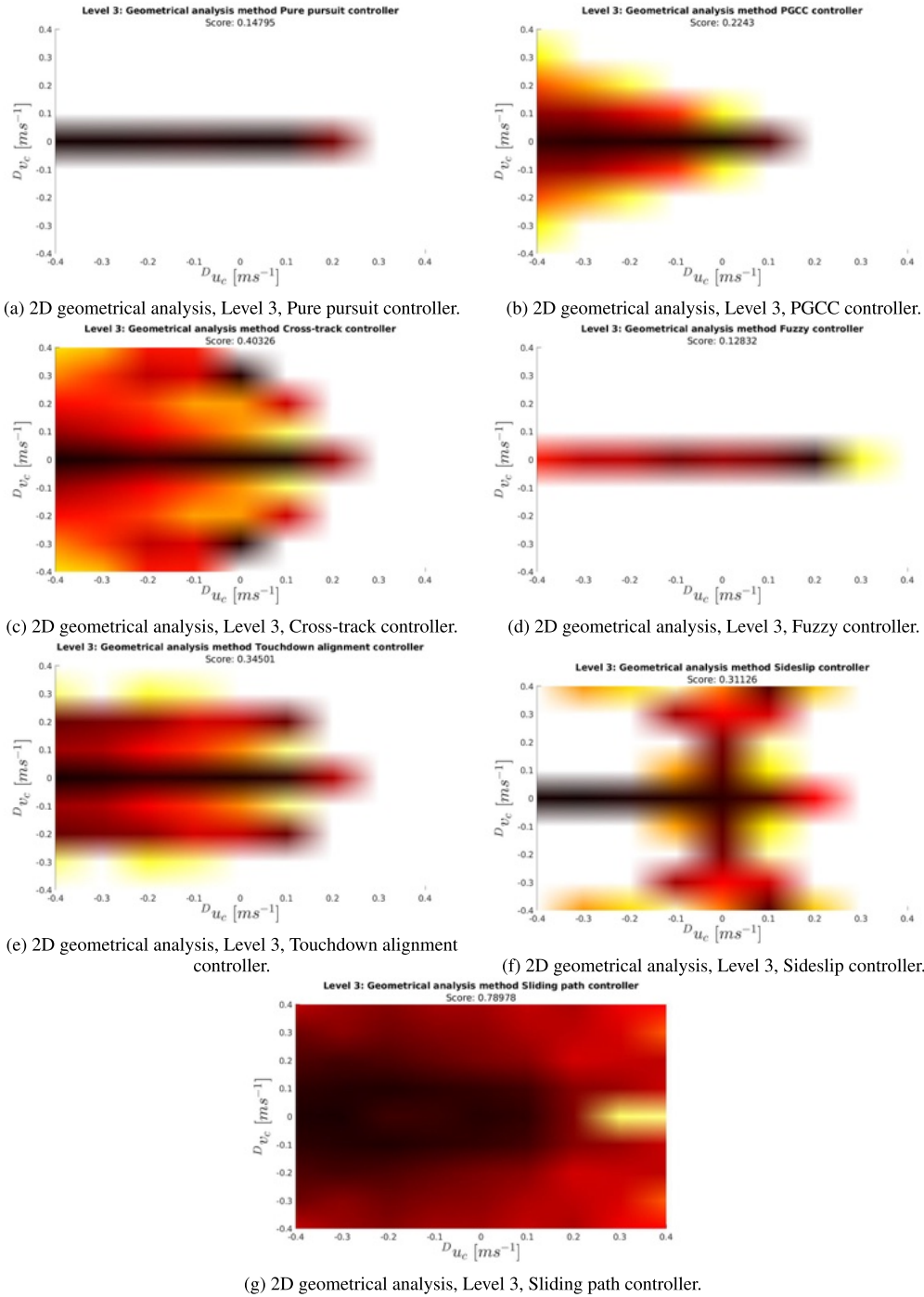


FIGURE 27. 2D representation of the geometrical analysis for the noisy measurements simulations with a docking velocity of 0.3 m/s. The value of \hat{g} is represented by the 'hot' color map, according to Fig. 19.

the sensitivity of the controller. For this reason, when the noise in the sensors' measurements is taken into account, the system is noticeably affected, failing to enter the DS in the majority of the cases at Level 2. If the parameters recommended by the original authors - gains according to Table 1 and membership functions according to Fig. 9 - are used, the score at Level 1 improves from 0.395 to 0.599, and the vehicle enters in practically all of the scenarios. However, when the noise in the DS localization is taken into account, the results do not show relevant improvements.

E. TOUCHDOWN ALIGNMENT CONTROLLER

The Touchdown alignment controller achieves excellent results at Level 1 (0.824) but only acceptable results at Levels 2 and 3 (0.348 and 0.345 respectively).

The Touchdown alignment controller is a cross-track controller with a final heading correction. In Level 1, where no noise is present in the localization of the DS, it achieves the best results (by adapting the heading), to enter in a smooth way. However, when the DS location is uncertain, it shows worse scores than the Cross-track controller. This results from the fact that the heading correction depends directly on the relative position between the AUV and the DS.

F. SIDESLIP CONTROLLER

The Sideslip controller achieves average results. At Level 1 it reaches a score of 0.347 (with especially good results in case of longitudinal ocean currents), at Level 2 its score is 0.207, while at Level 3 the algorithm scores 0.311.

This method tries to correct the heading of the AUV in a smooth way, during the final part of the path. The results show that it is significantly affected by the low level controllers of the Sparus II, not being able to accomplish the maneuver in several cases, and showing better results when the docking velocity is low. The control algorithm is also notably affected by the noisy localization of the DS, since the heading depends on it directly. This fact can be appreciated by comparing the scores between Level 1 and Level 2.

G. SLIDING PATH CONTROLLER

Using the parameters proposed in the original paper, the performance obtained with this method is acceptable at Level 1 and 2 (0.436 and 0.402 respectively), but surprisingly, it is excellent at Level 3 (0.790), where it performs best.

At high docking velocities (approximately 1 m/s) the sliding path controller exhibits good results for medium and low ocean currents, but not for high currents. Overall, the system appears robust to noisy sensor measurements. The observed errors come from the ILOS controller, which does not seem to have enough space to stabilize the vehicle within the sliding path section, in cases of fast ocean currents.

At Level 3, this method has the same problem as the PGCC controller and the Cross-track controllers, when the longitudinal ocean current velocity component is close to, or greater

than, the docking velocity. However, in this method the AUV follows a trajectory parallel to the center-line of the DS, rather than one coincident with it, and when the AUV reaches the sliding path section, the previous cross-track error is automatically eliminated. This happens due to the shape of the sliding path trajectory itself. This feature, coupled with the fact that at Level 3 the docking velocity is equal to 0.3 m/s, gives the vehicle more time to correct the final sliding path using the ILOS controller, making it work with all ocean current configurations at this level.

If the longitude of the sliding path is increased from 20 m (the distance used in the original paper) to 50 m, the score obtained at Level 1 increases up to 0.523, resulting in the AUV docking in practically all ocean current conditions. This improvement can be understood because the ILOS controller has more time to correct the position of the AUV, in the extreme cases.

VIII. CONCLUSION

This paper has compared seven docking methods in the presence of ocean currents, using the same setup: a funnel-shaped DS and a Sparus II AUV. These methods were selected after an exhaustive literature survey. They are: the Pure pursuit controller, the Pure Guidance with Current Compensation controller, the Cross-track controller, the Fuzzy controller, the Touchdown alignment controller, the Sideslip controller, and the Sliding path controller. Three scenarios have been simulated. In the first one (called Level 1), the controller knew the exact position of the DS and the ocean current velocity vector; also, the docking velocity was set to 1 m/s. In the second scenario (called Level 2), the controller used a realistic USBL model to estimate the position of the DS and a DVL model to estimate the ocean current velocity vector; the docking velocity was also set to 1 m/s. Finally, Level 3 was performed following the Level 2 conditions, but with a docking velocity of 0.3 m/s. Moreover, a new metric has been developed to be able to quantify the quality of the entrance of the AUV into the DS.

In the analysis of Level 1, it has been determined that the method that has the best performance is the Touchdown controller. This controller utilizes a Cross-track controller to minimize the cross-track error, correcting the effects of the ocean currents by applying a crab angle, and in the final moment it corrects the crab angle to dock in alignment with the DS.

At Level 2 the method that shows the best performance is the Cross-track controller.

At Level 3, the best performing method was the Sliding path controller. In this scenario, when the ocean current component parallel to the DS is directed towards it, and the current velocity is similar to the docking velocity, the AUV does not have the capacity to maintain the docking velocity, while effectively minimizing the cross-track error. The reason why the Sliding path controller outperforms the other methods is due to its final maneuver, where the AUV is able

to compensate for the cross-track error that occurred in the approaching path. This level reveals an interesting problem to study, that is, how to minimize the cross-track error when the ocean current is favourable and close to or larger than the docking velocity. In future work, a new algorithm will be developed and tested, to take into account the ocean currents that push a non-holonomic AUV towards the DS.

ABBREVIATIONS

AUV	Autonomous underwater vehicle
ROV	Remotely operated vehicle
DS	Docking station
USBL	Ultra short baseline
PGCC	Pursuit guidance with current compensation
PID	Proportional-integral-derivative controller
ILOS	Integral line of sight
SRG	Speed regulated guidance
COLA2	Component orientated layer-based architecture for autonomy
ROS	Robot operating system
IMU	Inertial measurement unit
DVL	Doppler velocity log
GPS	Global positioning system
POM	Polyoxymethylene
FFT	Fast Fourier transform
HIL	Hardware-in-the-loop
3D	Three dimensions
2D	Two dimensions

NOTATION

$\mathbf{D}\mathbf{P}_D = [{}^Dx_D \ {}^Dy_D \ {}^D\psi_D]^T$:	Docking station position in the $\{D\}$ frame (see Fig. 5)
$\mathbf{D}\boldsymbol{\eta} = [{}^Dx_B \ {}^Dy_B \ {}^D\psi_B]^T$:	AUV position in the $\{D\}$ frame (see Fig. 5)
$\mathbf{D}\mathbf{P}_p = [{}^Dx_p \ {}^Dy_p]^T$:	Point position in the $\{D\}$ frame
$\mathbf{D}\mathbf{P}_{cp2} = [{}^Dx_{cp2} \ {}^Dy_{cp2}]^T$:	Change point 2 position in the $\{D\}$ frame
Δx :	Distance in the x axis of the $\{D\}$ frame
Δy :	Distance in the y axis of the $\{D\}$ frame
u :	Surge velocity of the AUV
u_{dock} :	Surge velocity of the AUV set to dock
u_d :	Desired surge velocity of the AUV
${}^B u_{B,w}$:	Surge velocity of the AUV with respect to the water
$\mathbf{v}_c \in \mathbb{R}^2$:	Ocean current velocity
$\mathbf{D}\mathbf{v}_c = [{}^D u_c \ {}^D v_c]^T$:	Ocean current velocity in the $\{D\}$ frame
$\mathbf{B}\mathbf{v}_c = [{}^B u_c \ {}^B v_c]^T$:	Ocean current velocity in the $\{B\}$ frame

ψ_d :	Desired yaw angle of the AUV
ψ_{crab} :	Crab angle of the AUV to compensate the ocean currents
ψ_{nc} :	Heading angle of the AUV without ocean currents
e :	Distance error in the Cross-track controller
β :	Heading of the AUV when it starts the final maneuver
r_{max} :	Maximum yaw rate of the AUV
d :	Distance between the AUV and the DS in the x axis of the $\{D\}$ frame used in the Touchdown alignment controller
d_f :	Distance in the x axis of the $\{D\}$ frame where the touchdown maneuver starts
$d_{f,min}$:	Minimum distance in the x axis of the $\{D\}$ frame where the touchdown maneuver starts
ρ :	Distance between the AUV and the DS in the Sideslip controller
e_x :	Distance on the x axis of the $\{D\}$ frame between the AUV and the DS in the Sideslip controller
e_y :	Distance on the y axis of the $\{D\}$ frame between the AUV and the DS in the Sideslip controller
χ_s :	Angle between the AUV and the DS, see Fig. 11c
ρ_0 :	Distance between the AUV and the DS at the moment when the final maneuver starts in the Sideslip controller, see Fig. 11c
$e_{x,0}$:	Distance on the x axis of the $\{D\}$ frame between the AUV and the DS at the moment when the final maneuver starts in the Sideslip controller, see Fig. 11c
$e_{y,0}$:	Distance on the y axis of the $\{D\}$ frame between the AUV and the DS at the moment when the final maneuver starts in the Sideslip controller, see Fig. 11c
$\chi_{s,0}$:	Angle between the AUV and the DS in the moment when the final maneuver starts, see Fig. 11c
σ :	A gain
Δ :	Look-ahead distance
y_a :	Distance between the center-line and the approaching path in the Sliding path controller, see Fig. 12a

l :	Length of the sliding path
k_u :	A gain
ϕ_{dock} :	External diameter of the funnel of the DS
m_l :	Momentum lost on the entrance due to the collisions and friction between the AUV and the DS
m_T :	Change of momentum generated by the thrusters between the first and the second section, see Fig. 17
m_{s1} :	Momentum of the AUV when crossing the first section, see Fig. 17
m_{s2} :	Momentum of the AUV when crossing the second section, see Fig. 17
$ \vec{v}_1 $:	Velocity of the AUV when crossing the first section, see Fig. 17
$ \vec{v}_2 $:	Velocity of the AUV when crossing the second section, see Fig. 17
M :	Mass of the AUV
F_t :	Force that the thrusters are producing in one instance
t_1 :	Time when the AUV crosses the first section, see Fig. 17
t_2 :	Time when the AUV crosses the second section, see Fig. 17
α :	Heading of the AUV in the $\{D\}$ frame when it crosses the entrance section, see Fig. 18
α_o :	Optimal heading of the AUV in the $\{D\}$ frame when it crosses the entrance section, see Fig. 18
e_α :	Difference between α and α_o
w :	A weight
g :	Geometrical analysis value

REFERENCES

- [1] L. L. Whitcomb, "Underwater robotics: Out of the research laboratory and into the field," in *Proc. Millennium Conf., IEEE Int. Conf. Robot. Automat. Symposia*, vol. 1, Apr. 2000, pp. 709–716.
- [2] J. W. Nicholson and A. J. Healey, "The present state of autonomous underwater vehicle (AUV) applications and technologies," *Mar. Technol. Soc. J.*, vol. 47, no. 5, pp. 5–6, 2013.
- [3] D. Ribas, N. Palomeras, P. Ridao, M. Carreras, and A. Mallios, "Girona 500 AUV: From survey to intervention," *IEEE/ASME Trans. Mechatronics*, vol. 17, no. 1, pp. 46–53, Feb. 2012.
- [4] R. S. McEwen, B. W. Hobson, L. McBride, and J. G. Bellingham, "Docking control system for a 54-cm-Diameter (21-in) AUV," *IEEE J. Ocean. Eng.*, vol. 33, no. 4, pp. 550–562, Oct. 2008.
- [5] C. Yang, S. Peng, S. Fan, S. Zhang, P. Wang, and Y. Chen, "Study on docking guidance algorithm for hybrid underwater glider in currents," *Ocean Eng.*, vol. 125, pp. 170–181, Oct. 2016.
- [6] T. Kawasaki, T. Fukasawa, T. Noguchi, and M. Baino, "Development of AUV 'Marine Bird' with underwater docking and recharging system," in *Proc. 3rd Int. Workshop Sci. Use Submarine Cables Related Technol. (SSC)*, 2003, pp. 166–170.
- [7] H. Singh, J. G. Bellingham, F. Hover, S. Lemar, B. A. Moran, K. von der Heydt, and D. Yoerger, "Docking for an autonomous ocean sampling network," *IEEE J. Ocean. Eng.*, vol. 26, no. 4, pp. 498–514, Oct. 2001.
- [8] R. Stokey, B. Allen, T. Austin, R. Goldsborough, N. Forrester, M. Purcell, and C. von Alt, "Enabling technologies for REMUS docking: An integral component of an autonomous ocean-sampling network," *IEEE J. Ocean. Eng.*, vol. 26, no. 4, pp. 487–497, Oct. 2001.
- [9] M. D. Feezor, F. Y. Sorrell, P. R. Blankenship, and J. G. Bellingham, "Autonomous underwater vehicle homing/docking via electromagnetic guidance," *IEEE J. Ocean. Eng.*, vol. 26, no. 4, pp. 515–521, Oct. 2001.
- [10] T. Podder, M. Sibenac, and J. Bellingham, "AUV docking system for sustainable science missions," in *Proc. IEEE Int. Conf. Robot. Autom. (ICRA)*, Apr. 2004, pp. 4478–4485.
- [11] J. G. Bellingham, "Autonomous underwater vehicle docking," in *Springer Handbook of Ocean Engineering*. Cham, Switzerland: Springer, 2016, ch. 16, pp. 387–406.
- [12] A. M. Yazdani, K. Sammut, O. Yakimenko, and A. Lammas, "A survey of underwater docking guidance systems," *Robot. Auto. Syst.*, vol. 124, Feb. 2020, Art. no. 103382.
- [13] N. Palomeras, G. Vallicrosa, A. Mallios, J. Bosch, E. Vidal, N. Hurtos, M. Carreras, and P. Ridao, "AUV homing and docking for remote operations," *Ocean Eng.*, vol. 154, pp. 106–120, Apr. 2018.
- [14] P. Cieslak, "Stonefish: An advanced open-source simulation tool designed for marine robotics, with a ROS interface," in *Proc. OCEANS Marseille*, 2019, pp. 1–6.
- [15] J. C. Evans, K. M. Keller, J. S. Smith, P. Marty, and V. Rigaud, "Docking techniques and evaluation trials of the SWIMMER AUV: An autonomous deployment AUV for work-class ROVs," in *Proc. Oceans Conf. Rec. (IEEE)*, vol. 1, 2001, pp. 520–528.
- [16] J. Evans, P. Redmond, C. Plakas, K. Hamilton, and D. M. Lane, "Autonomous docking for Intervention-AUVs using sonar and video-based real-time 3D pose estimation," in *Proc. Oceans, Celebrating Past. Teaming Toward Future*, 2003, pp. 2201–2210.
- [17] T. Matsuda, T. Maki, K. Masuda, and T. Sakamaki, "Resident autonomous underwater vehicle: Underwater system for prolonged and continuous monitoring based at a seafloor station," *Robot. Auto. Syst.*, vol. 120, Oct. 2019, Art. no. 103231.
- [18] Z. Yan, D. Xu, T. Chen, J. Zhou, S. Wei, and Y. Wang, "Modeling, strategy and control of UUV for autonomous underwater docking recovery to moving platform," in *Proc. 36th Chin. Control Conf. (CCC)*, Jul. 2017, pp. 4807–4812.
- [19] G. D. Watt, A. R. Roy, J. Currie, C. B. Gillis, J. Giesbrecht, G. J. Heard, M. Birsan, M. L. Seto, J. A. Carretero, R. Dubay, and T. L. Jeans, "A concept for docking a UUV with a slowly moving submarine under waves," *IEEE J. Ocean. Eng.*, vol. 41, no. 2, pp. 471–498, Apr. 2016.
- [20] L. Brignone, M. Perrier, and C. Viala, "A fully autonomous docking strategy for intervention AUVs," in *Proc. OCEANS Eur.*, Jun. 2007, pp. 1–6.
- [21] S. Krupiński, F. Maurelli, G. Grenon, and Y. Petillot, "Investigation of autonomous docking strategies for robotic operation on intervention panels," in *Proc. OCEANS*, 2008, pp. 1–10.
- [22] J. Wallen and Z. Song, "Development of an adaptive docking station for resident underwater vehicles," in *Proc. OCEANS-Marseille*, Jun. 2019, pp. 1–7.
- [23] E. I. Sarda and M. R. Dhanak, "Launch and recovery of an autonomous underwater vehicle from a station-keeping unmanned surface vehicle," *IEEE J. Ocean. Eng.*, vol. 44, no. 2, pp. 290–299, Apr. 2019.
- [24] M. Wirtz, M. Hildebrandt, and C. Gaudig, "Design and test of a robust docking system for hovering AUVs," in *Proc. Oceans*, Oct. 2012, pp. 1–6.
- [25] P. W. Kimball, E. B. Clark, M. Scully, K. Richmond, C. Flesher, L. E. Lindzey, J. Harman, K. Huffstutler, J. Lawrence, S. Lelievre, J. Moor, B. Pease, V. Siegel, L. Winslow, D. R. Blankenship, P. Doran, S. Kim, B. E. Schmidt, and W. C. Stone, "The ARTEMIS under-ice AUV docking system," *J. Field Robot.*, vol. 35, no. 2, pp. 299–308, Mar. 2018.
- [26] Kawasaki Heavy Industries. *Close-Range Subsea Pipeline Inspection by Autonomous Underwater Vehicle (AUV)*. Accessed: Oct. 10, 2020. https://global.kawasaki.com/en/corp/newsroom/news/detail/?f=20200715_8265
- [27] T. Kawasaki, T. Noguchi, T. Fukasawa, S. Hayashi, Y. Shibata, T. Iimori, N. Okaya, K. Fukui, and M. Kinoshita, "'Marine Bird', a new experimental AUV—Results of docking and electric power supply tests in sea trials," in *Proc. Ocean MTS/IEEE Techno-Ocean, Bridges Across Oceans Conf.*, vol. 3, Nov. 2004, pp. 1738–1744.
- [28] B. R. Page and N. Mahmoudian, "AUV docking and recovery with USV: An experimental study," in *Proc. OCEANS-Marseille*, Jun. 2019, pp. 1–5.
- [29] A. Kukulya, A. Plueddemann, T. Austin, R. Stokey, M. Purcell, B. Allen, R. Littlefield, L. Freitag, P. Koski, E. Gallimore, J. Kemp, K. Newhall, and J. Pietro, "Under-ice operations with a REMUS-100 AUV in the arctic," in *Proc. IEEE/OES Auto. Underwater Vehicles*, Sep. 2010, pp. 1–8.
- [30] B. Allen, T. Austin, N. Forrester, R. Goldsborough, A. Kukulya, G. Packard, M. Purcell, and R. Stokey, "Autonomous docking demonstrations with enhanced REMUS technology," in *Proc. OCEANS*, Sep. 2006, pp. 1–6.
- [31] J.-Y. Park, B.-H. Jun, P.-M. Lee, J.-H. Oh, and Y.-K. Lim, "Underwater docking approach of an under-actuated AUV in the presence of constant ocean current," *IFAC Proc. Volumes*, vol. 43, no. 20, pp. 5–10, Sep. 2010.

- [32] K. Teo, E. An, and P.-P.-J. Beaujean, "A robust fuzzy autonomous underwater vehicle (AUV) docking approach for unknown current disturbances," *IEEE J. Ocean. Eng.*, vol. 37, no. 2, pp. 143–155, Apr. 2012.
- [33] J.-Y. Park, B.-H. Jun, K. Kim, P.-M. Lee, J.-H. Oh, and Y.-K. Lim, "Improvement of vision guided underwater docking for small AUV ISiML," in *Proc. OCEANS*, Oct. 2009, pp. 1–5.
- [34] A. Sans-Muntadas, K. Y. Pettersen, E. Brekke, and V. F. Henriksen, "A hybrid approach to underwater docking of AUVs with cross-current," in *Proc. OCEANS MTS/IEEE Monterey*, Sep. 2016, pp. 1–7.
- [35] N. Palomeras, A. El-Fakdi, M. Carreras, and P. Ridao, "COLA2: A control architecture for AUVs," *IEEE J. Ocean. Eng.*, vol. 37, no. 4, pp. 695–716, Oct. 2012.
- [36] R. C. Craig, "Implementation of the pure pursuit path tracking algorithm," Tech. Rep. [Online]. Available: <https://apps.dtic.mil/sti/citations/ADA255524>
- [37] N. Hurtos, A. Mallios, N. Palomeras, J. Bosch, G. Valllicosa, E. Vidal, D. Ribas, N. Gracias, M. Carreras, and P. Ridao, "LOON-DOCK: AUV homing and docking for high-bandwidth data transmission," in *Proc. OCEANS Aberdeen*, Jun. 2017, pp. 1–7.
- [38] J.-Y. Park, B.-H. Jun, P.-M. Lee, Y.-K. Lim, and J.-H. Oh, "Docking problem and guidance laws considering drift for an underactuated AUV," in *Proc. OCEANS IEEE-Spain*, Jun. 2011, pp. 1–7.
- [39] B. W. Hobson, R. S. McEwen, J. Erickson, T. Hoover, L. McBride, F. Shane, and J. G. Bellingham, "The development and ocean testing of an AUV docking station for a 21' AUV," in *Proc. OCEANS*, Sep. 2007, pp. 1–6.
- [40] T. I. Fossen, "Marine control systems," *J. Guid. Control Dyn.*, vol. 28, no. 9, pp. 1689–1699, 2002.
- [41] K. Teo, B. Goh, and O. K. Chai, "Fuzzy docking guidance using augmented navigation system on an AUV," *IEEE J. Ocean. Eng.*, vol. 40, no. 2, pp. 349–361, Apr. 2015.
- [42] W. Caharija, K. Y. Pettersen, M. Bibuli, P. Calado, E. Zereik, J. Braga, J. T. Gravdahl, A. J. Sorensen, M. Milovanovic, and G. Bruzzone, "Integral line-of-sight guidance and control of underactuated marine vehicles: Theory, simulations, and experiments," *IEEE Trans. Control Syst. Technol.*, vol. 24, no. 5, pp. 1623–1642, Sep. 2016.
- [43] M. Carreras, C. Candela, D. Ribas, A. Mallios, L. L. Magí, E. Vidal, N. Palomeras, and P. Ridao, "Sparus II, design of a lightweight hovering AUV," in *Proc. 5th Int. Workshop Marine Technol. (Martech)*, 2013, pp. 152–155.
- [44] M. Carreras, J. D. Hernandez, E. Vidal, N. Palomeras, D. Ribas, and P. Ridao, "Sparus II AUV—A hovering vehicle for seabed inspection," *IEEE J. Ocean. Eng.*, vol. 43, no. 2, pp. 344–355, Apr. 2018.
- [45] M. Quigley, B. Gerkey, K. Conley, J. Faust, T. Foote, J. Leibs, E. Berger, R. Wheeler, and A. Ng, "ROS: An open-source robot operating system," in *Proc. ICRA Workshop Open Source Softw.*, 2009.
- [46] J. Tong, X. Xu, L. Hou, Y. Li, J. Wang, and L. Zhang, "An ultra-short baseline positioning model based on rotating array & reusing elements and its error analysis," *Sensors*, vol. 19, no. 20, p. 4373, Oct. 2019.



PATRYK CIEŚLAŁK was born in Krakow, Poland, in 1986. He received the Ph.D. degree from the Department of Robotics and Mechatronics, AGH University of Science and Technology, Kraków, in 2016. During his Ph.D. studies, he was involved in several projects focused around mechatronic design and control design in mobile robotics and manipulator systems. In his Ph.D. thesis, he tackled a difficult problem of designing a new balancing mono-wheel robot, from the mechanical

structure, through model-based control, and to the software and firmware architecture. Since 2017, he has been working with the Underwater Vision and Robotics Lab (CIRS), University of Girona, Spain. He is currently a Postdoctoral Researcher with the Computer Vision and Robotics Research Institute (VICOROB), University of Girona. He started his work at CIRS as a Marie Skłodowska-Curie Postdoctoral Fellow, after being awarded a grant for a project aimed at developing control algorithms to enable compliant control for an I-AUV performing an autonomous non-destructive testing operation. During this project, he visited Heriot-Watt University, Edinburgh, U.K., where he worked at the Ocean Systems Laboratory (OSL), for a period of two months. After the successful completion of the grant-supported project, he continued his research in underwater manipulation, tackling tasks related to obstacle avoidance, motion planning, and cooperative manipulation utilising two I-AUVs. He is continuing his research at CIRS, working on underwater intervention for inspection, maintenance, and repair (IMR) operations in offshore wind farms. He is the coauthor of a commercial rehabilitation robot called Prodrobot, which is a stationary lower limbs exoskeleton, used in the learning and improvement of natural gait patterns in children. He is the author of an advanced open-source robot simulator called Stonefish, designed for marine robotics, which simulator is currently used in all underwater related research at CIRS, other institutions around the world, and can be found on Github.



NARCÍS PALOMERAS (Member, IEEE) was born in Vilafant, Spain, in 1981. He received the Ph.D. degree from the University of Girona, Spain, in 2011. He is currently a Postdoctoral Researcher with the Computer Vision and Robotics Research Institute (VICOROB), University of Girona. He is the Coordinator of a Joint Degree Erasmus Mundus on Intelligent Field Robotic Systems. He has participated in several research projects, all related to underwater robotics, both national

and European, including TRIDENT, PANDORA, MORPH, MERBOTS, LOONDOCK, TWINBOT, 3DAUV, and ATLANTIS, as well as in different European competitions for AUVs, such as SAUC-E and ERL. His research interests include underwater robotics in topics, like planning, exploration, intelligent control architectures, mission control, and localization.



PERE RIDAO (Member, IEEE) was born in Girona, Spain, in 1969. He received the Ph.D. degree in industrial engineering from the University of Girona, Spain, in 2001. He has directed nine Ph.D. theses (with four more currently under direction) and 14 M.S. theses. He is currently the Director of the Computer Vision and Robotics Research Institute (VICOROB), the Head of the Underwater Robotics Research Center (CIRS), and an Associate Professor with the Department of Computer Engineering, University of Girona. He is the coauthor of four licenses and one Spanish/European patent and the author of more than 100 publications. He is a co-founder of Iqua Robotics S.L.—a spin-off company. Since 1997, he has been participating in 24 research projects (15 European and nine National). His research interests include designing and developing autonomous underwater vehicles for 3-D mapping and intervention. He has served as the Chair for the IFAC's Technical Committee on Marine Systems.



JOAN ESTEBA was born in Girona, Spain, in 1994. He received the bachelor's degree in industrial technologies engineering and the M.Sc. degree in industrial engineering from the University of Girona (UdG), in 2016 and 2018, respectively, where he is currently pursuing the Ph.D. degree with the Computer Vision and Robotics Research Institute (VICOROB). He has been working for several years developing vision and robotic technologies in the automobile industry

and leading different projects. He has been leading some development projects in the food industry. He is a Registered Professional Engineer in Catalonia. His research interest includes docking systems for autonomous underwater robotic systems.

3

DEVELOPMENT OF THE DOCKING STRATEGY

IN this chapter a novel controller for a non-holonomic **AUV** with two horizontal thrusters, focused on the docking maneuver in a funnel-shaped **DS** is presented. Demonstrating it theoretically, and simulating it in the same framework where the rest of the algorithms were compared in the previous chapter. Obtaining a solution for the needs of the Sparus II **AUV**.

Title: Managed Surge Controller : A Docking Algorithm for a Non-Holonomic AUV (Sparus II)
in the Presence of Ocean Currents for a Funnel-Shaped Docking Station

Authors: **Joan Esteba**, Patryk Cieslak, Narcís Palomeras, and Pere Ridao

Journal: Sensors

Volume: 23, Published: 2023

DOI: [10.3390/s23010241](https://doi.org/10.3390/s23010241)

Quality index: JCR2021 Engineering, Electrical & Electronic, Impact Factor: 3.847, Q2 (92/276)



Article

Managed Surge Controller: a Docking algorithm for a Non-holonomic AUV (Sparus II) in the Presence of Ocean Currents for a funnel-shaped Docking Station

Joan Esteba *, Patryk Cieślak , Narcís Palomeras , and Pere Ridao

Computer Vision and Robotics Research Institute (VICOROB), University of Girona, 17003 Girona, Spain.

* Corresponding author: Joan Esteba (joan.esteba@udg.edu).

† This work has been developed in the context of the ATLANTIS "The Atlantic Testing Platform for Maritime Robotics: New Frontiers for Inspection and Maintenance of Offshore Energy Infrastructures" project. Founded from the European Union's Horizon 2020 research and innovation programme, under the Grant Agreement number 871571.

Abstract: This paper presents a novel algorithm to dock a non-holonomic Autonomous Underwater Vehicle (**AUV**) into a funnel-shaped Docking Station (**DS**), in the presence of ocean currents. In a previous work, the authors have compared several docking algorithms through Monte Carlo simulations. In this paper, a new control algorithm is presented with a goal to improve over the previous ones to fulfil the specific needs of the ATLANTIS project. Performance of the new proposed algorithm has been compared with the results of the previous study, using the same environment on the Stonefish hardware-in-the-loop simulator.

Keywords: Docking, AUV, ocean currents, non-holonomic



Citation: Esteba, J.; Cieślak, P.; Palomeras, N.; Ridao, P. Esteba, J.; Cieślak, P.; Palomeras, N.; Ridao, P. Managed Surge Controller: a Docking algorithm for a Non-holonomic AUV (Sparus II) in Presence of Ocean Currents for a funnel-shaped Docking Station. *Sensors* **2022**, *1*, 0. <https://doi.org/>

Received:

Accepted:

Published:

Publisher's Note: MDPI stays neutral with regard to jurisdictional claims in published maps and institutional affiliations.



Copyright: © 2022 by the authors. Licensee MDPI, Basel, Switzerland. This article is an open access article distributed under the terms and conditions of the Creative Commons Attribution (CC BY) license (<https://creativecommons.org/licenses/by/4.0/>).

1. Introduction

The **AUV** technologies presented a significant improvement during the last years. Several autonomous missions were developed in the field [1,2]. Nowadays, the common operating procedure of the **AUVs** is to deploy them (usually with a ship), develop the mission, and, finally, recover; in most of the cases during the same operational day. The natural next development for the consolidation of this technology is the creation of **DSs**, which can allow the **AUVs** to extend the operational time in the field. The **DS** have to offer protection, high-bandwidth communication channels, and the capacity to recharge the vehicle's batteries. In the literature, several examples of **DS** systems can be found [3–8]. Each **DS** concept was tailored to a specific **AUV** and used own perception and docking strategies. Several descriptive surveys about docking can be already found in the literature: [9–11].

Previously, the team from the University of Girona developed a prototype of funnel-shape **DS** that relied on an acoustic transponder and light beacons, in order to localize it from the vehicle [12]. The conclusions of that experiments have shown the need of developing a controller that considers the ocean currents. Moreover, in turbid water scenarios, the vision system was not appropriate. In the ATLANTIS project [13], one of the technologies that must be demonstrated is the semi-permanent deployment of the Sparus II **AUV**, using a docking station on the seabed. With this motivation, the authors have developed the following study.

In a previous publication [14], several algorithms have been studied to cope with the autonomous docking, using a non-holonomic **AUV**, in the presence of ocean currents: the Pursuit Guidance with current compensation controller presented by [4,15], the Cross-track controller used in [3,16], the Fuzzy controller used in [17,18], the Touchdown alignment controller described in [19], the Sideslip controller based on [20], and the Sliding path

controller described in [21]. None of the studied solutions offers a satisfactory behavior when dealing with ocean current velocities higher than the docking velocity. Thus a proposal of a novel control algorithm is presented in this work.

The paper is organized as follows: Section 2 presents the novel algorithm. Section 3 presents the experimental setup used in order to test the algorithm. Section 4 analyses the performance of the algorithm in different scenarios. Obtained results and the comparison with the other methods are presented in Section 5, discussed in Section 6, and finally, the conclusions are drawn in Section 7.

2. Proposal: Managed surge controller

This section presents the novel method to deal with the ocean currents controlling a non-holonomic AUV. The proposed method is called Managed Surge Controller (**MSC**).

2.1. Assumptions

2.1.1. Assumption 1

We assume that the **AUV** motion is described using two degrees of freedom: surge and yaw. This is a consequence of the commonly adopted strategy of neglecting sway for under-actuated vehicles, maneuvering at low speed.

2.1.2. Assumption 2

The inner loop controllers can track the desired surge velocity (u_d) and the desired yaw (ψ_d) with good accuracy.

2.1.3. Assumption 3

The velocity of the ocean currents is constant, irrotational, and bounded.

2.1.4. Assumption 4

The vehicle can measure its surge velocity, yaw angle, and the ocean current velocity.

2.1.5. Assumption 5

The vehicle can measure its relative position with respect to the **DS**.

2.2. Concepts

Inspired by the analysis done in [14], the present method improves the results obtained with the previously studied methods because it can deal with ocean currents, the velocity of which are larger than the velocity of docking of the **AUV**.

Fig. 1 presents the basic variables involved in the process. Two different reference frames are presented, the $\{D\}$ frame located at the position of the **DS**, and the $\{B\}$ frame attached to the **AUV** body. The velocity in the $\{D\}$ frame are with respect to the ground symbolised by \dot{x} and \dot{y} , and the velocities in the $\{B\}$ frame are with respect to the water represented by u and v .

Fig. 2 shows the velocities involved in the controller: 1) the ground speed ($D\dot{\eta}_{1B} = [\dot{x} \dot{y}]^T$), and 2) the through water velocity ($Bv_{1B} = [u v]^T$). Finally, the ocean current vector ($D\dot{\eta}_c = [\dot{x}_c \dot{y}_c]^T$) as well as the desired docking velocity ($D\dot{\eta}_{1D} = [\dot{x}_D 0]^T$) are represented in the inertial $\{D\}$ frame.

2.2.1. Model of the system

The kinematic system is represented by the following equations, recall Fig. 1 and Fig. 2:

$$D\dot{\eta}_{1B} = D\dot{R}_B \cdot Dv_{1B} + D\dot{\eta}_c \quad (1)$$

$$\begin{bmatrix} \dot{x} \\ \dot{y} \end{bmatrix} = \begin{bmatrix} \cos(\psi) & -\sin(\psi) \\ \sin(\psi) & \cos(\psi) \end{bmatrix} \cdot \begin{bmatrix} u \\ v \end{bmatrix} + \begin{bmatrix} \dot{x}_c \\ \dot{y}_c \end{bmatrix} \quad (2)$$

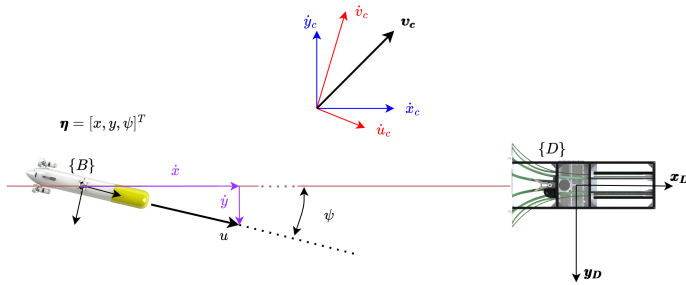


Figure 1: Geometrical representation of basic variables. Two different reference frames are presented, the $\{D\}$ frame located at the position of the DS, and the $\{B\}$ frame attached to the AUV body. The velocity in the $\{D\}$ frame are with respect to the ground symbolised by \dot{x} and \dot{y} , and the velocities in the $\{B\}$ frame are with respect to the water represented by u and v .

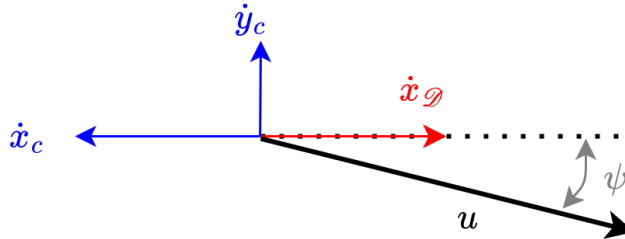


Figure 2: Geometrical representation of basic velocities.

which, assuming a negligible sway velocity (*Assumption 1*), simplifies to:

$$\dot{x} = u \cos(\psi) + \dot{x}_c, \quad (3)$$

$$\dot{y} = u \sin(\psi) + \dot{y}_c. \quad (4)$$

2.2.2. Docking scenarios

According to Fig. 3, three docking scenarios can be defined, depending on the robot ($D\mathbf{v}_1$), current ($D\mathbf{v}_c$) and docking ($D\mathbf{v}_{1D}$) velocities in the x_D axis:

- Scenario A ($\dot{x}_c \leq 0$): The current opposes to the robot speed. Therefore, a higher through water robot speed is required to achieve the desired inertial docking velocity.
- Scenario B ($\dot{x}_c > 0$ and $\dot{x}_c < \dot{x}_{1D}$): The current speed, being smaller than the desired docking velocity, adds to the through water robot velocity to achieve the inertial docking speed.
- Scenario C ($\dot{x}_c \geq \dot{x}_{1D}$): A current speed higher than the docking velocity, requires a backward through-water robot velocity to achieve the desired inertial docking velocity.

In scenarios A and B the surge velocity will normally be positive and the AUV heading will be opposite to \dot{y}_c . In contrast, in scenario C, the surge velocity will normally be negative and the heading will be in the direction of \dot{y}_c .

2.2.3. Crab angle

To be able to compensate the lateral ocean current (\dot{y}_c) with a non-holonomic AUV it is necessary to use a crab angle (ψ_c). This crab angle has the goal of aligning the robot to the axis of the DS ($\dot{y} = 0$), while keeping the desired docking velocity ($D\dot{\eta}_{1D}$). Therefore (2) can be rewritten as:

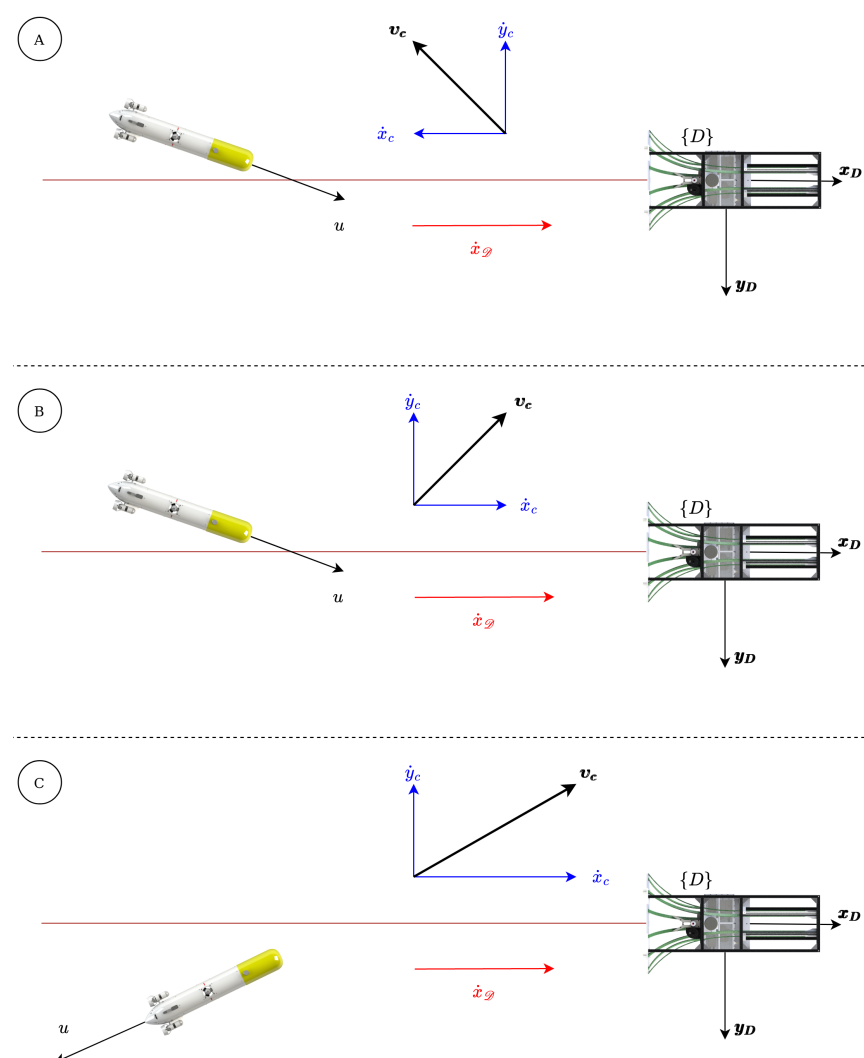


Figure 3: Possible docking scenarios.

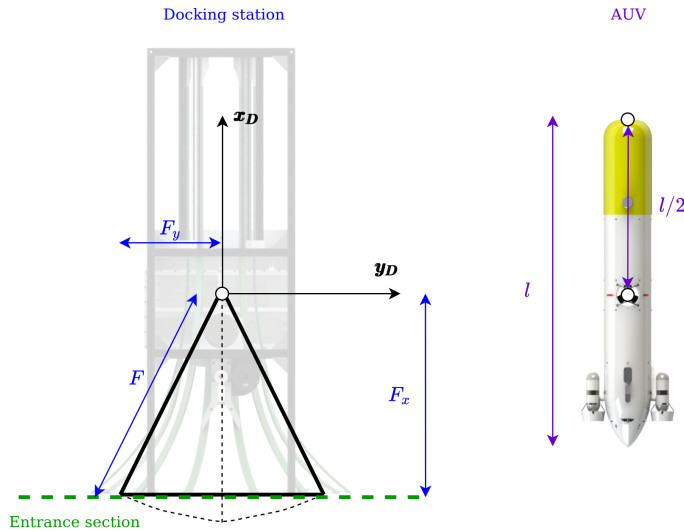


Figure 4: Geometrical problem simplification.

$$\begin{bmatrix} \dot{x}_c \\ 0 \end{bmatrix} = \begin{bmatrix} \cos(\psi_c) & -\sin(\psi_c) \\ \sin(\psi_c) & \cos(\psi_c) \end{bmatrix} \begin{bmatrix} u \\ 0 \end{bmatrix} + \begin{bmatrix} \dot{x}_c \\ \dot{y}_c \end{bmatrix}. \quad (5)$$

Solving the system, the crab angle can be expressed as:

$$\tan(\psi_c) = \frac{-\dot{y}_c}{\dot{x}_c - \dot{x}_c}, \quad (6)$$

assuming $\dot{x}_c - \dot{x}_c \neq 0$.

2.2.4. Entrance problem

The problem of making a torpedo-shaped AUV enter a funnel-shaped DS can be modeled with the simplification that the DS is represented by an isosceles triangle and the AUV by a straight line directed along its main axis (see Fig. 4).

If the symmetry of the system is taken into account, there are only three successful docking scenarios (Fig. 5):

- Scenario I: It represents the ideal entrance, where the AUV enters in a straight line with the same heading as the DS and aligned with its origin DS.
- Scenario II: The robot heading is not aligned to the x_D axis, but misaligned to the right.
- Scenario III: The robot heading is not aligned to the x_D axis, but misaligned to the left.

In Scenario II and III, the AUV completes the docking thanks to the geometrical properties of the system. Both scenarios differ in the energy lost during the collision, being Scenario III the one with the highest losses. Following the analysis of energy lost during the collision (reported in [14]), the AUV should try to perform Scenario I if possible, targeting Scenario II alternatively, and using Scenario III as the last resort. It is worth noting that Scenario I is not easy to perform with Sparus II AUV, in presence of ocean currents, due to its non-holonomic nature.

2.2.5. Path

A crab angle is needed to compensate for the ocean currents, therefore the method creates a path parallel to the DS axis at an appropriate distance from it, to take advantage of the torpedo-like shape of the AUV and the funnel-shaped DS, see Fig. 6. The path is

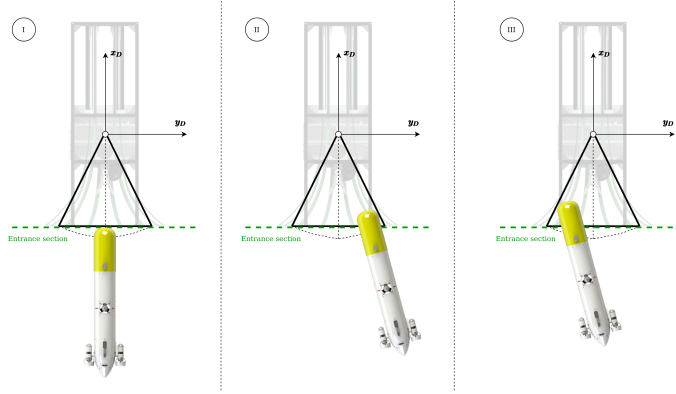


Figure 5: Successful entrance scenarios.

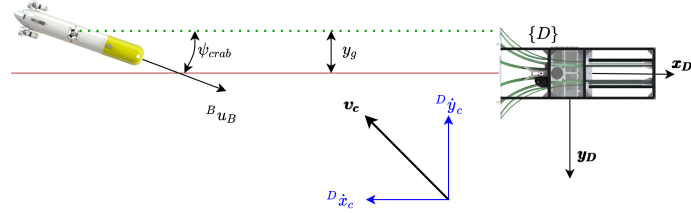


Figure 6: Path concept representation.

created calculating a gap (y_g), with respect to the axis of the DS using the crab angle, the DS and the AUV geometry. In order to calculate this gap, let us consider the geometry of the problem when the AUV reaches the DS in scenarios II and III (Fig. 7). For the entrance in Scenario II, the gap can be calculated as:

$$y_{g,II} = (F + l/2) \sin(-\psi_c). \quad (7)$$

The maximum crab angle admissible to enter to the DS in Scenario II is computed using the simplified funnel shape:

$$\psi_{c,II} = \tan(F_y/F_x), \quad (8)$$

This allows to calculate the maximum gap as:

$$y_g = (F + l/2) \sin(\tan(F_y/F_x)). \quad (9)$$

For crab angles larger than $\psi_{c,II}$ the system needs to perform the entrance Scenario III. The maximum crab angle for the entrance Scenario III, in case of $2F_y < l/2$ (that fulfils the mechanic characteristics of the system presented), can be calculated as (see Fig. 8, and recall Fig. 5):

$$\psi_{c,III} = \frac{\pi}{2} - \tan(F_y/F_x), \quad (10)$$

in order to guarantee that the AUV does not hit a disfavoured part of the DS. In this case the $y_{g,III}$ is fixed to be equal to $F_y/2$, remind Fig. 7. In summary, (11) sets the value of y_g for all the cases as:

$$y_g = \begin{cases} -(F + l/2) \sin(\psi_c), & -\psi_{c,II} \leq \psi_c \leq \psi_{c,II} \\ -\text{sign}(\psi_c) F_y/2, & |\psi_c| > \psi_{c,II}. \end{cases} \quad (11)$$

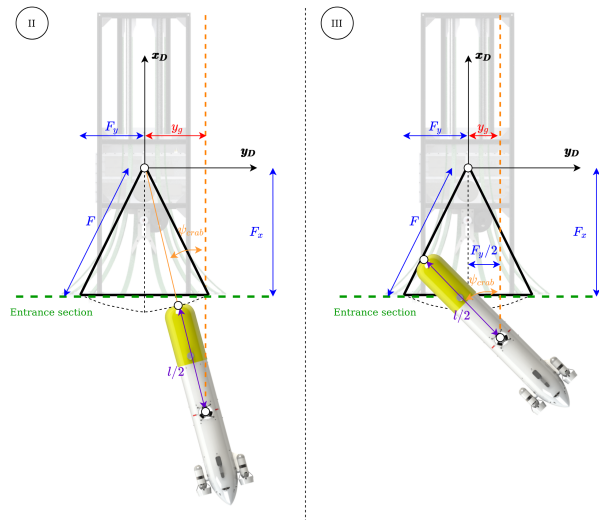


Figure 7: Gap calculus concept.

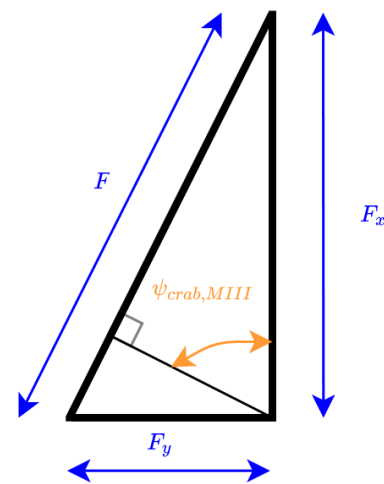


Figure 8: Maximum entrance Scenario III gap calculus concept.

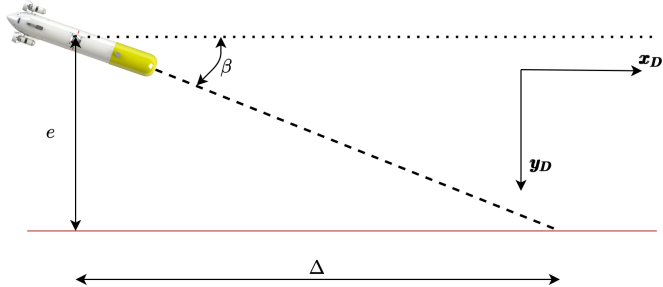


Figure 9: Beta concept representation.

2.2.6. Path following

The Sparus II AUV has direct control over the surge velocity (i.e., u) as well as over the heading (i.e., ψ). Let the cross-track path error be defined as:

$$e = y - y_g \quad (12)$$

With this notation, the objectives of the path following controller are to achieve:

$$\lim_{t \rightarrow \infty} e(t) = 0 \quad (13)$$

$$\lim_{t \rightarrow \infty} \psi_d(t) = \psi_c \quad (14)$$

$$\lim_{t \rightarrow \infty} u_d(t) = \frac{\dot{x}_g - \dot{x}_c}{\cos(\psi_c)}, \quad (15)$$

2.3. Control law

The control law regulates the desired heading (ψ_d) and the desired surge (u_d). The desired heading is defined as:

$$\psi_d = \psi_c + \beta, \quad (16)$$

where β is a correction term depending on the look-ahead distance (Δ) and the cross-track error (e), see Fig. 9:

$$\tan(\beta) = -\frac{e}{\Delta}, \quad (17)$$

where Δ is defined by a constant value ($k_\Delta > 0$) and a sign criteria (21):

$$\Delta = \frac{k_\Delta}{\text{sign}(\dot{x}_{ss})}, \quad (18)$$

being \dot{x}_{ss} the through water velocities of the AUV in the steady state in the $\{D\}$ frame (i.e., when e is zero). The desired surge velocity is given by:

$$u_d = \frac{\dot{x}_{ss}}{\cos(\psi)} - c, \quad (19)$$

where c is a correction term, introduced to adjust the response of the system:

$$c = k_1 \text{atan}(k_2 e) \text{ sign}(\psi); k_1, k_2 > 0 \quad (20)$$

The correction modifies the basic velocity representation from Fig. 2 into the one shown in Fig. 10. The steady state inertial velocities can be calculated as:

$$\dot{x}_{ss} = \dot{x} - \dot{x}_c, \quad (21)$$

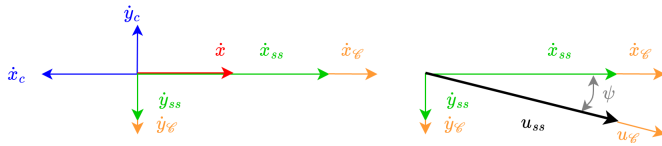


Figure 10: Geometrical representation of corrected velocities. Here, \dot{x}_{ss} , and \dot{y}_{ss} are through water velocities of the AUV in the steady state in the $\{D\}$ frame (i.e., when e is zero); u_{ss} the through water velocity of the AUV in the steady state in the $\{D\}$ frame; and $\dot{x}_{\mathcal{C}}$, $\dot{y}_{\mathcal{C}}$, and $u_{\mathcal{C}}$ the velocities due to c .

$$\dot{y}_{ss} = -\dot{y}_c, \quad (22)$$

where \dot{x} is set as $\dot{x}_{\mathcal{D}}$.

2.3.1. State space formulation

The system evolution is represented by the cross-track error (12), which, according to (4), has the following time derivative:

$$\dot{e} = u \sin(\psi) + \dot{y}_c. \quad (23)$$

Now, assuming $u = u_d$ and $\psi = \psi_d$, the error dynamics are given by:

$$\dot{e} = \left[\frac{\dot{x}_{ss}}{\cos(\psi_d)} - k_1 \tan(k_2 e) \operatorname{sign}(\psi_d) \right] \sin(\psi_d) + \dot{y}_c \quad (24)$$

2.3.2. Equilibrium points

An equilibrium point is reached when $\dot{e} = 0$, i.e., when $\psi_d = \psi_c$. If this condition is applied to (24), it follows that $e_{eq} = 0$ if $\dot{x}_c \neq \dot{x}_{\mathcal{D}}$, $\Delta \neq 0$, $k_1 > 0$, and $k_2 > 0$. In order to fulfill this condition, and because $\dot{x}_{\mathcal{D}}$ is a value that we can set, in the case of having $\dot{x}_{\mathcal{D}} = \dot{x}_c$ the $\dot{x}_{\mathcal{D}}$ will be increased according to:

$$\dot{x}_{\mathcal{D}} = \begin{cases} \dot{x}_{\mathcal{D}}, & \dot{x}_{ss} \in \mathbb{R} \setminus (-0.2, 0.2) \\ \dot{x}_c + 0.2, & \dot{x}_{ss} \in [0.0, 0.2) \\ \dot{x}_c - 0.2, & \dot{x}_{ss} \in (-0.2, 0.0) \end{cases} \quad (25)$$

2.3.3. Setting the gains

The definition of k_1 and k_2 corresponds to the maximum velocity and acceleration that the correction c (20) will impose on the system. Considering the characteristics of the Sparus II, a maximum correction velocity of 0.7 m/s , and a maximum correction acceleration of 0.5 m/s^2 are desirable.

In order to set k_1 , the function $y = \operatorname{atan}(x)$ is analysed. This function has a horizontal asymptote at $y = \pi/2$ and in $y = -\pi/2$. Taking into account the performance of Sparus II, the horizontal asymptote of (20) must be set to $y = 0.7 \text{ m/s}$, consequently $k_1 = 0.7 \cdot 2/\pi \approx 0.4456 \text{ m/s}$. To compute the maximum rate of change of the correction, both k_2 and k_{Δ} must be known. For this reason, in a first step k_2 is set as 1 m^{-1} .

The parameter k_{Δ} is computed in the Appendix, assuming $k_2 = 1 \text{ m}^{-1}$, in order to fulfil the stability conditions formulated in Section 2.3.5.

2.3.4. Domain of the controller

In order to evaluate the controller presented in this paper, a certain domain is set:

$$\begin{cases} \mathcal{X} = \{\dot{x}_c \mid -0.5 \leq \dot{x}_c \leq 0.5\} [m/s] \\ \mathcal{Y} = \{\dot{y}_c \mid -0.5 \leq \dot{y}_c \leq 0.5\} [m/s] \\ \mathcal{E} = \{e \mid -10 \leq e \leq 10\} [m] \end{cases} \quad (26)$$

Ocean current velocities must be within the range of those that the Sparus II AUV can withstand. Since the docking maneuver begins after a homing process, we can ensure that the cross-track error of the AUV position belongs to the stability domain. If during the maneuver, the cross-track error falls outside of the domain, the docking maneuver is cancelled and the whole process is repeated.

2.3.5. Stability

In order to demonstrate the stability of the system using the Lyapunov Direct Method, the following Lyapunov candidate is proposed:

$$V(e) = \frac{1}{2} e^2, \quad (27)$$

that fulfills the first and second Lyapunov conditions: $V(0) = 0$, and $V(e) > 0 \forall e \neq 0$.

The first order time derivative of the Lyapunov candidate can be expressed as:

$$\dot{V} = e \dot{e}. \quad (28)$$

To demonstrate exponential stability, we show that the system fulfills the condition (following [22]):

$$\dot{V} \leq -\lambda V, \quad (29)$$

for some $\lambda > 0$. The mathematical proof of stability is given in the Appendix.

2.3.6. Maximum acceleration verification

In Section 2.3.3, a $k_2 = 1 m^{-1}$ was assumed to be able to calculate a k_Δ that fulfils the stability conditions. In order to verify that the obtained gains do not result in surpassing the assumed capabilities of the Sparus II, for the presented controller, an optimization problem was formulated. In the problem, a maximum rate of change of the correction (c') is searched for, to check that it is not exceeding the maximum assumed acceleration of the robot $\dot{c} = 0.5 m/s^2$. First, we simplify (20) as:

$$c' = k_1 \text{atan}(k_2 e), \quad (30)$$

to avoid deriving the signum function, and because the maximum value of c' is not affected. The rate of change of c' is given by:

$$\dot{c}' = \frac{k_1 k_2}{k_2^2 e^2 + 1} \dot{e}. \quad (31)$$

The optimization problem is formulated as follows:

$$\begin{aligned} & \max_{\dot{x}_c, \dot{y}_c, e} && c' \\ & \text{s.t.} && \dot{x}_c \in \mathcal{X} \\ & && \dot{y}_c \in \mathcal{Y} \\ & && e \in \mathcal{E} \end{aligned} \quad (32)$$

Considering the domain set for the controller (Section 2.3.4), the parameters:

$$\begin{cases} \dot{x}_{\mathcal{D}} = 0.3 \text{ m/s} \\ k_1 = 0.4456 \text{ m/s} \\ k_2 = 1 \text{ m}^{-1}, \end{cases} \quad (33)$$

and together with (25), it can be deduced that three optimization problems must be solved for three subsets of the \dot{x}_c domain: $\mathcal{X}_1 = [-0.5, 0.1]$, $\mathcal{X}_2 = [0.1, 0.3]$ and $\mathcal{X}_3 = [0.3, 0.5]$, and the maximum of these three problems is the solution in the whole domain (26). The problem (32) was solved using the IPOPT [23] solver and yielded a result of 0.44979 m/s^2 .

2.3.7. Minimum docking distance

With the control laws defined, the minimum necessary distance to successfully perform docking, from a kinematic point of view, can be calculated, by solving (24). Considering the domain of Section 2.3.4 together with the parameters:

$$\begin{cases} \dot{x}_{\mathcal{D}} = 0.3 \text{ m/s} \\ k_1 = 0.4456 \text{ m/s} \\ k_2 = 1 \text{ m}^{-1} \\ k_{\Delta} = 6 \text{ m}, \end{cases} \quad (34)$$

applying the correction presented in (25). The maximum time to reach the equilibrium ($|e| \leq 0.05 \text{ m}$) can be calculated. This time applied to the desired docking velocity gives an approximation of the minimum necessary docking distance:

$$D_{min} = \dot{x}_{\mathcal{D}} t. \quad (35)$$

The minimum distance necessary to dock, in the worst case scenario, is close to 25 m. Note that the maximum velocity and acceleration in yaw have not been taken into account, because (for the set parameters) it has a low influence when the working yaw angle is reached. Note also that this is a controller defined for the docking maneuver (starting at $\pm 10 \text{ m}$ in y_D , with a heading favourable to the DS, i.e. $-1.5 > \psi < 1.5$), the homing maneuver will require its own additional distance.

3. Experimental setup

In order to do a consistent comparison, the same experimental setup, as presented in [14], was used.

3.1. Hardware

The non-holonomic AUV used for this test was the torpedo-shaped Sparus II [24,25], see Fig. 11. The AUV comes equipped with three thrusters, one vertical and a pair of horizontal, allowing for control in the surge, heave, and yaw. The control system supports inputs in force, velocity, and position. In this study we chose to control the vehicle in velocity, for the surge and heave, and in position, for the yaw.

The funnel-shaped DS developed by the University of Girona [12] (see Fig. 12) was represented in simulation.

3.2. Simulation

In this research an advanced open-source marine robotics simulator, called Stonefish [26], was used. Full dynamics and hydrodynamics of Sparus II were simulated, including ocean current influence, together with a complete suite of its sensors, see Fig. 13. Moreover, the docking station model was recreated in the simulation, with a high attention to details, allowing for realistic assessment of docking performance. Specifically for this research the



Figure 11: Photography of the Sparus II.

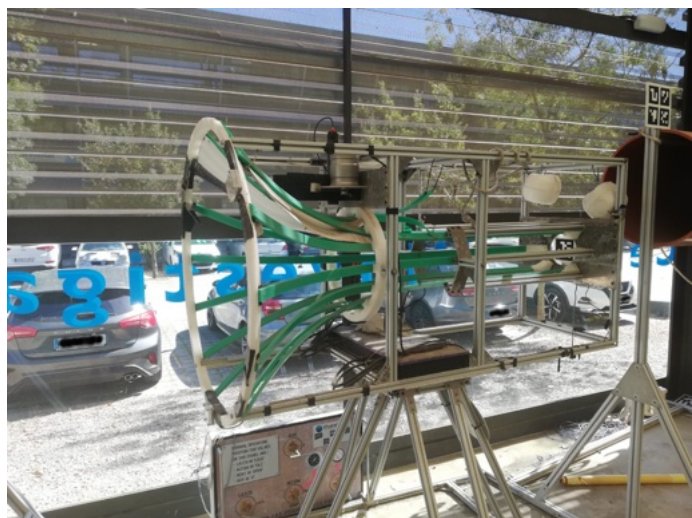


Figure 12: Photography of the docking station.

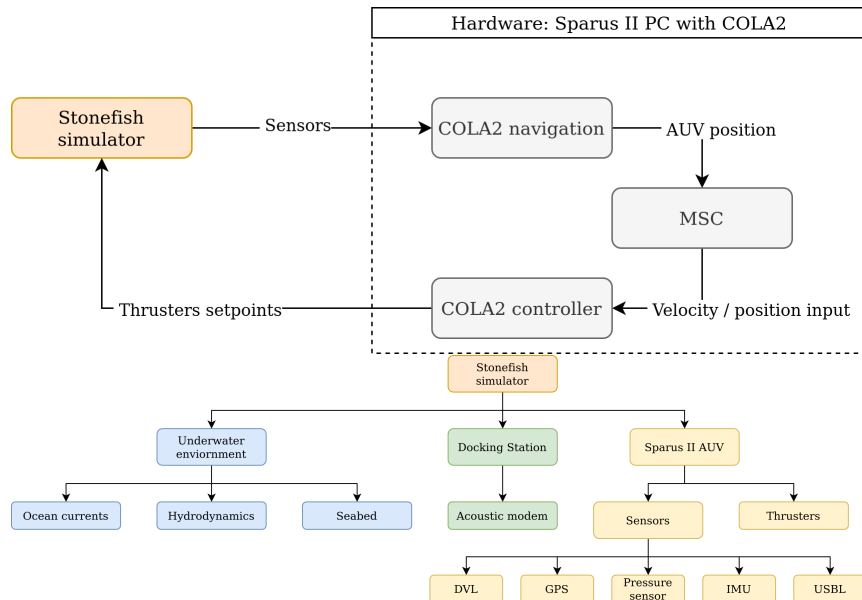


Figure 13: Conceptual representation of the hardware-in-the-loop simulation. The Sparus II architecture is in communication with the Stonefish simulator, which disposes of a model of the DS, the AUV with its sensors and thrusters [25], and the representation of the underwater environment.

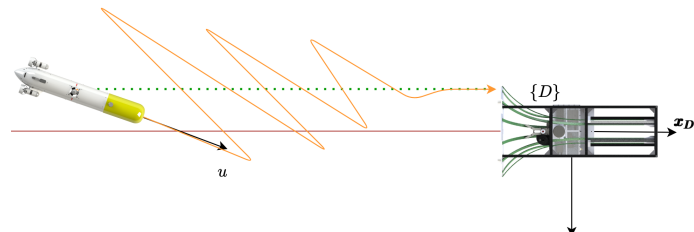


Figure 14: Conceptual performance representation.

simulator was extended to support acoustic communication and positioning devices. More details can be found in the previous work [14].

4. Performance

The objective of this section is to show the performance of the algorithm in the simulated scenario. The concept utilized to develop the high-level controller presented in this paper is to use the strong features of the Sparus II, to achieve maximum possible performance. The Sparus II AUV, as a non-holonomic robot without a rudder, requires a combined action of its two horizontal thrusters, in order to control the heading. This fact added to the non-symmetric behavior of the thrusters makes a notably lower response in the heading input than in the surge velocity.

The controller presented utilizes mainly the surge in order to correct the position of the AUV and reduce e , see Fig. 14.

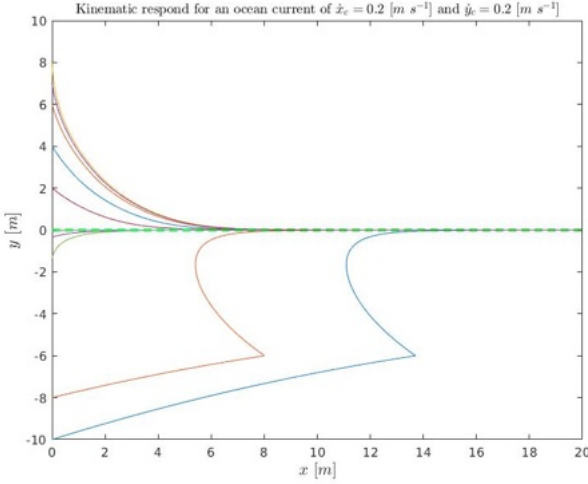


Figure 15: Kinematic simulation for the conditions (36) relative to position. The color lines represents the different simulations and the green discontinuous line the acceptance tolerance.

4.1. Docking scenarios A and B

For the docking scenarios A and B, remind Fig. 3, the heading of the AUV is opposite to \dot{y}_c , it can be seen in the video [27]. It can be understood, analyzing the velocity vectors, i.e., $\dot{x}_{\mathcal{D}}$ is bigger than \dot{x}_c , that the surge velocity has to be positive, being this case (and taking into consideration that we have a non-holonomic AUV) the surge has to point in the opposite direction to the \dot{y}_c , in order to be able to compensate for it.

A set of initial conditions are simulated (36), for kinematics (solving (3) and (4)), and plotted in Fig. 15 and Fig. 16. They are also simulated in dynamics (using Stonefish) and plotted in Fig. 17 in order to compare both results.

$$\begin{cases} \dot{x}_{\mathcal{D}} = 0.3 \text{ m/s} \\ \dot{x}_c = 0.2 \text{ m/s} \\ \dot{y}_c = 0.2 \text{ m/s} \\ e \in [-10 : 2 : 10] \text{ m} \\ k_1 = 0.4456 \text{ m/s} \\ k_2 = 1 \text{ m}^{-1} \\ k_{\Delta} = 6 \text{ m}, \end{cases} \quad (36)$$

4.2. Docking scenario C

For the docking scenario C, the heading of the AUV is the same as the direction of \dot{x}_c , see the video [28]. Again, analyzing the velocity vectors, i.e., $\dot{x}_{\mathcal{D}}$ is smaller than \dot{x}_c , the surge velocity has to be negative, so the surge has to point in the same direction as the \dot{y}_c , in order to be able to compensate for it.

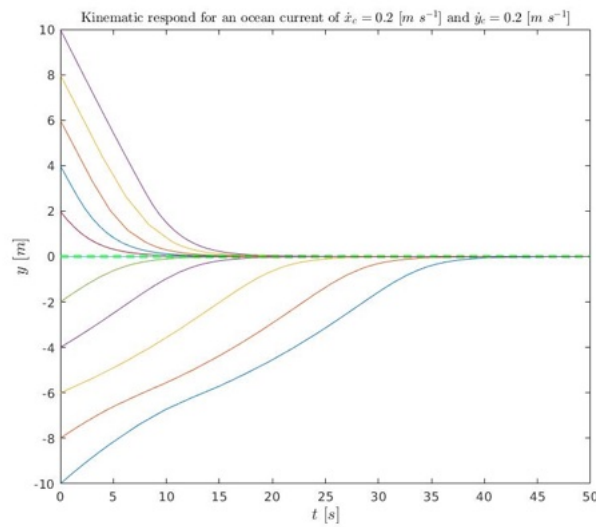


Figure 16: Kinematic simulation for the conditions (36) relative to time. The color lines represents the different simulations and the green discontinuous line the acceptance tolerance.

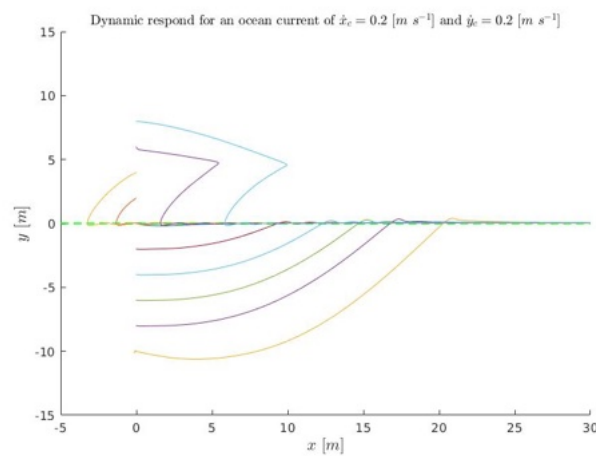


Figure 17: Dynamic simulation for the conditions (36). The color lines represents the different simulations and the green discontinuous line the acceptance tolerance.

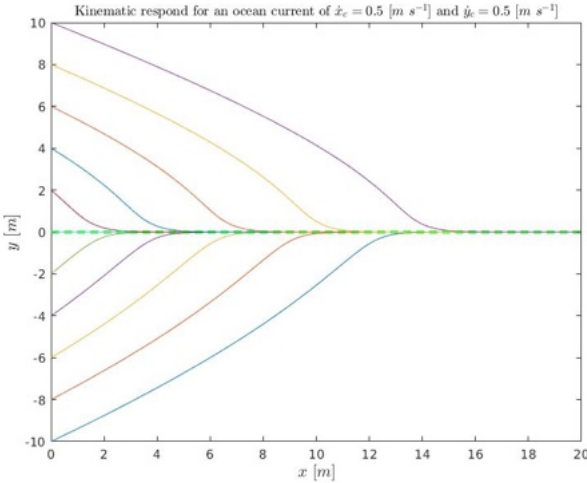


Figure 18: Kinematic simulation for the conditions (37) relative to position. The color lines represents the different simulations and the green discontinuous line the acceptance tolerance.

A set of initial conditions are simulated (37) for kinematics (solving (3) and (4)) and plotted in Fig. 18 and Fig. 19. They are also simulated in dynamics (using Stonefish) and plotted in Fig. 20 in order to compare both results.

$$\begin{cases} \dot{x}_{\mathcal{D}} = 0.3 \text{ m/s} \\ \dot{x}_c = 0.5 \text{ m/s} \\ \dot{y}_c = 0.5 \text{ m/s} \\ e \in [-10 : 2 : 10] \text{ m} \\ k_1 = 0.4456 \text{ m/s} \\ k_2 = 1 \text{ m}^{-1} \\ k_{\Delta} = 6 \text{ m}, \end{cases} \quad (37)$$

4.3. Entrance scenario II

An example of the performance achieved in the entrance scenario II can be found in [29], remind Fig. 5.

4.4. Entrance scenario III

An example of the performance achieved in the entrance scenario III can be found in [30], remind Fig. 5.

5. Results

In order to compare the new algorithm with the state of the art, the data obtained in the article [14] is used. In these previous article, different algorithms, already published in the literature, were compared at different levels. Being the level 3 the most representative for the authors' needs, the data from this level is used to compare with the proposed algorithm, since it was tested at the same level.

As it was presented in [14], in order to estimate the quality of the docking process in a funnel-shaped DS, a novel technique based on the geometrical analysis of the entrance of

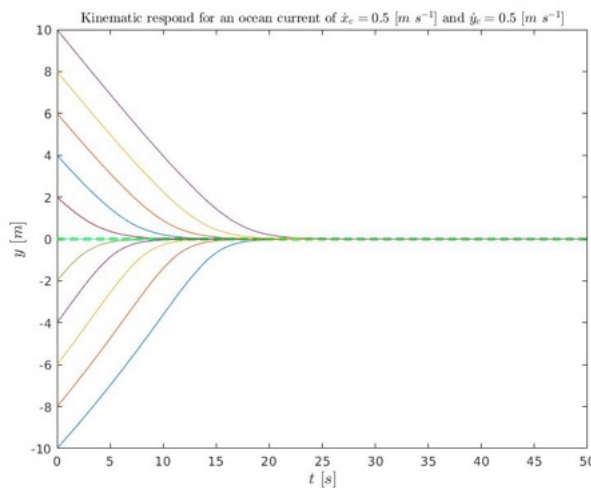


Figure 19: Kinematic simulation for the conditions (37) relative to time. The color lines represents the different simulations and the green discontinuous line the acceptance tolerance.

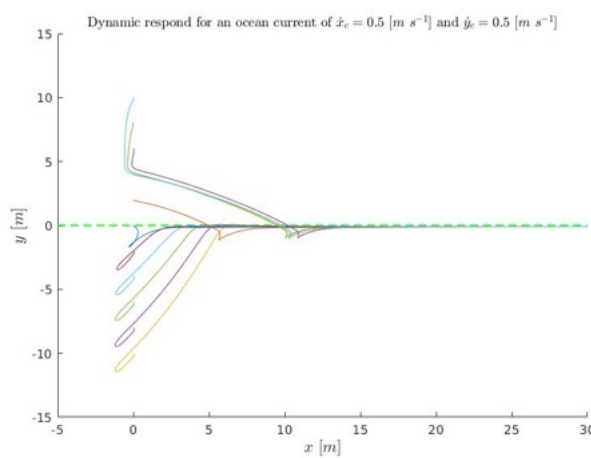


Figure 20: Dynamic simulation for the conditions (37). The color lines represents the different simulations and the green discontinuous line the acceptance tolerance.

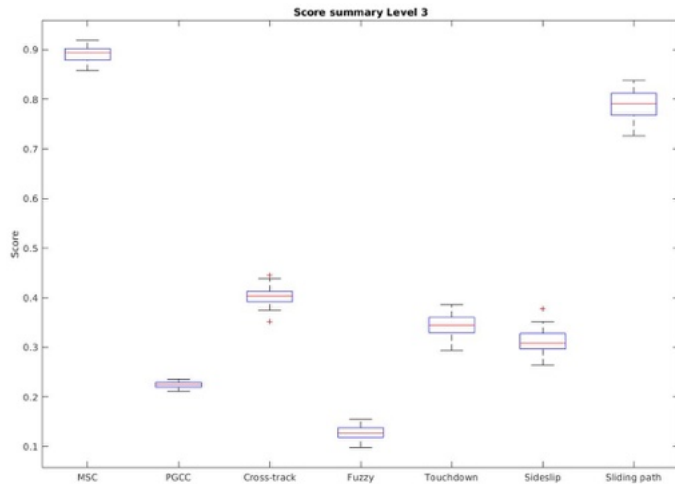


Figure 21: Score summary comparison between the different methods, taking the results of [14], using a box plot.

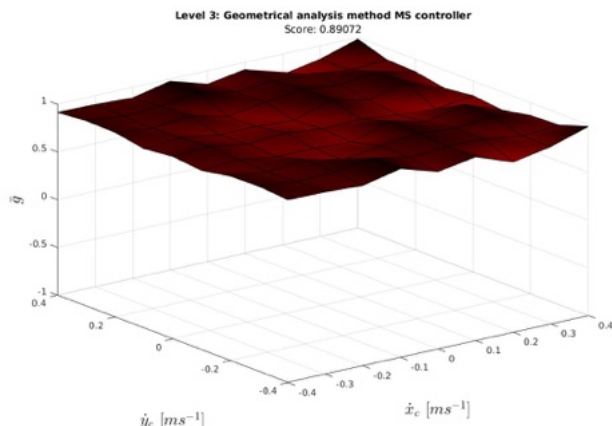


Figure 22: 3D Geometrical analysis for the Managed surge controller

the AUV was used. With this technique, we can evaluate the methods with a ‘score’ that ranges from 0 to 1, with 1 being the perfect docking.

In order to represent the comparison, a Boxplot is presented in Fig. 21.

The 3D plot of the results is presented in Fig. 22, and the 2D plot in Fig. 23.

A table with the numerical results compared can be seen in Table 1.

6. Discussion

The Managed Surge Controller achieved a mean score of 0.891, being the highest value for the proposed conditions. The controller is able to dock the robot in all the ocean currents conditions tested in the previous study (e.g., from -0.4 m/s to 0.4 m/s on both axis). As it can be seen in Fig. 21, it not only has the best mean scores, but also a low standard deviation, showing that the results are consistent.

As the score indicates and as can be further appreciated in Fig. 22 and Fig. 23, a good performance in all the ocean current conditions tested during the exercise was achieved. Ocean current velocity values larger than the ones studied in the previous paper were also

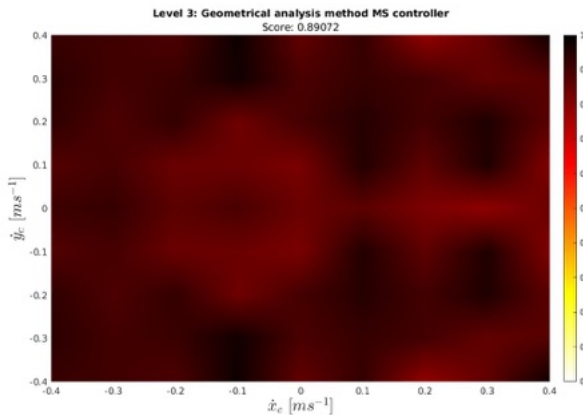


Figure 23: 2D Geometrical analysis for the Managed surge controller

studied in simulation, presenting also good results. However, it is not recommended to operate the Sparus II in more harsh conditions.

The Sparus II is a torpedo-shaped AUV equipped with three thrusters. It is designed to perform extended surveys, where the precision of the position is not crucial, implying that it is not capable of performing complicated maneuvers with high precision. One of the facts that are not reflected in the score is the simplicity of the maneuver, from a practical point of view. The more simple the maneuver, the more easy it is to perform it, using the real vehicle. In the docking maneuver, the MSC follows a straight-line, focusing on utilizing the horizontal thrusters optimally to work against the ocean current forces and correcting the cross-track error.

If the MSC is compared with the Sliding path controller (presented in [21] and implemented in [14]), that achieved a mean score of 0.790, one of the main differences is the developed maneuver. The Sliding path controller implies a notable precision in the maneuver to be able to enter exactly in the desired position, which is hard to achieve using the Sparus II. It is also not capable to minimize the cross-track error when the ocean current velocity is favorable and close to or larger than the docking velocity, when it is in the approaching path. However, during the sliding path it still can compensate for the error.

7. Conclusions

This paper has presented a novel controller to dock with a non-holonomic AUV, in a funnel-shaped DS, dealing with ocean currents. The paper proves the stability of the controller and the expected behavior is further confirmed using a very realistic dynamic simulator. In a previous work [14], after exhaustive survey, several algorithms to face the same problem were implemented and tested in the context of the ATLANTIS project, using the Stonefish simulator. This previous work concluded with a problem to study: how to minimize the cross-track error when the ocean current velocity is favorable and close to or larger than the docking velocity. In this article, the authors have developed an algorithm capable of dealing with this problem while maintaining or improving the rest of the evaluated criteria.

The novel proposal was compared with the state of the art algorithms, with the criteria developed in [14], presenting the best results. In future work, this controller will be implemented in Sparus II and tested in real scenarios. Also, a new funnel-shaped DS will be designed and built, in order to meet the requirements of the ATLANTIS project. The authors expect to be able to achieve docking without the use of vision systems, and if it is the case with the presence of ocean currents in the context of the project.

Method	Score	
	mean	std
Managed surge controller	0.891	0.013
PGCC controller	0.224	0.008
Cross-track controller	0.403	0.019
Fuzzy controller	0.128	0.014
Touchdown alignment controller	0.345	0.022
Sideslip controller	0.311	0.021
Sliding path controller	0.790	0.025

Table 1: Score results comparison between the different methods, taking the results of the level 3 of [14].

8. Acknowledgment

The authors would like to distinguish the counsel and guidance of António Pascoal from the Institute for Systems and Robotics for the development of this work.

Also, the authors would like to thank the ATLANTIS project to motivate this study and the following ones that would come, related to that.

Abbreviations

AUV Autonomous Underwater Vehicle

DS Docking Station

MSC Managed Surge Controller

3D Three dimensions

2D Two dimensions

Notation

${}^D\boldsymbol{\eta} = [x \ y \ \psi]^T$: AUV position in the $\{D\}$ frame (see Fig. 1)

${}^D\boldsymbol{v}_{1B} = [u \ v]^T$: Robot velocity in the $\{B\}$ frame with respect to the water

${}^D\dot{\boldsymbol{\eta}}_{1B} = [\dot{x} \ \dot{y}]^T$: AUV velocity in the $\{D\}$ frame with respect to the ground

${}^D\dot{\eta}_{1\varnothing} = [\dot{x}_\varnothing \ 0]^T$: Desired velocity of the robot when it impacts to the DS

${}^D\dot{\eta}_c = [\dot{x}_c \ \dot{y}_c]^T$: Ocean current velocity in the $\{D\}$ frame

u_d : Desired surge velocity of the AUV

u_{ss} : Surge velocity of the AUV in the stationary state

$\dot{x}_{ss}, \dot{y}_{ss}$: Robot velocities in the $\{D\}$ frame with respect to water in the stationary state

\dot{u}_c : Surge velocity of the AUV due to c

\dot{x}_c, \dot{y}_c : Robot velocities with respect to water in the $\{D\}$ frame due to c

ψ_d : Desired yaw angle of the AUV

ψ_c : Crab angle of the AUV to compensate the ocean currents

ψ_{cII} : Maximum crab angle admissible to enter to the DS in Scenario II

ψ_{cIII} : Maximum crab angle admissible to enter to the DS in Scenario III

β : Relation between a look-ahead distance and the cross-track error

F : Longitud of the twin sides of the isosceles triangle that represents the DS, see Fig. 4

F_x : Height of the isosceles triangle that represents the DS, see Fig. 4

F_y : Base (half) of the isosceles triangle that represents the DS, see Fig. 4

l : Longitude of the AUV

y_g : Distance between the maneuver path and the axis of the DS

y_{gII} : Distance between the maneuver path and the axis of the DS in Scenario II

y_{gIII} : Distance between the maneuver path and the axis of the DS in Scenario III

y_{gM} : Maximum distance that can be set between the maneuver path and the axis of the DS

Δ : Look-ahead distance

k_Δ : Gain of the look-ahead distance

e : Cross-track error

\dot{e} : Time derivative of e

e_{eq} : Cross-track error in the equilibrium

c : Velocity correction of the controller

k_1 : Gain to set the maximum velocity of the correction

k_2 : Gain to set the maximum acceleration of the correction

V : Lyapunov candidate

\dot{V} : Time derivative of V

λ : Parameter to control the exponential stability

D_{min} : Approximation of the minimum necessary docking distance

t : Time

A_1 : Declared variable for a better comprehension of the mathematical expressions

A_2 : Declared variable for a better comprehension of the mathematical expressions

A_3 : Declared variable for a better comprehension of the mathematical expressions

Appendix A Exponential stability proof

Computing the time derivative of the Lyapunov function candidate

$$V(e) = \frac{1}{2} e^2 \quad (\text{A1})$$

yields

$$\dot{V} = e \dot{e}, \quad (\text{A2})$$

where

$$\dot{e} = \left[\frac{\dot{x}_{ss}}{\cos(\psi_d)} - c \right] \sin(\psi_d) + \dot{y}_c, \quad (\text{A3})$$

In what follow we show that

$$\dot{V} \leq -\lambda V, \quad (\text{A4})$$

where $\lambda > 0$, leads to exponential stability. Substituting (A3) into (A2)

$$\dot{V} = (\dot{x}_{ss} \tan(\psi_d) + \dot{y}_c) e - c \sin(\psi_d) e, \quad (\text{A5})$$

where

$$\dot{y}_c = -\dot{y}_{ss}, \quad (\text{A6})$$

$$\dot{y}_{ss} = \dot{x}_{ss} \tan(\psi_c), \quad (\text{A7})$$

$$c = k_1 \operatorname{atan}(k_2 e) \operatorname{sign}(\psi_d), \quad (\text{A8})$$

$$\psi_d = \psi_c + \beta. \quad (\text{A9})$$

Substituting (A6), (A7), (A8), and (A9) into (A5) yields

$$\begin{aligned} \dot{V} = & (\dot{x}_{ss} \tan(\psi_c + \beta) - \dot{x}_{ss} \tan(\psi_c)) e \\ & - k_1 \operatorname{atan}(k_2 e) \operatorname{sign}(\psi_d) \sin(\psi_d) e. \end{aligned} \quad (\text{A10})$$

If the trigonometrical relation $\tan(x + y) = \frac{\tan(x) + \tan(y)}{1 - \tan(x)\tan(y)}$ is applied to (A10), then

$$\dot{V} = \dot{x}_{ss} e \left[\frac{\tan(\psi_c) + \tan(\beta)}{1 - \tan(\psi_c)\tan(\beta)} - \tan(\psi_c) \right] - k_1 \text{atan}(k_2 e) \text{sign}(\psi_d) \sin(\psi_d) e, \quad (\text{A11})$$

$$\dot{V} = \dot{x}_{ss} e \frac{\tan(\beta) + \tan^2(\psi_c)\tan(\beta)}{1 - \tan(\psi_c)\tan(\beta)} - k_1 \text{atan}(k_2 e) \text{sign}(\psi_d) \sin(\psi_d) e, \quad (\text{A12})$$

$$\dot{V} = \dot{x}_{ss} e \frac{\tan(\beta)}{1 - \tan(\psi_c)\tan(\beta)} [1 + \tan^2(\psi_c)] - k_1 \text{atan}(k_2 e) \text{sign}(\psi_d) \sin(\psi_d) e, \quad (\text{A13})$$

where

$$\tan(\beta) = \frac{-e \text{sign}(\dot{x}_{ss})}{k_\Delta}, \quad (\text{A14})$$

$$\tan(\psi_c) = \frac{\dot{y}_{ss}}{\dot{x}_{ss}}. \quad (\text{A15})$$

Applying (A14) and (A15) to (A13) one obtains

$$\dot{V} = - \frac{e^2 \dot{x}_{ss} \text{sign}(\dot{x}_{ss})}{k_\Delta + \frac{\dot{y}_{ss}}{\dot{x}_{ss}} e \text{sign}(\dot{x}_{ss})} \left[1 + \frac{\dot{y}_{ss}^2}{\dot{x}_{ss}^2} \right] - k_1 \text{atan}(k_2 e) \text{sign}(\psi_d) \sin(\psi_d) e. \quad (\text{A16})$$

Inserting (A16) in condition (A4) yields

$$- \frac{e^2 \dot{x}_{ss} \text{sign}(\dot{x}_{ss})}{k_\Delta + \frac{\dot{y}_{ss}}{\dot{x}_{ss}} e \text{sign}(\dot{x}_{ss})} \left[1 + \frac{\dot{y}_{ss}^2}{\dot{x}_{ss}^2} \right] - k_1 \text{atan}(k_2 e) \text{sign}(\psi_d) \sin(\psi_d) e \leq -\frac{\lambda e^2}{2}, \quad (\text{A17})$$

and, rewriting $|x| \equiv x \text{sign}(x)$, the following condition is obtained:

$$\lambda \leq \frac{2 |\dot{x}_{ss}|}{k_\Delta + \frac{|\dot{y}_{ss}|}{|\dot{x}_{ss}|} e} \left[1 + \frac{\dot{y}_{ss}^2}{\dot{x}_{ss}^2} \right] + \frac{2 k_1 \text{atan}(k_2 e)}{e} |\sin(\psi_d)|. \quad (\text{A18})$$

In order to fulfil the exponential stability condition, $\lambda > 0$, (A18) can be simplified to

$$0 < \frac{2 |\dot{x}_{ss}|}{k_\Delta + \frac{|\dot{y}_{ss}|}{|\dot{x}_{ss}|} e} \left[1 + \frac{\dot{y}_{ss}^2}{\dot{x}_{ss}^2} \right] + \frac{2 k_1 \text{atan}(k_2 e)}{e} |\sin(\psi_d)|, \quad (\text{A19})$$

from which it can be obtained that

$$k_\Delta > -\frac{\dot{y}_{ss}}{|\dot{x}_{ss}|} e - \frac{|\dot{x}_{ss}|}{k_1 \operatorname{atan}(k_2 e) |\sin(\psi_d)|} e - \frac{\dot{y}_{ss}^2}{|\dot{x}_{ss}| k_1 \operatorname{atan}(k_2 e) |\sin(\psi_d)|} e, \quad (\text{A20})$$

is the new condition that must be fulfilled in order to ensure exponential stability. For the sake of clarity, the following variables are defined:

$$A_1 \triangleq -\frac{\dot{y}_{ss}}{|\dot{x}_{ss}|} e, \quad (\text{A21})$$

$$A_2 \triangleq -\frac{|\dot{x}_{ss}|}{k_1 \operatorname{atan}(k_2 e) |\sin(\psi_d)|} e, \quad (\text{A22})$$

$$A_3 \triangleq -\frac{\dot{y}_{ss}^2}{|\dot{x}_{ss}| k_1 \operatorname{atan}(k_2 e) |\sin(\psi_d)|} e, \quad (\text{A23})$$

and consequently

$$k_\Delta > A_1 + A_2 + A_3. \quad (\text{A24})$$

Being $\operatorname{sign}(x) \equiv \operatorname{sign}(\operatorname{atan}(x))$, implies $A_2 \leq 0$ and $A_3 \leq 0$. Assuming $|\sin(\psi_d)| = 1$ is a conservative solution, consequently, the expression

$$k_\Delta > -\frac{\dot{y}_{ss}}{|\dot{x}_{ss}|} e - \frac{|\dot{x}_{ss}|}{k_1 \operatorname{atan}(k_2 e)} e - \frac{\dot{y}_{ss}^2}{|\dot{x}_{ss}| k_1 \operatorname{atan}(k_2 e)} e \quad (\text{A25})$$

still represents the condition to fulfill the exponential stability for the controller. In order to calculate k_Δ a nonlinear optimization problem of the following form was solved:

$$\begin{aligned} \max_{\dot{x}_c, \dot{y}_c, e} \quad & A_1 + A_2 + A_3 \\ \text{s.t.} \quad & \dot{x}_c \in \mathcal{X} \\ & \dot{y}_c \in \mathcal{Y} \\ & e \in \mathcal{E} \end{aligned} \quad (\text{A26})$$

Considering the domain set for the controller:

$$\left\{ \begin{array}{l} \mathcal{X} = \{\dot{x}_c \mid -0.5 \leq \dot{x}_c \leq 0.5\} [\text{m/s}] \\ \mathcal{Y} = \{\dot{y}_c \mid -0.5 \leq \dot{y}_c \leq 0.5\} [\text{m/s}] \\ \mathcal{E} = \{e \mid -10 \leq e \leq 10\} [\text{m}] \\ \dot{x}_\emptyset = 0.3 \text{ m/s} \\ k_1 = 0.4456 \text{ m/s} \\ k_2 = 1 \text{ m}^{-1} \end{array} \right. \quad (\text{A27})$$

together with (25), it can be deduced that three optimization problems have to be solved, for three subsets of the \dot{x}_c domain: $\mathcal{X}_1 = [-0.5, 0.1]$, $\mathcal{X}_2 = [0.1, 0.3]$ and $\mathcal{X}_3 = [0.3, 0.5]$, and the maximum of these three problems is the solution in the whole domain (A27). The problem (A26) was solved using the IPOPT solver and yielded a result of 5.1441. Consequently, for this domain, the controller is guaranteed to achieve exponential stability if

$$k_\Delta > 5.1441, \quad (\text{A28})$$

where k_Δ is a value that can be set by the designer.

References

1. Nicholson, J.; Healey, A. The Present State of Autonomous Underwater Vehicle (AUV) Applications and Technologies. *Marine Technology Society Journal* **2013**, *47*, 5–6. <https://doi.org/10.4031/MTSJ.47.5.17>.
2. Clague, D.A.; Paduan, J.B.; Caress, D.W.; McClain, J.; Zierenberg, R.A. Lava Flows Erupted in 1996 on North Gorda Ridge Segment and the Geology of the Nearby Sea Cliff Hydrothermal Vent Field From 1-M Resolution AUV Mapping. *Frontiers in Marine Science* **2020**, *7*, 1–25. <https://doi.org/10.3389/fmars.2020.00027>.
3. McEwen, R.S.; Hobson, B.W.; Bellingham, J.G.; McBride, L. Docking control system for a 54-cm-diameter (21-in) AUV. *IEEE Journal of Oceanic Engineering* **2008**, *33*, 550–562. <https://doi.org/10.1109/JOE.2008.2005348>.
4. Yang, C.; Peng, S.; Fan, S.; Zhang, S.; Wang, P.; Chen, Y. Study on docking guidance algorithm for hybrid underwater glider in currents. *Ocean Engineering* **2016**, *125*, 170–181. <https://doi.org/10.1016/j.oceaneng.2016.08.002>.
5. Kawasaki, T.; Fukasawa, T.; Noguchi, T.; Baino, M. Development of AUV "Marine Bird" with underwater docking and recharging system. *SSC 2003 - 3rd International Workshop on Scientific Use of Submarine Cables and Related Technologies* **2003**, pp. 166–170. <https://doi.org/10.1109/SSC.2003.1224134>.
6. Singh, H.; Bellingham, J.G.; Hover, F.; Lerner, S.; Moran, B.A.; Von Der Heydt, K.; Yoerger, D. Docking for an autonomous ocean sampling network. *IEEE Journal of Oceanic Engineering* **2001**, *26*, 498–514. <https://doi.org/10.1109/48.972084>.
7. Stokey, R.; Allen, B.; Austin, T.; Goldsborough, R.; Forrester, N.; Purcell, M.; Von Alt, C. Enabling technologies for REMUS docking: An integral component of an autonomous ocean-sampling network. *IEEE Journal of Oceanic Engineering* **2001**, *26*, 487–497. <https://doi.org/10.1109/48.972082>.
8. Feezor, M.D.; Sorrell, F.Y.; Blankinship, P.R.; Bellingham, J.G. Autonomous underwater vehicle homing/docking via electromagnetic guidance. *IEEE Journal of Oceanic Engineering* **2001**, *26*, 515–521. <https://doi.org/10.1109/48.972086>.
9. Podder, T.; Sibenac, M.; Bellingham, J. AUV docking system for sustainable science missions. *Proceedings - IEEE International Conference on Robotics and Automation* **2004**, *2004*, 4478–4485. <https://doi.org/10.1109/robot.2004.1302423>.
10. Bellingham, J.G. Autonomous Underwater Vehicle Docking. In *Springer Handbook of Ocean Engineering*; Springer, Cham, 2016; chapter 16, pp. 387–406. https://doi.org/https://doi.org/10.1007/978-3-319-16649-0_16.
11. Yazdani, A.M.; Sammut, K.; Yakimenko, O.; Lammas, A. A survey of underwater docking guidance systems. *Robotics and Autonomous Systems* **2020**, *124*. <https://doi.org/10.1016/j.robot.2019.103382>.
12. Palomeras, N.; Vallicrosa, G.; Mallios, A.; Bosch, J.; Vidal, E.; Hurtos, N.; Carreras, M.; Ridao, P. AUV homing and docking for remote operations. *Ocean Engineering* **2018**, *154*, 106–120. <https://doi.org/10.1016/j.oceaneng.2018.01.114>.
13. Pinto, A.M.; Marques, J.V.; Campos, D.F.; Abreu, N.; Matos, A.; Jussi, M.; Berglund, R.; Halme, J.; Tikka, P.; Formiga, J.; et al. ATLANTIS - The Atlantic Testing Platform for Maritime Robotics. *Oceans Conference Record (IEEE)* **2021**, 2021-Septe, 1–5. <https://doi.org/10.23919/OCEANS44145.2021.9706059>.
14. Esteba, J.; Cieslak, P.; Palomeras, N.; Ridao, P. Docking of Non-holonomic AUVs in Presence of Ocean Currents: a Comparative Survey. *IEEE Access* **2021**. <https://doi.org/10.1109/ACCESS.2021.3083883>.
15. Park, J.Y.; Jun, B.H.; Lee, P.M.; Lim, Y.K.; Oh, J.H. Docking problem and guidance laws considering drift for an underactuated AUV. *OCEANS 2011 IEEE - Spain* **2011**, pp. 1–7. <https://doi.org/10.1109/Oceans-Spain.2011.6003574>.
16. Hobson, B.W.; McEwen, R.S.; Erickson, J.; Hoover, T.; McBride, L.; Shane, F.; Bellingham, J.G. The development and ocean testing of an AUV docking station for a 21" AUV. *Oceans Conference Record (IEEE)* **2007**, pp. 1–6. <https://doi.org/10.1109/OCEANS.2007.07449318>.
17. Teo, K.; An, E.; Beaujean, P.P.J. A robust fuzzy autonomous underwater vehicle (AUV) docking approach for unknown current disturbances. *IEEE Journal of Oceanic Engineering* **2012**, *37*, 143–155. <https://doi.org/10.1109/JOE.2011.2180058>.
18. Teo, K.; Goh, B.; Chai, O.K. Fuzzy Docking Guidance Using Augmented Navigation System on an AUV. *IEEE Journal of Oceanic Engineering* **2015**, *40*, 349–361. <https://doi.org/10.1109/JOE.2014.2312593>.
19. Park, J.Y.; Jun, B.H.; Lee, P.M.; Oh, J.H.; Lim, Y.K. Underwater docking approach of an under-actuated AUV in the presence of constant ocean current. *IFAC Proceedings Volumes (IFAC-PapersOnline)* **2010**, *43*, 5–10. <https://doi.org/10.3182/20100915-3-DE-3000065>.
20. Park, J.Y.; Jun, B.H.; Kim, K.; Lee, P.M.; Oh, J.H.; Lim, Y.K. Improvement of vision guided underwater docking for small AUV ISiMI. *MTS/IEEE Biloxi - Marine Technology for Our Future: Global and Local Challenges, OCEANS 2009 2009*, pp. 1–5. <https://doi.org/10.23919/OCEANS.2009.5422241>.
21. Sans-Muntadas, A.; Pettersen, K.Y.; Brekke, E.; Henriksen, V.F. A hybrid approach to underwater docking of AUVs with cross-current. *OCEANS 2016 MTS/IEEE Monterey, OCE 2016 2016*, pp. 1–7. <https://doi.org/10.1109/OCEANS.2016.7761213>.
22. Khalil, H.K. Nonlinear systems, 2007. https://doi.org/10.1007/978-3-540-71225-1_5.
23. Wächter, A.; Lorenz T. Biegler. *Catalogue of an exhibition of the works of Dante Alighieri March to October 1909*; Vol. 57, 2006; pp. 25–57.
24. Carreras, M.; Candela, C.; Ribas, D.; Mallios, A.; Magí, L.L.; Vidal, E.; Palomeras, N.; Ridao, P. Sparus [II], design of a lightweight hovering [AUV]. *Proceedings of the 5th international workshop on marine technology. Martech'13 2013*, pp. 152–155.
25. Carreras, M.; Hernandez, J.D.; Vidal, E.; Palomeras, N.; Ribas, D.; Ridao, P. Sparus II AUV - A Hovering Vehicle for Seabed Inspection. *IEEE Journal of Oceanic Engineering* **2018**, *43*, 344–355. <https://doi.org/10.1109/JOE.2018.2792278>.

-
- 26. Cieslak, P. Stonefish: An Advanced Open-Source Simulation Tool Designed for Marine Robotics, With a ROS Interface. *OCEANS 2019 - Marseille* **2019**, pp. 1–6. <https://doi.org/10.1109/oceanse.2019.8867434>.
 - 27. J. Esteba. Performance example 0202. <https://youtu.be/Ag0Hj9vIdsE>. [Online; accessed 2021-09-01].
 - 28. J. Esteba. Performance example 0505. <https://youtu.be/cnuAa7iNAXs>. [Online; accessed 2021-09-01].
 - 29. J. Esteba. Performance example 0202. <https://youtu.be/SJBucM-229M>. [Online; accessed 2021-09-01].
 - 30. J. Esteba. Performance example 0202. <https://youtu.be/M943vUTJPuk>. [Online; accessed 2021-09-01].

4

EXPERIMENTAL IMPLEMENTATION

IN this chapter an experimental autonomous docking application for a non-holonomic **AUV** in a funnel-shaped **DS** is presented. Developing, building, and coding a new prototype of **DS**. Integrating an acoustic sensor for localization to the **AUV** navigation. Applying the controller developed in the previous publication. And finally, testing the application in two different scenarios in the sea.

Title: Sparus Docking Station: A Current Aware Docking Station For a Non-holonomic AUV
Authors: **Joan Esteba**, Patryk Cieslak, Narcís Palomeras, and Pere Ridao
Journal: Journal of Field Robotics
Volume: , Published:
Quality index: JCR2021 Robotics, Impact Factor: 6.385, Q2 (8/30)

Sparus Docking Station: A Current Aware Docking Station For a Non-holonomic AUV

Joan Esteba*

Computer Vision and Robotics Research Institute (VICOROB)
 University of Girona
 17003 Girona, Spain
 joan.esteba@udg.edu

Patryk Cieślak

Computer Vision and Robotics Research Institute (VICOROB)
 University of Girona
 17003 Girona, Spain
 patryk.cieslak@udg.edu

Narcís Palomeras

Computer Vision and Robotics Research Institute (VICOROB)
 University of Girona
 17003 Girona, Spain
 narcis.palomeras@udg.edu

Pere Ridao

Computer Vision and Robotics Research Institute (VICOROB)
 University of Girona
 17003 Girona, Spain
 pere.ridao@udg.edu

Abstract

This paper presents the design and development of a funnel-shaped Sparus Docking Station (SDS) intended for the non-holonomic torpedo-shaped Sparus II Autonomous Underwater Vehicles (AUV). The SDS is equipped with sensors and batteries, allowing for a stand-alone long-term deployment of the AUV. An inverted Ultra Short BaseLine (USBL) system is used to locate the Docking Station (DS) as well as to provide long-term drift-less AUV navigation. The SDS is able to observe the ocean currents using a Doppler Velocity Log (DVL), being motorized to allow its self-alignment with the current. Moreover, a docking algorithm accounting for the current is used to guide the robot during the docking maneuver. The paper reports experimental results of the docking maneuver in sea trials.

*This work has been developed in the context of the ATLANTIS "The Atlantic Testing Platform for Maritime Robotics: New Frontiers for Inspection and Maintenance of Offshore Energy Infrastructures" project. Founded from the European Union's Horizon 2020 research and innovation programme, under the Grant Agreement number 871571. Also, in collaboration with the projects Platform for Long-lasting Observation of Marine Ecosystems PLEC2021-007525, Despliegue Permanente de Vehículos Submarinos Autónomos Bi-Manuales para la Intervención PID2020-115332RB-C32, and Vehículo Inalámbrico Híbrido Operador Autónoma/Remotamente - OPTHIROV PDC2021-120791-C21.

1 Introduction

During the last years, AUVs have been developed and improved to satisfy the needs for more complex and demanding tasks. This trend will surely rise, considering many fields that can benefit from this technology, including oil and gas industry, marine life monitoring and research, and renewable energy production (e.g., through offshore wind farms) (Page and Mahmoudian, 2020), (Whitcomb, 2000), (Nicholson and Healey, 2013). AUVs can provide new capabilities by performing tasks that are not achievable using Remotely Operated Vehicles (ROV)s, for example, an AUV can carry out large autonomous mapping or inspection missions (Carreras et al., 2018) that an ROV can not execute due to the limitations imposed by its tether. In addition, the use of AUVs can drastically reduce the high operational costs associated with the use of ROVs due to the reduced dependence on large support vessels, as well as the necessity of a smaller support crew. On the other hand, the fact that AUVs are not wired, limits their operating time to their battery capacity. The lack of a cable also drastically reduces the communication bandwidth. To perform missions that extend beyond their operating time, AUVs must be recovered to recharge or replace their batteries, and to download gathered data that can hardly be transmitted otherwise.

One solution already explored in the literature (Bellingham, 2016), that can be applied in places where it is necessary to conduct actions on a regular basis, is the development of an underwater support infrastructure, named DS, where the AUV can be docked to recharge its batteries and/or transmit collected data. A DS provides a resting place for an AUV, at which it can recharge, transfer the data collected during the mission, and wait for further instructions. It removes the need for retrieving the AUV after each task and, in consequence, reduces significantly the operational costs. All these concepts lie in the interest of the Long Term Deployment (LTD) research in underwater robotics. The main concept of the LTD is to allow the AUVs to remain at the operational site for a period ranging from days to months. This will allow the AUVs to perform new tasks, such as continuous surveillance or persistent inspection of underwater industrial infrastructures. This research provides both hardware and software innovations as well as field results to progress toward this goal. Nowadays, the LTD research is developed in multiple research projects (Pinto et al., 2021), (Universitat de Girona, b), (Universitat de Girona, a), (Mbari,), (Bluelogic,). One of them is the H2020 ATLANTIS project that aims to establish a pioneer pilot infrastructure capable of demonstrating key enabling robotic technologies for inspection and maintenance of offshore wind farms (Pinto et al., 2021). Within the scope of this project, both the aerial and underwater parts of a wind farm must be inspected autonomously, on a regular basis. To achieve the LTD proposed in the ATLANTIS project, a DS has been designed and built and an inspection-capable AUV has been adapted to this scenario. Next, an autonomous docking controller has been developed to follow the appropriate docking maneuver. For the controller to work, a localization system between the AUV and the DS has been implemented.

In this work, the authors present all the steps from hardware designs to field tests which resulted in a complete solution for the LTD of the Sparus II AUV. Starting from a state of the art of the experimental docking systems in literature, summarized in Section 2. Continuing with the presentation of the proposed LTD system for the Sparus II AUV presented in Section 3. Containing the hardware development, presenting the non-invasive LTD upgrade of the AUV in Section 3.1 and the main characteristics of the developed DS prototype in Section 3.2. And the software development, explaining the docking strategy in Section 3.3 and the navigation upgrade developed in the AUV in Section 3.4. And finalizing with the presentation of successful sea results in Section 4, developed in two different locations: in the Mediterranean sea (Spain) and in the Atlantic Ocean (Portugal).

2 State of the art

AUV docking stations have been under development since 1997 (Stokey et al., 1997) and multiple solutions have been already proposed in the literature, summarized in (Bellingham, 2016), (Yazdani et al., 2020), (Esteba et al., 2021). The challenges faced by the researchers developing DS systems include: detecting the DS, estimating a good localization between the DS and the vehicle, controlling the AUV till completing the

docking maneuver, latching the vehicle in the DS, and establishing a connection between the DS and the AUV to transmit data and/or power when possible. Considering these challenges, multiple designs, tailored to different applications and requirements, have been proposed.

Docking systems can be classified from different points of view being the most important one the capture mechanism and the perception systems used to detect the DS, as well as to estimate the relative position between the AUV and the DS. Regarding the capture mechanism, some of the most popular solutions are: pole docking (Singh et al., 2001), (Sarda and Dhanak, 2019), where the AUV catches a pole using a device designed for this purpose, usually installed on the front of the vehicle; landing docking (Kawasaki et al., 2004), where the AUV touches down over the DS; net docking (Kukulya et al., 2010), where the AUV collides with a trapping net; and funnel docking systems (McEwen et al., 2008), where the robot is introduced into a funnel-shaped structure. While some of these systems take into consideration the presence of ocean currents by construction (e.g., pole docking) most of these systems have a well-defined approaching direction that can be difficult to follow in presence of ocean currents, especially for nonholonomic vehicles. It is worth noting that controlling a nonholonomic vehicle to follow a given trajectory is more challenging, as it can not be actuated in all the degrees of freedom it can move.

The perception system, used to detect the DS as well as to estimate the relative position between the vehicle and the DS, is also an important element that clearly differentiates the application and requirements of one docking system with respect to another. Perception systems can be based on acoustics, mainly from position measurements (i.e., USBL) (McEwen et al., 2008); vision, with passive or active markers (Park et al., 2010); or a combination of several systems (Palomeras et al., 2018), (Fletcher et al., 2017).

Looking at all these solutions, it is clear that not all systems can be used in all situations. For instance, DS that use a pole or a net capturing mechanism can be useful to recover the vehicle but not to protect it for a large period of time. Also, systems that heavily rely on vision can not be used in places where water clarity can not be guaranteed.

After reviewing the main published systems, and considering applications that face long-term deployment requirements, the most popular capture mechanism for the application at hand is the funnel-shaped system that may provide data and power communication to the AUV as well as protection. Perception systems used for this typology of DS include position-based acoustics combined with passive or active landmarks that can be detected with a vision system. Regarding ocean currents, funnel-shaped systems are not the best suited because they enforce a very restricted approaching angle. However, two contributions, one in the form of modifications to the standard funnel-shaped DS hardware and the other in the control algorithm, are presented in this paper to overcome this problem.

Table 1 summarizes some of the most cited funnel-based systems that have been taken from the design phase to field experiments as well as their main characteristics. It compares the most determinant parameters from the DS systems:

1. **Localization system:** consists of the typology of the perception system used for localizing the DS from the AUV.
2. **Currents:** evaluates if the publication considers the ocean currents velocity vector.
3. **Comms and power:** considers if the published system presents a solution for connecting the AUV with the DS to transmit data (communication) and power.
4. **LTD or LaRS:** considers if the publication is developed as a Long Term Deployment system or a Launch and Recovery System.
5. **Controller:** considers the control system for the path-following of the AUV during the docking maneuver.

6. **Success rate:** evaluates the number of successful attempts against the total attempts published for each solution.

Authors	(Stokey et al., 2001)	(Feezor et al., 2001)	(Allen et al., 2006)	(McEwen et al., 2008)	(Park et al., 2009)	(Circle, 2012)	(Fletcher et al., 2017)	(Palomeras et al., 2018)
Localization system	Acoustics	Electro-magnetic	Acoustics	Acoustics	Vision	Acoustics	Acoustics and vision	Acoustics and vision
Currents	Yes	Yes	No	Yes	Yes	Yes	No	No
Comms and power	Yes	Yes	Yes	Yes	No	No	No	Comms only
LTD or LaRS	LTD	LaRS	LTD	LTD	LTD	LaRS	LaRS	LTD
Controller	Not published	PID	Not published	Cross-track	Custom	Pure pursuit	Pure pursuit	Pure pursuit
Success rate	Not published	5/8	17/29	4/4	Not published	7/11	6/25	12/15

Table 1: Summary of the most representative funnel-shaped DS systems published in the literature that achieved experimental results.

All the works presented in Table 1 use funnel-shaped DS that show experimental results. In (Stokey et al., 1997), a planar nose cone, to accommodate the vehicle, and four individual wide-band hydrophone signals, to estimate the DS location, were used. Field works are mentioned in the text but statistical results (related to the success rate) are not provided. In 2006, another experimental study was conducted (Allen et al., 2006) using a USBL as the main localization system. Experimental results provided in the article indicate 17 successful trials out of 29 attempts, which constitutes a 58% success rate. In 2008 (McEwen et al., 2008) designed and tested a funnel-shaped DS that was also using a USBL system for localization. Trials were carried out at 300 meters deep with an AUV that had to find the DS and then dock. The authors were able to perform four consecutive successful autonomous dockings. In 2012, the HYDRIOD group implemented an autonomous docking system also using a USBL system for localization purposes. The reported success rate for this system was 77% (Circle, 2012). In 2017, other sea experiments were performed (Fletcher et al., 2017), (Zhang et al., 2017), proving that funnel shape is a successful DS design. However, they do not take into consideration the effect of the currents in their trials. Finally, in 2018, a team from Universitat de Girona (UdG) developed another funnel-based solution that used a combination of acoustic ranges and active optical markers to localize the DS with respect to the AUV (Palomeras et al., 2018). Despite a success rate of 80%, the authors concluded that the system was not reliable in presence of ocean currents and that the optical part of the localization system was not suitable for high levels of water turbidity. Examining not only the systems mentioned above, but most of the articles on funnel-based docking published to date, the authors believe that it is possible to state that, to this day, there are still improvement needs in order to achieve a highly reliable solution for autonomous docking in real marine environments, especially when looking for long-term deployable systems in areas that may be affected by currents. Therefore, this article aims to provide novel solutions, both in the mechanical design and the localization and control software, that will help to achieve this goal.

3 Long Term Deployment system

This section describes the main developments of the different technologies that were needed to achieve the experimental results presented in this work. First, the AUV is presented as well as the hardware upgrades done to tackle the proposed LTD application. Second, the new prototype of a DS is presented. Third, the docking strategy, already explained in (Esteba et al., 2023), is presented. Finally, the navigation system implemented in the AUV to meet the necessary docking requirements is described.

3.1 Nonholonomic AUV: Sparus II

The Sparus II is an AUV developed primarily for seabed surveys and offshore structure inspection by the University of Girona, and recently commercialized by Iqua Robotics SL. (Carreras et al., 2013), (Carreras et al., 2018). It combines the classical concept of a torpedo-shaped vehicle with hovering capabilities (see Fig. 1). The main specifications and features of the Sparus II consist of:

- Length: 1.6 m.
- Hull diameter: 230 mm.
- Maximum width: 460 mm.
- Weight in air: 52 kg.
- Maximum depth: 200 m.
- Energy: 1.4 kWh Li-Ion battery.
- Endurance: from 8 to 10 hours.
- Maximum surge velocity: 3 kn.
- Propulsion system: 3 thrusters with magnetic coupling.
- Controllable Degree of Freedom (DoF): Surge, heave, and yaw.
- Building materials: Modular aluminum and acetal hull.
- Navigation sensors: DVL, Inertial Measurement Unit (IMU), pressure sensor, and Global Positioning System (GPS).
- Payload volume: 8 liters or 7 kg in air.
- Payload interface: Ethernet, RS-232, regulated 12 V and 24 V.
- Communications: WiFi, XBee, GSM/3G.

The shape of the AUV hull is optimized for navigation at medium/high velocities. The vehicle can be controlled in surge, heave, and yaw degrees of freedom independently by means of three thrusters (one vertical and two horizontal). It can reach a maximum velocity in surge of 3 kn. The vehicle is rated for up to 200 m depth. Its navigation suite includes an Inertial Measurement Unit (IMU), a Doppler Velocity Log (DVL), a Global Positioning System (GPS), a pressure sensor, and, optionally, a Ultra Short BaseLine (USBL). The latter can be used as a beacon to localize the AUV from the surface or, as inverted-USBL, to localize a target underwater, here the DS equipped with an acoustic beacon.

Its software architecture is based on Component Orientated Layer-based Architecture for Autonomy (COLA2) (Palomeras et al., 2012) which is utilizing the ROS open-source middleware (Quigley et al., 2009).



Figure 1: On the left, photography of the Sparus II AUV with the ATLANTIS project configuration. On the right, payload developed by Iqua Robotics that includes X150 USBL Beacon from Blueprint Subsea (Blueprint Design Engineering Ltd, b), Wireless charger prototype from INESCTEC, forward-looking camera from Iqua Robotics, and an Oculus M-Series from Blueprint Subsea (Blueprint Design Engineering Ltd, a).

The control system is divided into two parts: a guidance docking velocity controller based on the Managed Surge Controller (MSC) presented in section 3.3 and a low-level controller included within the COLA2.

To allow for the integration of mission-oriented equipment, the robot has a fully configurable payload area. In the ATLANTIS project, a new payload was designed and manufactured by Iqua Robotics (see Fig. 1). This payload was designed for mapping the seabed using a multibeam imaging sonar, allowing, also, for inductive charging, and including an USBL transceiver to locate the DS.

3.2 Sparus Docking Station

Given the torpedo shape of the non-holonomic AUV used, we opted for a funnel-shaped design, conceived as an evolution of the one presented in (Palomeras et al., 2018). The main difference with its predecessor is the capability to operate in low visibility environments using only acoustic feedback for its localization. Another significant advantage is the capability of self-alignment with the ocean currents to facilitate the docking. The SDS is made of two principal components, the tripod and the funnel, both of them described hereafter.

3.2.1 Tripod

The tripod is the base structure supporting the funnel. It is a tetrahedron frame made of 316 stainless steel pipes welded to laser-cut sheets. The tripod is designed to withstand the docking collision impacts transmitting the energy to the ground. The structure has two layers. The bottom one contains the pressure vessel (rated for 100-meter depth) with the batteries and the electronics. It is cabled to the SDS sensors, actuators, the inductive AUV charger, and the modems. The electronics (Fig. 5) include a Raspberry Pi 3 computer (Raspberry Pi,) and a microcontroller. The Raspberry Pi runs the Robot Operating System (ROS) (Quigley et al., 2009) middle-ware to manage the main system and the communication with the devices. The microcontroller manages the control of the motors and the power, implementing a sleep mode for battery consumption optimization. Finally, the cylinder hosts the battery (24 packs of NL2044 14.4V Lithium Ion Batteries). The top layer hosts the funnel rotation system. It consists of 4 elements: 1) the funnel orientation motor, 2) the linear actuator that brakes the rotation, 3) the gear system to transmit the torque, and 4) the two bearings of the funnel.

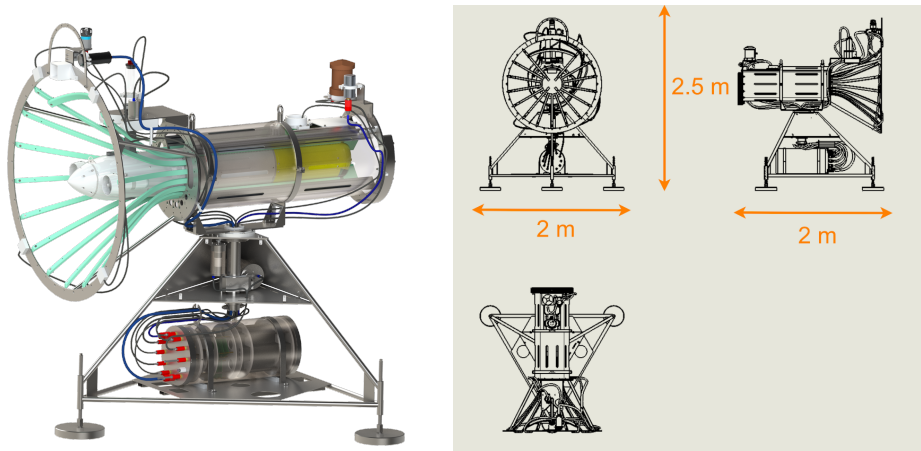


Figure 2: Conceptual representation of the Docking Station.

3.2.2 Funnel

The funnel is the assembly where the AUV docks, which includes (see Fig. 4) the following devices:

1. An USBL transponder/modem for localization and communication with the AUV (Blueprint Subsea Seatrack X110 (Blueprint Design Engineering Ltd, b)).
2. A camera to record the docking maneuvers.
3. A WiFi antenna for ultra-short-range high bandwidth communication. When docked, it allows the AUV to transmit the data logged during the mission to the DS.
4. A latching device, which clamps the AUV antenna to secure the position of the AUV inside the DS.
5. An inductive charger, developed by INESC TEC in the context of the ATLANTIS project.
6. An optical modem (10 MBs Luma X hydromea(Hydromea,)) , for wireless high bandwidth communication with the AUV.
7. A DVL to measure the ocean current vector at the DS site (NavQuest LinkQuest 600 Micro (LinkQuest Inc,)) to align the DS.

The funnel entrance is manufactured using polyethylene M AST PE-1000 which, thanks to its properties, helps to absorb the collision energy of the docking maneuver, passively guiding the AUV to the DS. The tripod is designed to receive the collision impacts transmitting the energy to the ground. Finally, to lower the power required to rotate the funnel, an adjustable counterweight is used for its balance.

3.3 Docking controller

The MSC is a guidance controller for a nonholonomic AUV (Esteba et al., 2023) which drives the vehicle to the DS selecting the appropriate surge-velocity and heading set-points. It guides the robot along a line parallel to the main axis of the DS. The line offset depends on the ocean current, ensuring that the AUV nose targets the center of the funnel. When the robot nose touches the funnel, a surge/pitch controller is used to push ensuring a smooth entrance. Fig. 6 shows the main variables involved in the controller. The

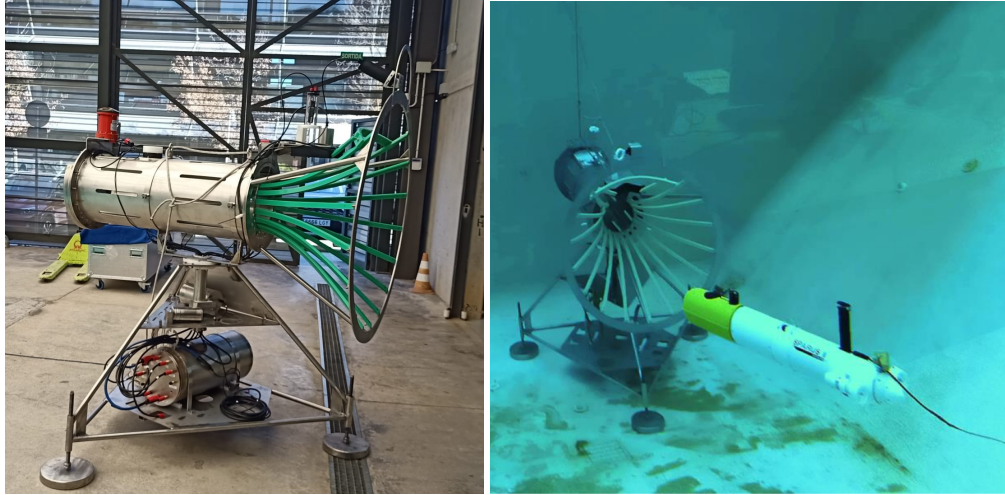


Figure 3: Docking Station photographies in the surface and into the CIRS (Centre d'Investigació en Robòtica Submarina) water tank with the Sparus II.

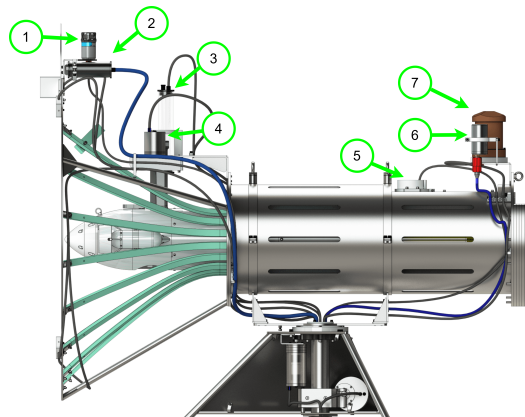


Figure 4: Sparus Docking Station funnel representation. 1) Acoustic modem from BluePrint Subsea, 2) camera, 3) WiFi antenna, 4) latching motor, 5) inductive charger from INESC TEC, 6) optical modem from Hydromea, 7) DVL from LinkQuest.

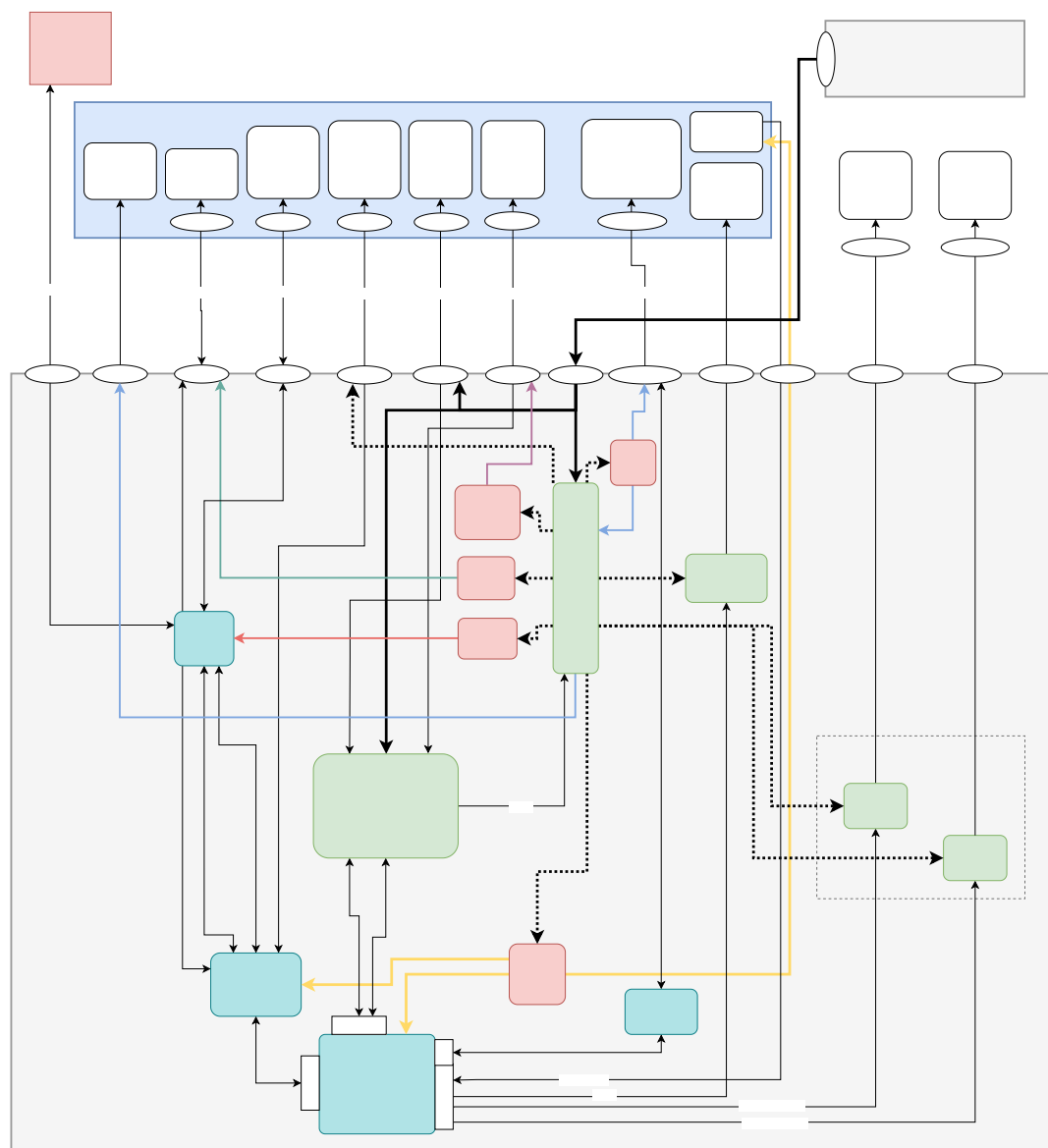


Figure 5: Docking Station basic electrical schematic from the main cylinder.

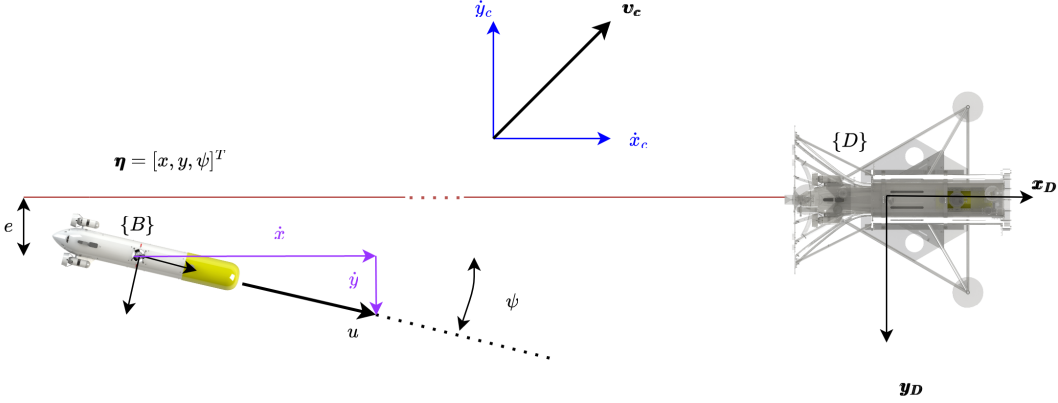


Figure 6: MSC basic variables representation.

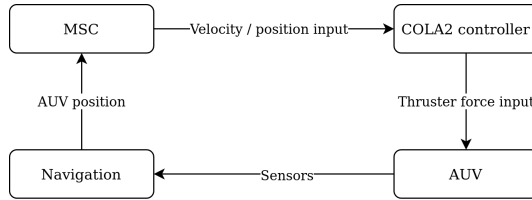


Figure 7: Conceptual representation of the Sparus II control system.

controller error dynamics are formulated as follows:

$$\dot{e} = u_d \sin(\psi) + \dot{y}_c, \quad (1)$$

where \dot{e} is the time derivative of the cross-track error, u_d is the desired surge velocity, ψ is the heading of the AUV, and \dot{y}_c is the projection of the ocean current velocity vector on the direction perpendicular to the DS main axis.

The controller law is defined as:

$$u_d = \frac{\dot{x}_{ss}}{\cos(\psi)} + c, \quad c = -k_1 \operatorname{atan}(k_2 e) \operatorname{sign}(\psi) \quad (2)$$

$$\psi_d = \psi_c - \operatorname{atan}\left(\frac{e}{\Delta}\right), \quad (3)$$

where \dot{x}_{ss} and \dot{y}_{ss} are the robot velocities with respect to water in the steady state (when the cross-track error vanishes to zero); k_1 , k_2 , and Δ are adjustable gains, e is the cross-track error, and ψ_c is a crab angle.

More details about the controller can be found in (Esteba et al., 2023), where its exponential stability is shown together with an exhaustive set of simulated results. The MSC was integrated into the vehicle's COLA2 (Palomeras et al., 2012) software architecture, acting as a guidance controller and issuing set-points to the velocity and heading vehicle controllers (see Fig. 7).

Once the AUV impacts the DS a constant surge velocity and a small pitch correction, are applied to achieve and smooth entrance. The pitch correction is achieved using the vertical thruster of the Sparus II AUV, taking advantage of the fact that the vehicle is touching with its nose the DS.

3.4 Inverted USBL navigation

In order to locate the DS, the AUV is equipped with an inverted USBL system, where the transceiver is mounted on the robot payload while the transponder is placed in the DS. To this aim, an Extended Kalman Filter (EKF) navigation method has been employed which fuses sensor data from a DVL, an Attitude and Heading Reference System (AHRS), a GPS, a depth sensor, and an USBL.

Following Fig. 8, let $\boldsymbol{\eta}_1 = [x \ y \ z]^T$ be the robot position in the NED *N-frame* and $\boldsymbol{\nu}_1 = [u \ v \ w]^T$ its linear velocity vector referenced to the body fixed *B-frame*, the robot state vector has been defined defined as:

$$\boldsymbol{x}_k = \begin{bmatrix} \boldsymbol{\eta}_1 \\ \boldsymbol{\nu}_1 \end{bmatrix} \quad (4)$$

Then, a constant velocity model with attitude input and acceleration noise is used as the motion model:

$$\bar{\boldsymbol{x}}_k = \mathbf{f}(\boldsymbol{x}_{k-1}, \boldsymbol{u}_k, \boldsymbol{w}_k) = \begin{bmatrix} \boldsymbol{\eta}_{1_{k-1}} + {}^N\mathbf{R}_B(\boldsymbol{u}_k + \boldsymbol{w}_{\boldsymbol{\eta}_{2_k}}) \left(\boldsymbol{\nu}_{k-1} \Delta t + \boldsymbol{w}_{\boldsymbol{\nu}_{1_k}} \frac{\Delta t^2}{2} \right) \\ \boldsymbol{\nu}_{k-1} + \boldsymbol{w}_{\boldsymbol{\nu}_{1_k}} \Delta t \end{bmatrix} \quad (5)$$

where $\boldsymbol{u}_k = [\phi \ \theta \ \psi]^T$ is the robot attitude measured with the AHRS, and $\boldsymbol{w}_k = [\boldsymbol{w}_{\boldsymbol{\eta}_{2_k}}^T \ \boldsymbol{w}_{\boldsymbol{\nu}_k}^T]^T$ is the motion model noise, composed of the AHRS noise $\boldsymbol{w}_{\boldsymbol{\eta}_{2_k}} = [w_\phi \ w_\theta \ w_\psi]^T$ and the acceleration noise $\boldsymbol{w}_{\boldsymbol{\nu}_k} = [w_{\dot{u}} \ w_{\dot{v}} \ w_{\dot{w}}]^T$. The filter is updated with the observations from the navigation sensors. The DVL, the AHRS, the GPS, and the depth sensor provide linear observations of components of the state vector:

$$\boldsymbol{z}_k = \mathbf{H}_k \cdot \boldsymbol{x}_k + \boldsymbol{v}_k \quad (6)$$

each one having its corresponding observation vector, matrix, and noise:

- **DVL:** Provides the robot velocity in the *B-frame*.

$$\begin{aligned} \boldsymbol{z}_{DVL} &= [z_u \ z_v \ z_w]^T, \quad \boldsymbol{v}_{DVL} = \mathcal{N}(\mathbf{0}, \mathbf{R}_{DVL}) \\ \boldsymbol{z}_{DVL} &= \mathbf{H}_k \cdot \boldsymbol{x}_k + \boldsymbol{v}_{DVL} \Rightarrow \mathbf{H}_k = [\mathbf{0}_{3 \times 3} \ \mathbf{I}_{3 \times 3}] \end{aligned}$$

- **GPS:** Provides the robot position in the *N-frame*.

$$\begin{aligned} \boldsymbol{z}_{GPS} &= [z_x \ z_y]^T, \quad \boldsymbol{v}_{GPS} = \mathcal{N}(\mathbf{0}, \mathbf{R}_{GPS}) \\ \boldsymbol{z}_{GPS} &= \mathbf{H}_k \cdot \boldsymbol{x}_k + \boldsymbol{v}_{GPS} \Rightarrow \mathbf{H}_k = [\mathbf{I}_{2 \times 2} \ \mathbf{0}_{2 \times 4}] \end{aligned}$$

- **Depth:** Provides the robot depth in the *N-frame*.

$$\begin{aligned} v_{depth} &= \mathcal{N}(0, \sigma_{depth}^2) \\ z_{depth} &= \mathbf{H}_k \cdot \boldsymbol{x}_k + v_{depth} \Rightarrow \mathbf{H}_k = [\mathbf{0}_{1 \times 2} \ 1 \ \mathbf{0}_{1 \times 3}] \end{aligned}$$

Regarding the USBL observation $\boldsymbol{z}_{USBL} = [z_x \ z_y \ z_z]^T$, the non-linear USBL observation equation is given by:

$$\begin{aligned} \boldsymbol{z}_{USBL} &= h_{USBL}(\boldsymbol{x}_k, \boldsymbol{v}_k) \\ &= \mathbf{F}_1^T \left((\ominus^B \boldsymbol{x}_U) \ominus (\mathbf{F}_1 \boldsymbol{\eta}_1 + \mathbf{F}_2 (\boldsymbol{\eta}_2 + \boldsymbol{v}_{AHRS})) \right) \oplus {}^N \boldsymbol{x}_D + \boldsymbol{v}_{USBL} \end{aligned} \quad (7)$$

where $\mathbf{F}_1 = [\mathbf{I}_{3 \times 3} \ \mathbf{0}_{3 \times 3}]^T$ and $\mathbf{F}_2 = [\mathbf{0}_{3 \times 3} \ \mathbf{I}_{3 \times 3}]^T$ are projection matrices, $\boldsymbol{\eta}_1$ is the robot position within the state vector, $\boldsymbol{u}_k = \boldsymbol{\eta}_2 = [\phi \ \theta \ \psi]^T$ is the robot attitude taken from the AHRS, ${}^N \boldsymbol{x}_D$ is the docking station pose in the *N-frame* and ${}^B \boldsymbol{x}_U$ is the pose of the USBL transponder in the *B-frame* (both of them

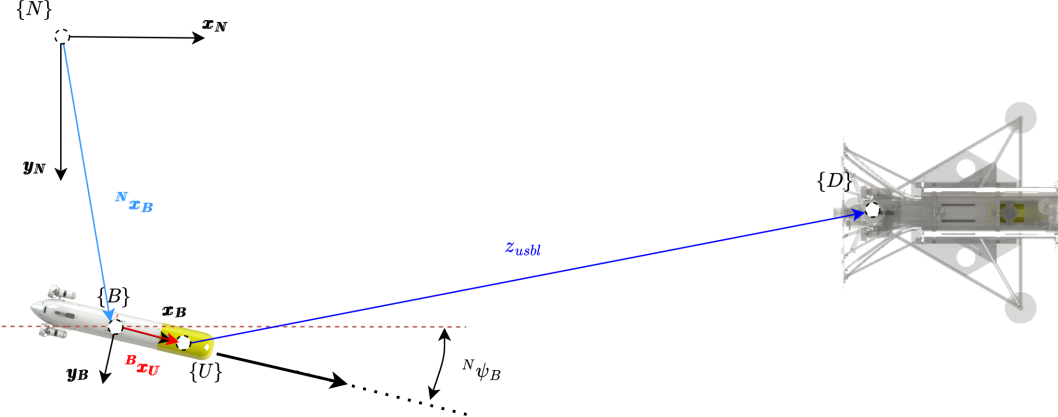


Figure 8: Reference systems used for the navigation.

constant and known a priori), while $\mathbf{v}_k = [v_{USBL}^T \ v_{AHRS}^T]^T = \mathcal{N}(\mathbf{0}, \mathbf{R}_k)$ is the observation noise. Then, the observation Jacobians are given by:

$$\begin{aligned} \mathbf{H}_k &= \frac{\partial h_{USBL}(\mathbf{x}_k, \mathbf{v}_k)}{\partial \mathbf{x}_k} = \frac{\partial h_{USBL}(\boldsymbol{\eta}_1, \boldsymbol{\eta}_2, \mathbf{v}_k)}{\partial [\boldsymbol{\eta}_1 \ \boldsymbol{\nu}_1]} = [\mathbf{F}_1^T \mathbf{J}_{1\oplus} \mathbf{J}_{2\ominus} \mathbf{F}_1 \quad \mathbf{0}_{3\times 3}] \\ \mathbf{V}_k &= \frac{\partial h_{USBL}(\mathbf{x}_k, \mathbf{v}_k)}{\partial \mathbf{v}_k} = \frac{\partial h_{USBL}(\mathbf{x}_k, \mathbf{v}_{USBL}, \mathbf{v}_{AHRS})}{\partial [\mathbf{v}_{USBL} \ \mathbf{v}_{AHRS}]} = [\mathbf{I}_{3\times 3} \quad \mathbf{F}_1^T \mathbf{J}_{1\oplus} \mathbf{J}_{2\ominus} \mathbf{F}_2] \end{aligned} \quad (8)$$

where $\mathbf{J}_{1\oplus}$ and $\mathbf{J}_{2\ominus}$ are the Jacobians of the 6 DoF compounding operation (Smith et al., 1990). Finally, it is worth noting that the observations update the filter only if they satisfy an individual compatibility Chi-Square test, at a certain confidence level, to avoid the adverse effect of the outliers.

4 Results

This section reports the results of the experimental validation of the proposed system. First, the experiment conceived for the validation is described in section 4.1. Next, the selected experimental sites are presented followed by the results (sections 4.3 and 4.4).

4.1 Validation Experiment

The validation experiment was conceived to emulate a typical survey during a LTD mission. The Sparus II AUV started docked at the DS (located at a priori known pose), then undocked, executed a survey, and docked again autonomously as shown in Fig. 9. Different surveys, of different duration, were tested in order to check the robot's capability to dock after a mission, the longest one reaching 90 min of duration and completing a successful dock. To evaluate the repeatability of the system, most of the surveys were reduced to a minimum duration. At the end of the survey (Fig. 10), the robot executed a docking maneuver. First, the robot navigated towards a home position (1) in front of the DS, receiving updates in position from the USBL (2), then it followed a straight line (3) towards the funnel entrance. As explained in Section 3.3, this line might be slightly misaligned with the DS axis, to account for the ocean current. An inverted USBL navigation method (Section 3.4) was used during the whole maneuver to cancel the drift, accumulated during the survey, of the DVL-based navigation (4). When the robot touched the funnel of the docking station (5) a

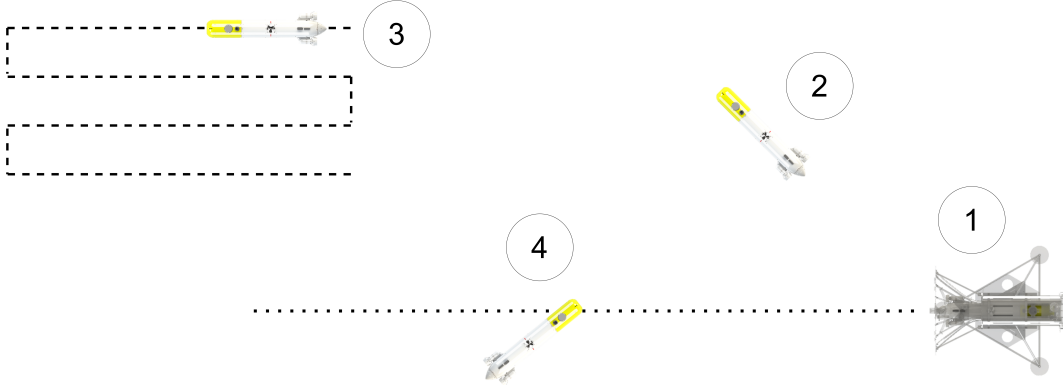


Figure 9: Experimental concept developed. 1) the Sparus II is inside the DS, 2) the Sparus II undocks and 3) performs the survey, 4) the docking maneuver is developed.

constant surge velocity and a small pitch correction, were applied to achieve a smooth entrance, completing the docking.

4.2 Experimental Setup

To test the experiment described above, the DS system was deployed in the calmed waters of the harbour of Sant Feliu (Girona, Spain), at 8 meters depth (Fig. 11, Fig. 12, and Fig. 13). Although the DS may self-orient according to the currents it measures, the absence of relevant currents in the harbour made us to adjust the DS heading manually (to maximise the maneuvering space) keeping it constant during the experiments. Therefore, the controller parameters were set as follows: $\psi_c = 0$; as reported in (Esteba et al., 2023) the gains were set as $k_1 = 0.4456 \text{ m/s}$, $k_2 = 1 \text{ m}^{-1}$, and $k_\Delta = 6 \text{ m}$. Finally, the desired docking velocity was set as $\dot{x}_{ss} = 0.3 \text{ m/s}$, to avoid strong collisions between the AUV and the DS. The controller was executed at a frequency of 100 Hz, with a navigation frequency of 15 Hz and including USBL fixes approximately every 2 seconds.

A second field deployment took place in the ATLANTIS Test Centre (INESC TEC,) (Fig.14), in Viana do Castelo (Porto, Portugal), at 8 meters depth with tides up to 2 meters. The DS location is shown in Fig.15. The test center is placed in the harbour, next to the mouth of the river Lima. There, the underwater visibility is very low as shown in Fig. 15 and Fig. 16, clearly justifying our docking strategy based only on acoustic sensor feedback. Again, the harbor protection made the current negligible.

4.3 Results in Sant Feliu

The validation began with several engineering tests to adjust the covariance matrices of the navigation sensors to achieve the required navigation accuracy. A batch of ten tests was performed first, achieving eight successful docking maneuvers and two failures. Fig. 17a shows the time evolution of the cross-tracking error of a representative successful test. It can be appreciated that at time -40 seconds an USBL fix (red line) arrives, updating the robot position estimate and, consequently, growing the cross-track error around 3 meters. This update is mostly attributed to the accumulated navigation drift. As expected, the MSC controller reacts, driving the robot in a direction minimizing the error, and successfully docking the vehicle. The MSC output variables, the heading, and the surge velocity are shown in Fig. 17. The heading is shown in Fig. 17b, where can be appreciated the reaction to the cross-track error, turning the robot towards the

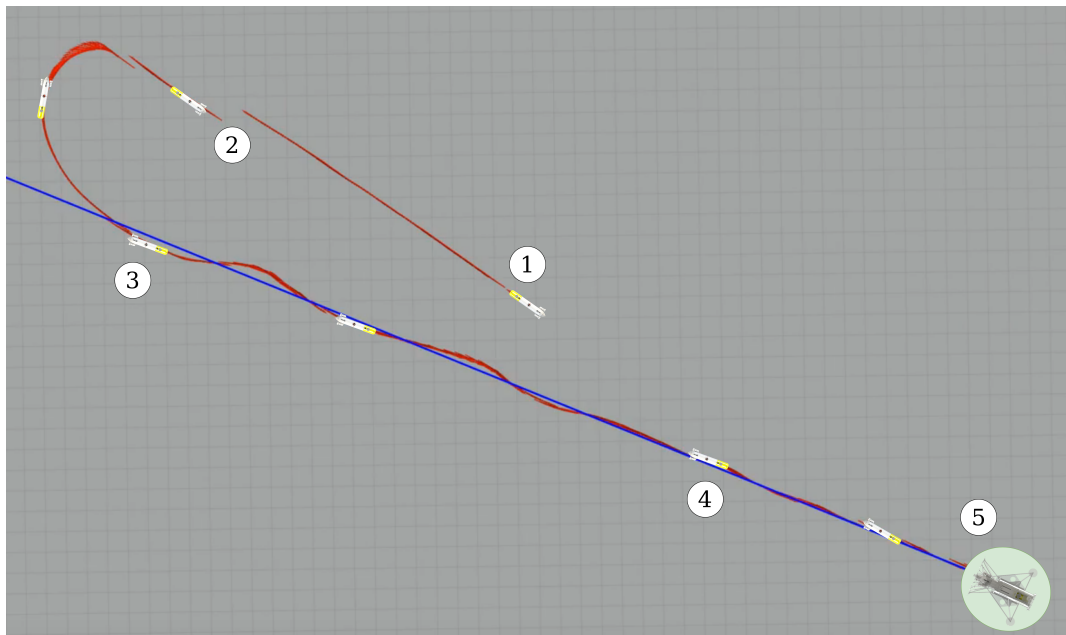


Figure 10: Navigation of one autonomous docking example. 1) The Sparus II receives the command to start the docking maneuver, 2) the USBL applies an update to the Sparus II position, 3) the MSC controller starts, 4) while the AUV gets closer to the DS it's position is updated and the MSC has to react, 5) the AUV successfully docks.

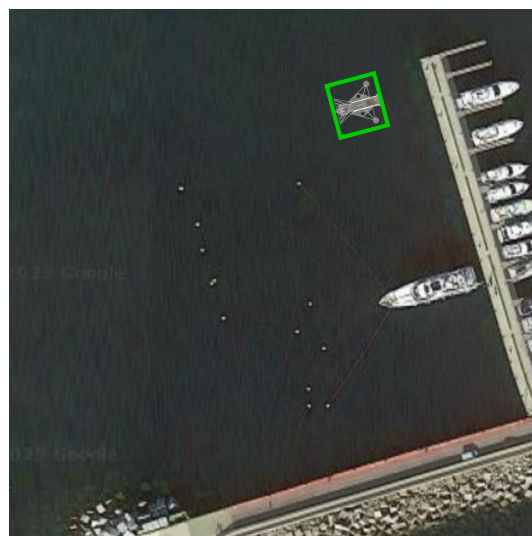


Figure 11: Location of the DS, Sant Feliu de Guíxols harbor. Image obtained from Google Maps. Note that for a better understanding, the DS is not in the correct scale.

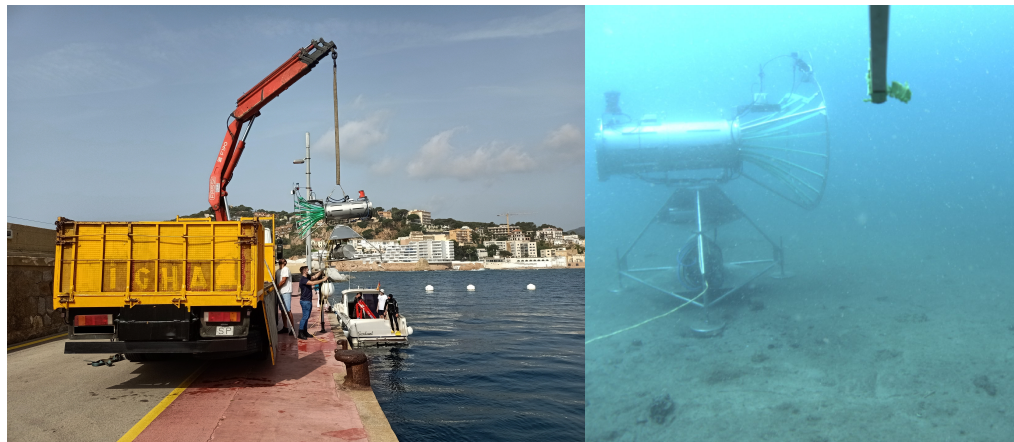


Figure 12: On the left deployment of the DS at Sant Feliu de Guíxols harbor. On the right, DS inside the harbor of Sant Feliu de Guíxols.

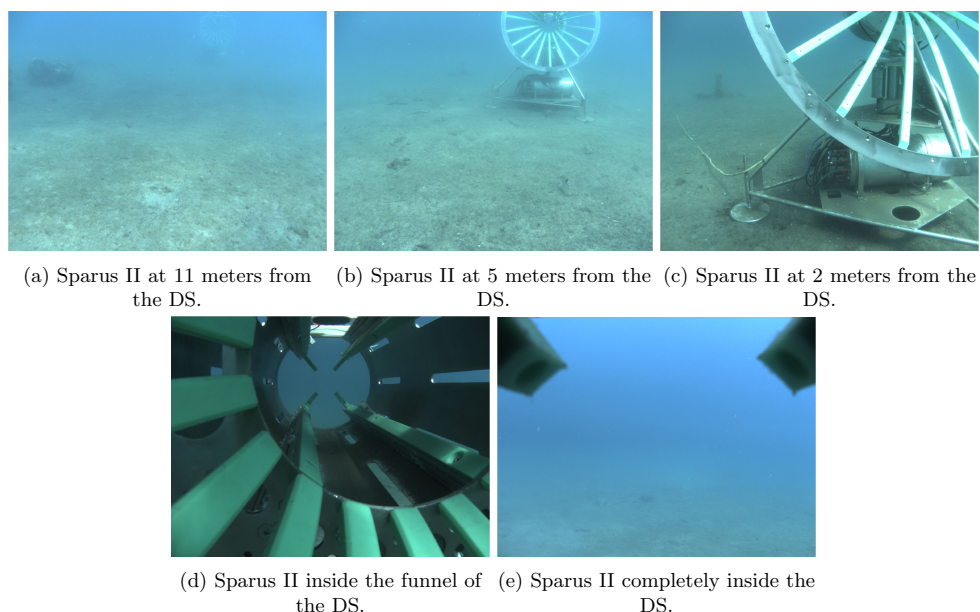


Figure 13: Frame sequence of the forward-looking camera of the Sparus II, developing an experimental autonomous docking in Sant Feliu de Guíxols.

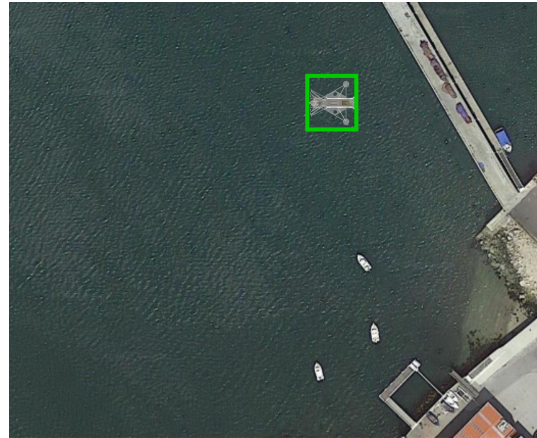


Figure 14: Location of the DS, Viana do Castelo harbor. Image obtained from Google Maps. Note that for a better understanding, the DS is not in the correct scale.

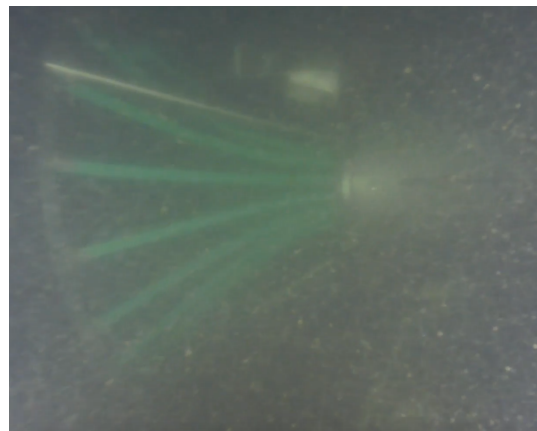


Figure 15: DS inside the harbor of Viana do Castelo.

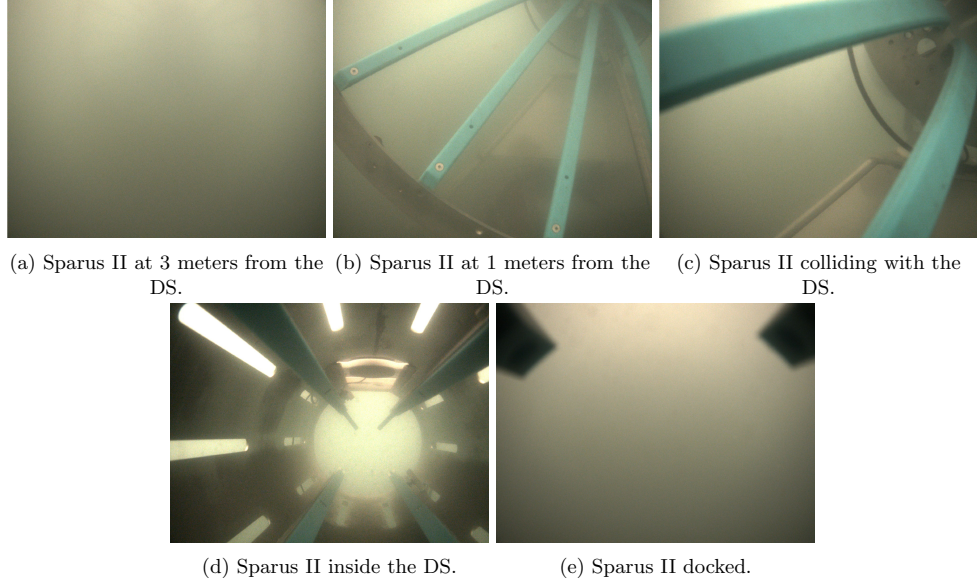


Figure 16: Frame sequence of the forward-looking camera of the Sparus II, developing an experimental autonomous docking in Viana do Castelo.

Quality of the entrance into the DS: Sant Feliu							
Trial	#1	#2	#3	#4	#5	#6	#7
g	0.1192	0.8399	0.5263	0.9460	0.1172	0.9036	0.8252

Table 2: Analysis of the quality in the entrance of the AUV when it impacts to the DS (Esteba et al., 2021), for the last batch of tests developed in Sant Feliu de Guíxols.

entrance line. The surge velocity set-point (eq. (2)), modifies the surge speed to reduce the cross-track error either accelerating or reducing the speed (Fig. 17c and Fig. 17d). It is worth noting that the AUV desired velocity set to impact the DS (\dot{x}_{ss}) is 0.3 m/s , from which it is applied the correction (c), recall (2). Fig. 13 shows a sequence of images gathered with the frontal camera of Sparus II AUV, to illustrate the docking maneuver. With respect to the failed experiments, the first one, shown in Fig. 18a, was due to the absence of USBL fixes during the last 20 seconds of the mission, which caused a navigation drift. In this case, the cross-track error was driven to zero, but due to the navigation drift, the actual error was higher than the radius of the funnel entrance failing the docking. In the case of the second failure (Fig. 18b), the USBL updates make the robot aware it was located at the left of the DS beginning, therefore, a correction action. Unfortunately, too late to achieve the docking. The navigation system caused both failures, and therefore, the noise covariance matrix was adjusted to rise the influence of the USBL updates. Finally, a second batch of tests was launched, achieving seven consecutive autonomous docking maneuvers (see Fig. 19 and table 2), being considered as successful trial.

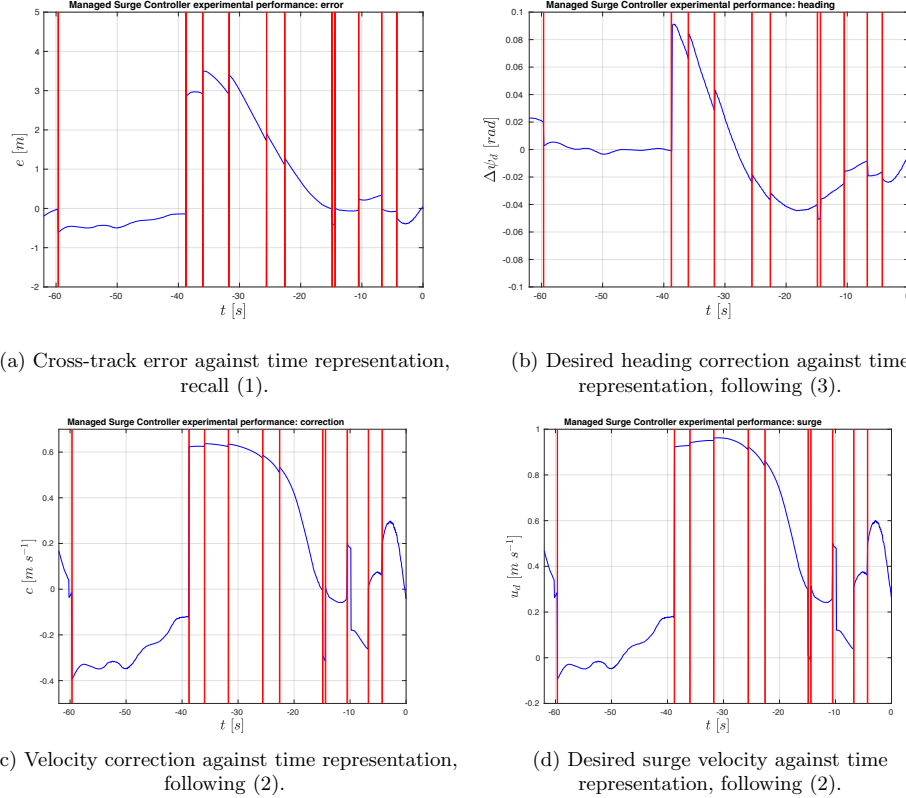


Figure 17: Representation of the performance of the MSC in one docking maneuver. Each vertical red line represents an update of the position of the AUV.

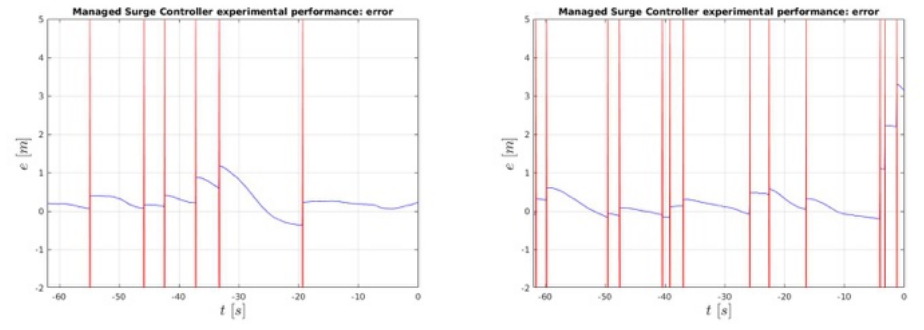


Figure 18: Representation of the error of the position of the AUV in the two failed maneuvers of the first test batch developed in Sant Feliu de Guíxols. Each vertical red line represents an update of the position of the AUV.

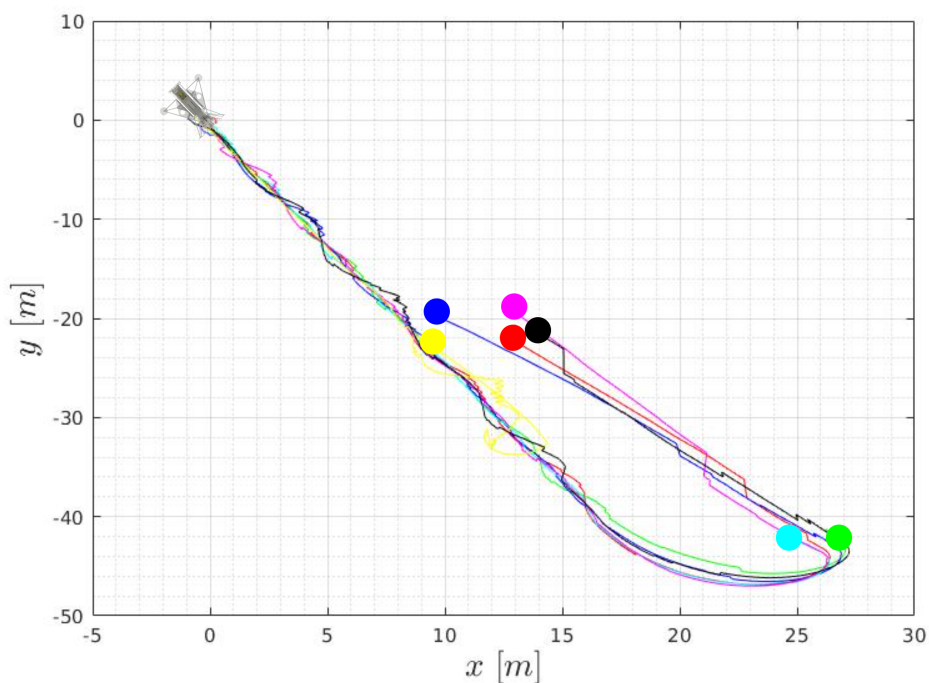


Figure 19: Representation of the seven autonomous docking maneuvers performed in Sant Feliu de Guíxols. Each color represents a different attempt. For the clarity of the image, the scale of the DS is not realistic, and a circle is represented at the beginning of each trajectory.

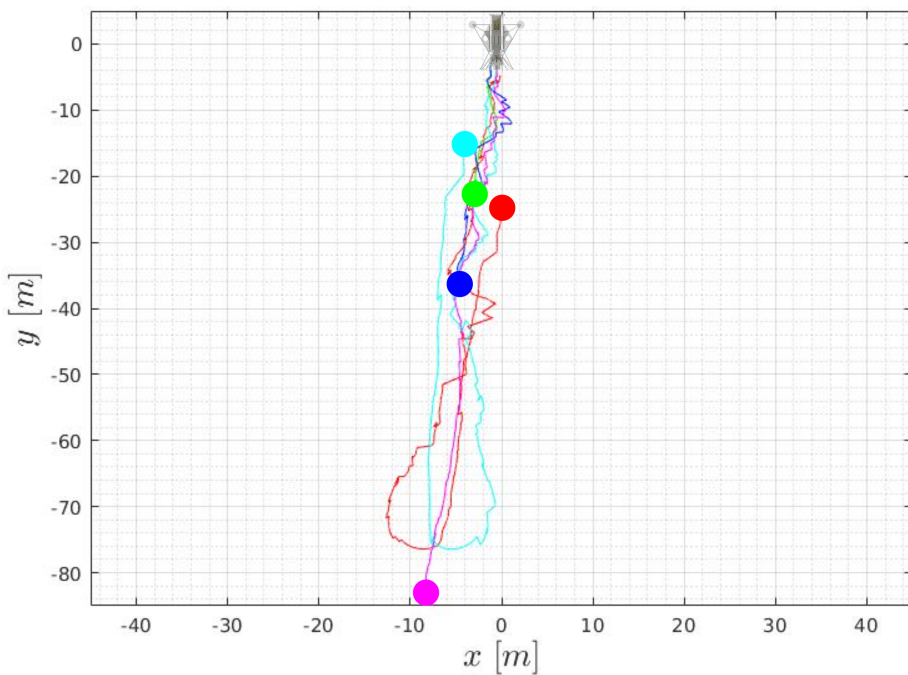


Figure 20: Representation of the seven autonomous docking maneuvers performed in Viana do Castelo. Each color represents a different attempt. For the clarity of the image, the scale of the DSis not realistic, and a circle is represented at the beginning of each trajectory.

Quality of the entrance into the DS: Viana					
Trial	#1	#2	#3	#4	#5
g	0.9513	0.4003	0.5765	0.7765	0.3881

Table 3: Analysis of the quality in the entrance of the AUV when it impacts to the DS (Esteba et al., 2021), for the last batch of tests developed in Viana do Castelo.

4.4 Results in Viana do Castello

Due to the water exchange between the river and the ocean, significant changes in salinity were observed depending on the area and depth. This affects the performance of the acoustic sensors, and degrades their performance, requiring further tuning of the navigation filter. Moreover, in this location, the time for testing was more restricted, due to the schedule of the experimental trials, the weather, and the vessel traffic. In these conditions, nine experiments were performed, the first four devoted to engineering trials and tuning, finalising with a batch of five consecutive docking maneuvers (table 3 and Fig. 20). Fig. 16 shows a camera frame sequence of a representative successful docking operation, where it can be appreciated the low visibility conditions of the area. As commented above, selecting a docking strategy based only on acoustic sensors feedback proved to be the right chose.

5 Conclusions

This paper presents a Long Term Deployment system for a non-holonomic AUV. The system is based on a motorized funnel-based docking station sensorized to be able to detect currents and self-align with them. The use of visual servoing methods to guide the docking has been explicitly avoided, to be able to operate in low visibility conditions. Therefore, the relative DS AUV navigation is tackled through an inverted USBL system conveniently integrated with the AUV navigation. The MSC algorithm, accounting for the ocean currents, has been employed to guide the docking. The system has been extensively tested in the field, using the Sparus II AUV, first in a harbor in Sant Feliu (Spain) and later on, in the ATLANTIS test center in Viana do Castelo (Portugal). In both cases with satisfactory results.

6 Future work

Future work will focus on testing the system under the influence of ocean currents. Unfortunately, this depends on the environmental conditions of the experimental site, as well as on the available logistics for the deployment, therefore, requiring detailed planning and preparation. Besides, we are conducting an energy consumption study and optimization of the DS, to guarantee long-term energetic autonomy.

Acknowledgments

The authors would like to thank the ATLANTIS consortium and in particular, the INESTEC team who provided the inductive charger used in the AUV and the DS.

Abbreviations

AUV Autonomous Underwater Vehicles

ROV Remotely Operated Vehicles

DS Docking Station

SDS Sparus Docking Station

MSC Managed Surge Controller

USBL Ultra Short BaseLine

EKF Extended Kalman Filter

AHRS Attitude and Heading Reference System

PID Proportional-integral-derivative controller

COLA2 Component orientated layer-based architecture for autonomy

ROS Robot Operating System

IMU Inertial Measurement Unit

DVL Doppler Velocity Log

GPS Global Positioning System

NED North, East, Down

LTD Long Term Deployment

LaRS Launch and Recovery System

UdG Universitat de Girona

DoF Degree of Freedom

COLA2 Component Orientated Layer-based Architecture for Autonomy

References

- Allen, B., Austin, T., Forrester, N., Goldsborough, R., Kukulya, A., Packard, G., Purcell, M., and Stokey, R. (2006). Autonomous Docking Demonstrations with Enhanced REMUS Technology. *Oceans 2006*, pages 1–6.
- Bellingham, J. G. (2016). Autonomous Underwater Vehicle Docking. In *Springer Handbook of Ocean Engineering*, chapter 16, pages 387–406. Springer, Cham.
- Bluelogic. Bluelogic subsea docking station. <https://www.bluelogic.no/news-and-media/subsea-docking-station-sds->. [Online; accessed 2023-01-31].
- Blueprint Design Engineering Ltd. Blueprint subsea oculus imaging sonar. <https://www.blueprintsubsea.com/oculus/oculus-m-series>. [Online; accessed 2022-09-21].
- Blueprint Design Engineering Ltd. Blueprint subsea seatrac x150 usbl beacon. <https://www.blueprintsubsea.com/seatrac/>. [Online; accessed 2022-09-21].
- Carreras, M., Candela, C., Ribas, D., Mallios, A., Magí, L. L., Vidal, E., Palomeras, N., and Ridao, P. (2013). Sparus {II}, design of a lightweight hovering {AUV}. *Proceedings of the 5th international workshop on marine technology. Martech'13*, pages 152–155.
- Carreras, M., Hernandez, J. D., Vidal, E., Palomeras, N., Ribas, D., and Ridao, P. (2018). Sparus II AUV - A Hovering Vehicle for Seabed Inspection. *IEEE Journal of Oceanic Engineering*, 43(2):344–355.
- Circle, B. N. (2012). Underwater mobile docking of autonomous underwater vehicles. *OCEANS 2012 MTS/IEEE: Harnessing the Power of the Ocean*, pages 1–15.
- Esteba, J., Cieslak, P., Palomeras, N., and Ridao, P. (2021). Docking of Non-holonomic AUVs in Presence of Ocean Currents: a Comparative Survey. *IEEE Access*.
- Esteba, J., Cieslak, P., Palomeras, N., and Ridao, P. (2023). Managed Surge Controller : A Docking Algorithm for a Non-Holonomic AUV (Sparus II) in the Presence of Ocean Currents for a Funnel-Shaped Docking Station. *Sensors*, 23.
- Feezor, M. D., Sorrell, F. Y., Blankinship, P. R., and Bellingham, J. G. (2001). Autonomous underwater vehicle homing/docking via electromagnetic guidance. *IEEE Journal of Oceanic Engineering*, 26(4):515–521.
- Fletcher, B., Martin, S., Flores, G., Jones, A., Nguyen, A., Brown, M. H., and Moore, D. L. (2017). From the lab to the ocean: Characterizing the critical docking parameters for a free floating dock with a REMUS 600. *OCEANS 2017 - Anchorage*, 2017-Janua:1–7.
- Hydromea. Luma x. <https://www.hydromea.com/underwater-wireless-communication>. [Online; accessed 2022-09-21].
- INESC TEC. Atlantis test center promotional video. <https://youtu.be/7QW24hzuo50>. [Online; accessed 2022-12-12].
- Kawasaki, T., Noguchi, T., Fukasawa, T., Hayashi, S., Shibata, Y., Iimori, T., Okaya, N., Fukui, K., and Kinoshita, M. (2004). "Marine Bird," a new experimental AUV - Results of docking and electric power supply tests in sea trials. *Ocean '04 - MTS/IEEE Techno-Ocean '04: Bridges across the Oceans - Conference Proceedings*, 3:1738–1744.
- Kukulya, A., Plueddemann, A., Austin, T., Stokey, R., Purcell, M., Allen, B., Littlefield, R., Freitag, L., Koski, P., Gallimore, E., Kemp, J., Newhall, K., and Pietro, J. (2010). Under-ice operations with a REMUS-100 AUV in the Arctic. *2010 IEEE/OES Autonomous Underwater Vehicles, AUV 2010*, pages 1–8.

- LinkQuest Inc. Navquest micro dvl 600. https://www.link-quest.com/html/intro_nq.htm. [Online; accessed 2022-09-21].
- Mbari. Mars system from mbari. <https://www.mbari.org/technology/monterey-accelerated-research-system-mars/>. [Online; accessed 2023-01-31].
- McEwen, R. S., Hobson, B. W., Bellingham, J. G., and McBride, L. (2008). Docking control system for a 54-cm-diameter (21-in) AUV. *IEEE Journal of Oceanic Engineering*, 33(4):550–562.
- Nicholson, J. and Healey, A. (2013). The Present State of Autonomous Underwater Vehicle (AUV) Applications and Technologies. *Marine Technology Society Journal*, 47(5):5–6.
- Page, B. R. and Mahmoudian, N. (2020). Simulation-Driven Optimization of Underwater Docking Station Design. *IEEE Journal of Oceanic Engineering*, 45(2):404–413.
- Palomeras, N., El-Fakdi, A., Carreras, M., and Ridao, P. (2012). COLA2: A control architecture for AUVs. *IEEE Journal of Oceanic Engineering*, 37(4):695–716.
- Palomeras, N., Vallicrosa, G., Mallios, A., Bosch, J., Vidal, E., Hurtos, N., Carreras, M., and Ridao, P. (2018). AUV homing and docking for remote operations. *Ocean Engineering*, 154(May 2017):106–120.
- Park, J. Y., huan Jun, B., mook Lee, P., and Oh, J. (2009). Experiments on vision guided docking of an autonomous underwater vehicle using one camera. *Ocean Engineering*, 36(1):48–61.
- Park, J. Y., Jun, B. H., Lee, P. M., Oh, J. H., and Lim, Y. K. (2010). Underwater docking approach of an under-actuated AUV in the presence of constant ocean current. *IFAC Proceedings Volumes (IFAC-PapersOnline)*, 43(20):5–10.
- Pinto, A. M., Marques, J. V., Campos, D. F., Abreu, N., Matos, A., Jussi, M., Berglund, R., Halme, J., Tikka, P., Formiga, J., Verrecchia, C., Langiano, S., Santos, C., Sa, N., Stoker, J. J., Calderoni, F., Govindaraj, S., But, A., Gale, L., Ribas, D., Hurtos, N., Vidal, E., Ridao, P., Chieslak, P., Palomeras, N., Barberis, S., and Aceto, L. (2021). ATLANTIS - The Atlantic Testing Platform for Maritime Robotics. *Oceans Conference Record (IEEE)*, 2021-Septe:1–5.
- Quigley, M., Gerkey, B., Conley, K., Faust, J., Foote, T., Leibs, J., Berger, E., Wheeler, R., and Ng, A. (2009). ROS: an open-source Robot Operating System. *ICRA workshop on open source software*.
- Raspberry Pi. Raspberry pi official website. <https://www.raspberrypi.com/products/raspberry-pi-3-model-a-plus/>. [Online; accessed 2023-01-31].
- Sarda, E. I. and Dhanak, M. R. (2019). Launch and Recovery of an Autonomous Underwater Vehicle from a Station-Keeping Unmanned Surface Vehicle. *IEEE Journal of Oceanic Engineering*, 44(2):290–299.
- Singh, H., Bellingham, J. G., Hover, F., Lerner, S., Moran, B. A., Von Der Heydt, K., and Yoerger, D. (2001). Docking for an autonomous ocean sampling network. *IEEE Journal of Oceanic Engineering*, 26(4):498–514.
- Smith, R., Self, M., and Cheeseman, P. (1990). *Estimating Uncertain Spatial Relationships in Robotics*, pages 167–193. Springer New York, New York, NY.
- Stokey, R., Allen, B., Austin, T., Goldsborough, R., Forrester, N., Purcell, M., and Von Alt, C. (2001). Enabling technologies for REMUS docking: An integral component of an autonomous ocean-sampling network. *IEEE Journal of Oceanic Engineering*, 26(4):487–497.
- Stokey, R., Purcell, M., Forrester, N., Austin, T., Goldsborough, R., Allen, B., and von Alt, C. (1997). Docking system for REMUS, an autonomous underwater vehicle. *Oceans Conference Record (IEEE)*, 2:1132–1136.
- Universitat de Girona. Ophirov research project official website. <https://ophirov.udg.edu/>. [Online; accessed 2022-12-21].

- Universitat de Girona. Plome research project official website. <https://plomeproject.es/>. [Online; accessed 2022-12-21].
- Whitcomb, L. L. (2000). Underwater robotics: out of the research laboratory and into the field. *Proceedings - IEEE International Conference on Robotics and Automation*, 1:709–716.
- Yazdani, A. M., Sammut, K., Yakimenko, O., and Lammas, A. (2020). A survey of underwater docking guidance systems. *Robotics and Autonomous Systems*, 124.
- Zhang, T., Li, D., and Yang, C. (2017). Study on impact process of AUV underwater docking with a cone-shaped dock. *Ocean Engineering*, 130(December 2016):176–187.

5

RESULTS AND DISCUSSION

IN this chapter the author summarizes and discusses not only the results published, but also presents the relevant results that had not been published yet.

5.1 Summary of the completed work

In this thesis, we have focused on developing the LTD technology. The main results published are related to the Sparus II AUV autonomous docking, but results complementary to that were also achieved.

Chapter 2 covers the state of the art of the main DS systems published in the literature. Its analysis lead us to the study of the state of the art strategies for docking a non-holonomic AUV in a funnel-shaped DS. A new metric to evaluate the quality of the entrance of the AUV inside the DS is proposed. This metric has been applied to the studied docking strategies within a common simulated framework, to compare them in a methodical way. Three simulated scenarios have been considered to evaluate each strategy. First, the ideal situation was considered, neglecting the noise in the localization and the ocean current detection, and assuming a docking velocity larger than the ocean currents velocity. The second scenario, included sensor noise, within the ocean current velocity and the AUV localization. From the authors' experience, Sparus II AUV can deal with ocean currents up to 0.5 m/s , and it was defined, as a design criterion, a docking velocity of 0.3 m/s . It is worth noting that, the docking velocity corresponds to the velocity with respect to the ground that the AUV is desired to have at the moment of impact to the DS and in extension, is the velocity with respect to the ground that the AUV will have approaching the DS. From these considerations, a new paradigm that was not considered before, from the author's knowledge, in the literature, appeared: how to develop a docking maneuver with an ocean current velocity bigger than the docking velocity. In the third scenario, the docking velocity was reduced to 0.3 m/s with the objective of analyzing the performance of the strategies with this new paradigm. This analysis concluded with a categorization of the strategies and an exposition of the strong points of each method, allowing us to conclude if the state of the art strategies fits the demands of the Sparus II AUV LTD DS system.

In Chapter 3, we proposed a new docking controller. When the ocean currents are considered for docking with a non-holonomic AUV, they used to be seen as a disadvantage; in this novel approach, they are used in favor of the maneuver. If a non-holonomic AUV has to follow a line in the presence of ocean currents it is needed to apply a crab angle to compensate for the effect of the lateral ocean current velocity. It is worth remarking that the crab angle, in the presence of ocean currents, allows the robot to follow a straight trajectory (with respect to the ground) maintaining an angular offset with respect to the surge velocity vector. The key point of the new proposal is to use the surge velocity not only to advance compensating for the ocean current, but also to reduce the cross-track error. The classical cross-track error controller relies on the control of the heading of the AUV to reduce the cross-track error. For a non-holonomic AUV like Sparus II, this leads to a slow convergence of the error. Our proposal combines the classical cross-track error controller for correcting big errors in a slower way, with the surge control to reduce faster the cross-track error when it is smaller. This strategy is inspired by the Sparus II thrusters configuration (two steering thrusters in the horizontal plane), allowing for a faster change of the surge velocity than the heading. Also, this novel proposal considers the situation previously presented in Chapter 2: when the ocean current velocity is bigger than the docking velocity. The exponential stability of this new strategy was demonstrated from a mathematical point of view, tested in simulation, and compared with the algorithms presented in Chapter 2 in the third scenario; obtaining the best performance.

In Chapter 4, we developed a new **DS** system for the Sparus II **AUV**. First, we designed and manufactured a new **DS**, explained more in detail in Appendix A. Then we integrated an inverse **USBL** system to the Sparus II navigation. Usually, in the **UdG** applications, the acoustic localization based on the **USBL** technology places the transceiver on the boat and the transponder on the **AUV**. In this development, we acquired a **USBL** system small enough to fit it in the Sparus II **AUV** payload, and in consequence, the transponder was assembled in the **DS**. This system allowed us to localize the position of the **DS** with respect to the **AUV**, considering that the position of the **DS** with respect to the world is known (from a previous calibration procedure), the position of the **AUV** with respect to the world was continuously updated. For achieving the integration of the **USBL** to the navigation of the **AUV**, several engineering tests were conducted. Finally, the docking algorithm presented in Chapter 3 was tested in a real environment. The trials took place in two different sites, in Sant Feliu de Guíxols (Spain) and in Viana do Castelo (Portugal). In the harbor of Sant Feliu de Guíxols, we were able to deploy and test the **DS** for several days without major vessel traffic disturbance, with neglectable ocean currents, and with good visibility, allowing us the use of monitoring cameras. As presented in Chapter 4, it can be considered that robust autonomous docking was achieved, being able to successfully dock seven consecutive times after different missions. In the context of the ATLANTIS research project, the system was tested later on in Viana do Castelo. In this case, the testbed offered a more restricted scenario. Testing time was more limited and conditioned by the vessel traffic and the weather. Also, being this testbed in the mouth of a river to the ocean some side-effects happened. First, the water density was not constant, affecting the performance of the acoustic sensors, increasing the dead reckoning error compared with the one usually observed in Sant Feliu. Second, because of the high amount of mud particles in the water, the light absorption was significant, not allowing intuitive monitoring of the system through cameras. Again, several consecutive autonomous docking maneuvers were achieved, proving the robustness of the system and proving the utility of the acoustic localization system in real conditions.

5.2 Ocean current observer

In this section, a proposal for a passive ocean current observer with a non-holonomic vehicle is presented.

5.2.1 Context and motivation

The ocean currents are a critical factor when a non-holonomic **AUV** has to develop the docking maneuver. With the purpose of reducing the required distance for the docking maneuver, it is desirable to know a priori the ocean current velocity vector; otherwise, it has to be calculated during the maneuver, increasing its length. In this thesis, the docking maneuver presented relies on the knowledge of the ocean current vector to calculate the crab angle, as it is presented in Chapter 3 and Chapter 4.

The original idea to estimate the ocean current velocity vector was to rely on the Doppler Velocity Log (**DVL**) from the **DS**. But the **DVL** used needs at least 15 meters of water column in order to calculate the ocean current velocity, being deployed in shallow water (8 meters), it was not able to obtain a reliable observation. In addition, the **DVL** of the Sparus II faced the same problem, navigating at approximately 2 meters of altitude, it was not able to estimate the ocean current velocity vector.

From this problem, the use of a passive observer is proposed.

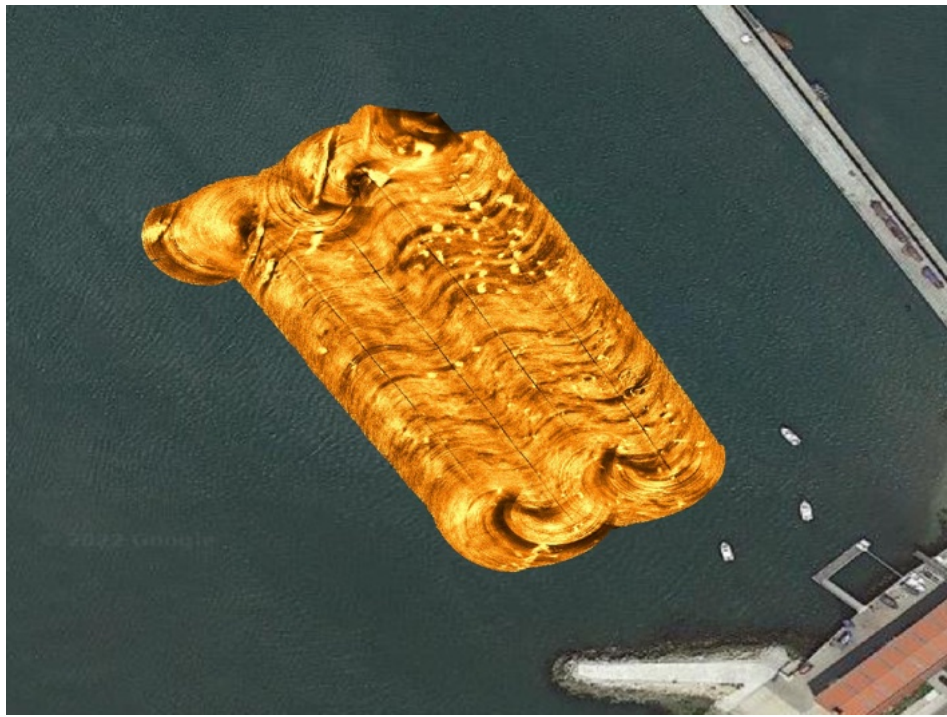


Figure 5.1: Example of the result of a survey developed with the Sparus II AUV, using a forward-looking sonar [18], processed with SounTiles [19] with the collaboration of IQUA Robotics. The survey was performed in Viana do Castelo (Portugal), in the context of the ATLANTIS research project [14].

5.2.2 Oportunity

A key point of the proposal is to understand the demands of the application developed for the ATLANTIS research project [14].

In the project, for maintenance (inspection) reasons, it was required that the Sparus II develop a survey, using a forward-looking sonar [18] for scanning the seabed related to the windfarm (or in the case of the tests, related to the pilot structure), see Fig. 5.1. The complete application about Sparus II AUV was to start from the DS, perform the survey, and return to the DS; all the tasks were performed in an autonomous way.

The proposal is based on taking profit of the survey performed for the seabed sonar observation, to observe the ocean current velocity vector.

5.2.3 Concept

When a non-holonomic AUV wants to follow a straight line and has to deal with a constant ocean current velocity, it has to apply a crab angle to compensate for the lateral ocean velocity with respect to the robot, recall Chapter 3. When the steady state is reached, the crab angle is constant.

The controller applied to perform the survey is a standard proportional cross-track error controller, that follows the nomenclature presented in Chapter 3:

$$\psi_d = \text{atan} \left(\frac{-e}{\Delta} \right). \quad (5.1)$$

Being ψ_d the desired heading of the AUV, e the cross-track error, and Δ a gain set to 5.5. When this controller achieves a steady state in the presence of ocean currents, it converges to

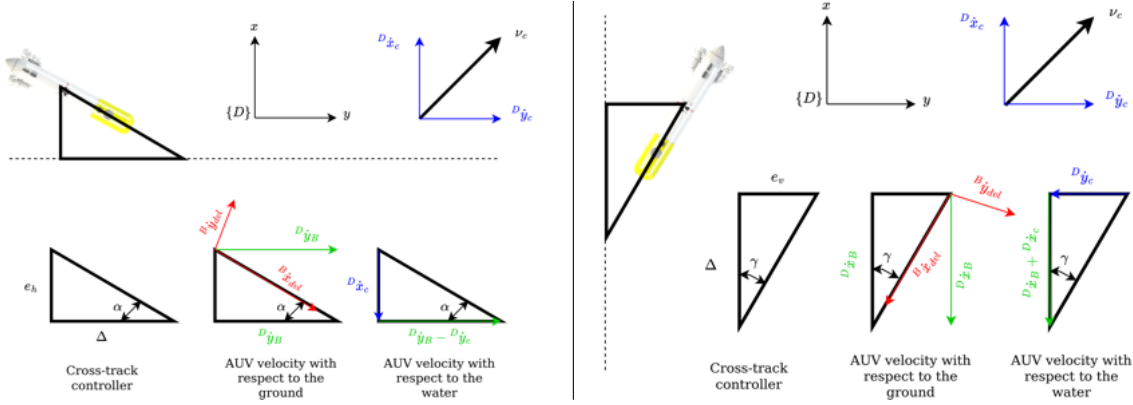


Figure 5.2: Representation of the horizontal (left) and the vertical (right) ocean current observation, when the steady state is achieved.

a constant e . The strategy of this ocean current observer is to achieve the steady state with the controller and observe the e .

To establish the ocean current velocity vector, two observations have to be done, ideally one perpendicular to the second. For simplification of the nomenclature, the first will be called horizontal observation, and the second, vertical observation.

5.2.3.1 Horizontal observation

The steady state of the horizontal case is represented on the left in Fig. 5.2; where $\{D\}$ represents the **DS** frame, $\{B\}$ the body (robot) frame, $\nu_c = [^D\dot{x}_c, ^D\dot{y}_c]$ the ocean current velocity, $[^B\dot{x}_{dvl}, ^B\dot{y}_{dvl}]$ the velocity with respect to the ground observed from the AUV's DVL, and $[^D\dot{x}_B, ^D\dot{y}_B]$ the robot velocity with respect to the ground on $\{D\}$ frame.

From Fig. 5.2, following the Tales theorem it can be obtained:

$$\frac{e_h}{\Delta} = \frac{^D\dot{x}_c}{^D\dot{y}_B - ^D\dot{y}_c}, \quad (5.2)$$

and from the second triangle,

$$^D\dot{y}_B = {}^B\dot{x}_{dvl,h} / \cos(\alpha). \quad (5.3)$$

Finally, applying the reference system of the robot, $\alpha = \psi_h - \pi/2$, to (5.2) and (5.3), it can be obtained:

$$^D\dot{x}_c = \frac{e_h \left[{}^B\dot{x}_{dvl,h} / \cos(\psi_h - \pi/2) - ^D\dot{y}_c \right]}{\Delta} \quad (5.4)$$

5.2.3.2 Vertical observation

The steady state of the vertical case is represented on the right in Fig. 5.2, from it, applying the Tales theorem can be obtained:

$$\frac{e_v}{\Delta} = \frac{^D\dot{y}_c}{^D\dot{x}_B + ^D\dot{x}_c}, \quad (5.5)$$

and from the second triangle:

$$^D\dot{x}_B = {}^B\dot{x}_{dvl,v} / \cos(\gamma). \quad (5.6)$$

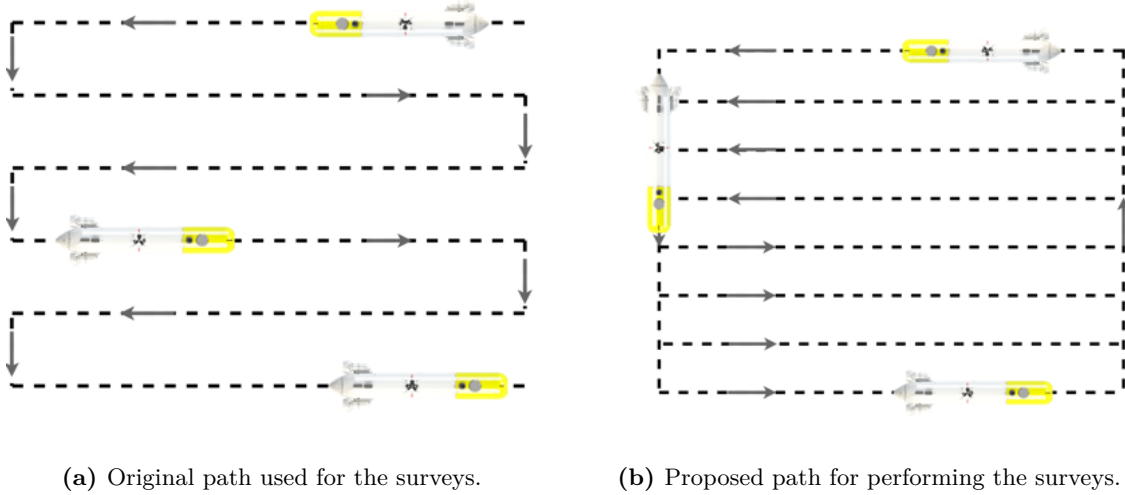


Figure 5.3: Conceptual path representation for the development of a survey with a forward-looking sonar.

Finally, applying the reference system of the robot, $\gamma = \psi_v - \pi$, to (5.5) and (5.6), it can be obtained:

$${}^D\dot{y}_c = \frac{e_v [{}^B\dot{x}_{dvl,v} / \cos(\psi_v - \pi) + {}^D\dot{x}_c]}{\Delta} \quad (5.7)$$

5.2.3.3 Computed observation

With the two observations obtained, the ocean current velocity vector can be computed by combining (5.4) with (5.7):

$${}^D\dot{x}_c = \frac{e_h [{}^B\dot{x}_{dvl,h} / \cos(\psi_h - \pi/2) - \frac{e_v}{\Delta} [{}^B\dot{x}_{dvl,v} / \cos(\psi_v - \pi) + {}^D\dot{x}_c]]}{\Delta}, \quad (5.8)$$

from which it can be obtained:

$${}^D\dot{x}_c = \frac{\Delta^2 e_h {}^B\dot{x}_{dvl,h} / \cos(\psi_h - \pi/2) - \Delta e_h e_v {}^B\dot{x}_{dvl,v} / \cos(\psi_v - \pi)}{\Delta^3 + \Delta e_v e_h}, \quad (5.9)$$

which combined with (5.7) the ocean current velocity vector can be build.

5.2.3.4 Application

In order to reach the steady state in an optimal way it is worth studying the path that the AUV has to follow to perform the survey. Regarding the SoundTiles [19] demands about the reconstruction of the forward-looking sonar data, it is necessary to have an overlap between the paths of the AUV, is for this reason that in ViCOROB it is common to perform a survey of the type presented in Fig. 5.3a. From which, considering the simplification mentioned previously, the AUV can optimally achieve the steady state from the horizontal but not from the vertical trajectory. Being necessary to achieve a steady state in both directions for applying this ocean current observer proposal, the authors suggest applying the path presented in Fig. 5.3b.

This ocean current observed was tested in simulation obtaining excellent results with surveys of 100x100 meters or larger. Notice that the minimum size of the survey depends on

the distance that the AUV requires to achieve the steady state. In the future, this proposed method will be tested in sea experiments.

6

CONCLUSIONS AND FUTURE WORK

THIS chapter closes this thesis with two last sections. First, the main conclusions of this work are summarized in Section 6.1. Then, new research lines for future work are proposed in Section 6.2.

6.1 Contributions of this thesis

This thesis has contributed to advancing the state of the art in underwater Long Term Deployment. Presenting a successful experimental application of an autonomous non-holonomic **AUV** docking system, and preparing the bases for the future. We can break down this main contribution into particular ones:

Literature survey and simulation comparison: The first contribution presented in this thesis was an extensive review of the different docking strategies for non-holonomic **AUV** in a funnel-shaped **DS**. In the article presented in Chapter 2, we developed a novel metric to evaluate in a qualitative way the entrance of the **AUV** inside the funnel-shaped **DS**. We also created a simulation environment to compare all the strategies in the same framework, obtaining a methodic comparison, showing the strong points of each strategy.

Novel docking strategy: In this thesis, we have also presented a novel strategy for dealing with ocean currents with a non-holonomic **AUV** to dock in a funnel-shaped **DS** using only acoustic feedback. In the article presented in Chapter 3, a novel controller is presented, probing the exponential stability. The strategy was tested in simulation, being compared with the rest of the strategies, obtaining the best results.

Self orientable funnel-shaped Docking Station: The third contribution is the development of a successful experimental autonomous docking system. Following the results of the article presented in Chapter 4, a new funnel-shaped **DS** for the Sparus II **AUV** was designed, built, and tested. The system was validated at sea with robust results in different sea environments.

Ocean current observer: We also presented in Chapter 5 a new proposal for a passive ocean current observer with a non-holonomic **AUV**, designed to optimize the docking maneuver, taking advantage of the most common Sparus II mission.

6.2 Future work

This thesis concludes with the development of the fundaments of the **LTD** research line, but with the pillars established, it is needed to continue constructing the building. Consequently, we finish this thesis by pointing out and discussing different developments to continue enhancing the **LTD** technology.

Continue the development of the Sparus Docking Station One of the main contributions of this thesis was the development of a new prototype of funnel-shaped **DS** for the Sparus II **AUV**. Despite most of its technologies were developed and achieved successful experimental results, some of them were not tested yet.

One of the main functionalities of the **DS** is to charge the batteries of the **AUV**. For doing that, in the presented design an inductive charger was considered. It will be necessary for the future to acquire or develop an inductive charger adapted to the **AUV** requirements.

Another key point of development is energetic autonomy. The performed tests were focused on the docking maneuver, and the energetic autonomy was not properly

studied yet. At the moment of writing this thesis, the **UdG** team is doing an energy consumption study of the devices, to design an optimal energy consumption strategy.

Test experimentally the ocean current effect The main contribution of this thesis was focused on the development of docking with a non-holonomic **AUV** in a funnel-shaped **DS**. One critical point to consider in this context is the effect of ocean currents. Despite developing all the tools and strategies to consider the ocean currents, it was not possible to test their effect in an experimental environment. From logistics, the tests developed during this thesis were enclosed in time, and we were not lucky enough to have significant ocean currents during the experiments. The next natural step from the work presented, will be to test the docking system in a sea environment where constant ocean currents are present.

Develop the LTD for the Girona AUV A side work from this thesis was the design and building of the Girona Docking Station, explained with more detail on Appendix B. Preparing the future of several developments that can be done related to the platform. In fact, at the moment of writing this thesis, two Master's Thesis are in development related to that. On one side, a visual localization and docking autonomous system are in development, and on the other, a grasping strategy for autonomously hooking the **DS** with an Intervention **AUV** (**I-AUV**) for launch and recovery operations is being tested.

As this Master Thesis points out, two main developments can be achieved. The first one is related to the docking strategy from the **AUV** to enter into the **DS**. Presenting in theory an easier docking maneuver compared to the Sparus II **AUV**, considering the holonomic movement of the Girona **AUV**. In the first iteration, a localization based on a vision system will be developed, trying to create a novel long-term passive visual marker, with the aim of being able to test it in the **CIRS** water tank. And in the future, a dual-**USBL** localization system will be integrated into the **AUV** navigation in order to localize in a robust way the **DS**.

The second one is related to the autonomous launch and recovery system for the **DS**. In the experiments developed during this thesis, a diver team was used to install the **DS** in the seabed, being this possible because it was deployed in shallow water. If in the future we pretend to deploy and recover the **DS** in a deeper seabed, a novel autonomous strategy has to be developed. The first proposal consists to consider that the **DS** is deployed on the seabed, and a chain coming from the boat has to be attached to the **DS** autonomously to be able to recover it.

Develop a launch and recovery system for the AUV The main focus of this thesis was in the **LTD**, but a parallel development to that is the launch and recovery system. The launch and recovery system consists in developing the technology to autonomously launch the **AUV** from the boat to the sea and to recover it from the sea to the boat. It is worth noting that the docking strategy that was developed in this thesis is compatible with this new concept.

The next natural step will be the adaptation of the Sparus Docking Station presented in this thesis to fit the launch and recovery system. Also to adapt the strategy to the new requirements and develop the operation in an autonomous way.

A

SPARUS DOCKING STATION

In this appendix, the Sparus Docking Station (see Fig. A.1) is presented in more details, focusing on the design and the experimental experience.

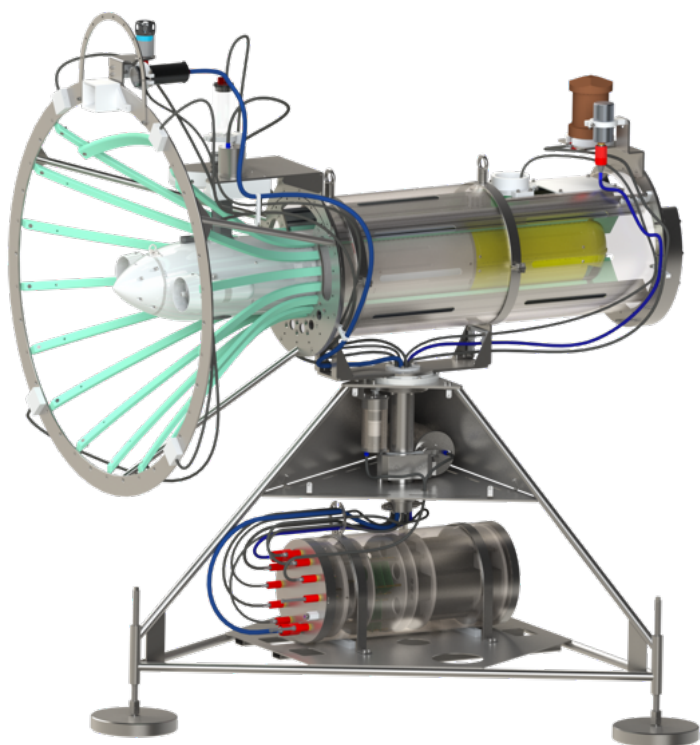


Figure A.1: Sparus Docking Station conceptual general view.

A.1 Context

As it is explained in this thesis, the **LTD** is a research line that the **UdG** team is focused on nowadays in several projects. For this reason, the first main design that was developed during the thesis was the Sparus Docking Station.

Inspired by the previous **UdG** design presented in [13], for the magnitude of research projects that **ViCOROB** is reaching, it was necessary to develop a robust design, closer to a real product than a first concept. This job presents a natural step forward after the previous experience.

The Sparus Docking Station pretends to build the base for the **LTD** of the Sparus II **AUV** for the future years in the **CIRS**. It was designed with the scope to be deployed in the Atlantic ocean at 100 meters depth.

A.2 Concept

Following the concept of the funnel-shaped **DS** used by several authors in the literature, a new **DS** development is presented in this thesis. As can be seen in Fig. A.1, it is designed to carry the Sparus II **AUV**, utilizing a funnel entrance to allow some tolerance. It can be divided into two main sections, the tripod and the funnel.

The main structure is built using 316 stainless steel for its mechanical and corrosion properties. The manufacturing consists mainly of a combination of the novel laser cutting process [20] with bending and welding, allowing to minimize significantly the production cost.

A.2.1 Tripod

The tripod presents the base where the funnel lies. It consists of a main structure of 316 stainless steel pipes welded with three layers of laser-cut sheets.

It is designed with three easy-to-adjust (by a diver or a robot) feet, to be able to adapt to the seabed, see Fig. A.2a. In the top part, there is a structure prepared for coupling a fixed key, that allows turning the main axis. This main axis is free in the bottom part, using the nuts combination, allowing the base of the feet to remain static in the ground. This combination of elements, allows easy installation in the seabed, permitting the adjustment of each foot without major effort.

In the bottom part of the tripod, it is located the main cylinder, see Fig. A.2b which contains the batteries and the main electronics. It consists of a housing for protecting the inner part and a removable structure with all the electronics. The housing is designed to support a hundred meters of depth pressure, following the requirements of the ATLANTIS research project; it consists of a 316 stainless steel pipe with two laser-cut lids welded and corrected with a Computerized Numerical Control (**CNC**) lathe. The lid consists also of a 316 stainless steel part manufactured with a **CNC** late. It uses the consolidated underwater technique to avoid the use of screws that can provoke corrosion in the long term, as can be seen in the left part of the image, using an O-Ring radial rod sealing [21]. Also, SubConn[®] connectors [22] were used to ensure the sealing and the quality of the signals. Finally, the lid has a SeaVent[®] Single Seal Face relief valve [23] for safety purposes. The electronics consist mainly of a Raspberry Pi 3 computer [24] and a microcontroller. The Raspberry Pi contains Robot Operation System (**ROS**) [25] to manage the main system and the communication with the devices. The microcontroller manages the control of the motors and the Raspberry Pi's power, allowing a sleep mode for battery consumption optimization. Finally, the cylinder contains

the battery, it used twenty-four packs of NL2044 14.4V Lithium Ion Batteries, which are the same used for Girona AUV, for logistics reasons.

In the top part, it is located the rotation system, see Fig. A.2c. It consists of five elements; the first one is the motor that controls the Degree of Freedom (DoF) of the orientation of the funnel, the second one is the linear actuator that brakes the previous DoF, the third is the gear system to transmit the torque, the fourth is the main bearing, and the fifth is the second bearing. The motor and the linear actuator are inside a housing designed for their protection, this housing uses the O-Ring [21] technology in order to ensure the sealing. As an example of the development, the housing of the motor that controls the DoF of the funnel is represented in Fig. A.2d. The main body of the housing consists of a tube welded with laser-cut cylinders, all of them from 316 stainless steel, corrected from the inside with a late to ensure the sealing surface demands. It contains several elements, which are explained below:

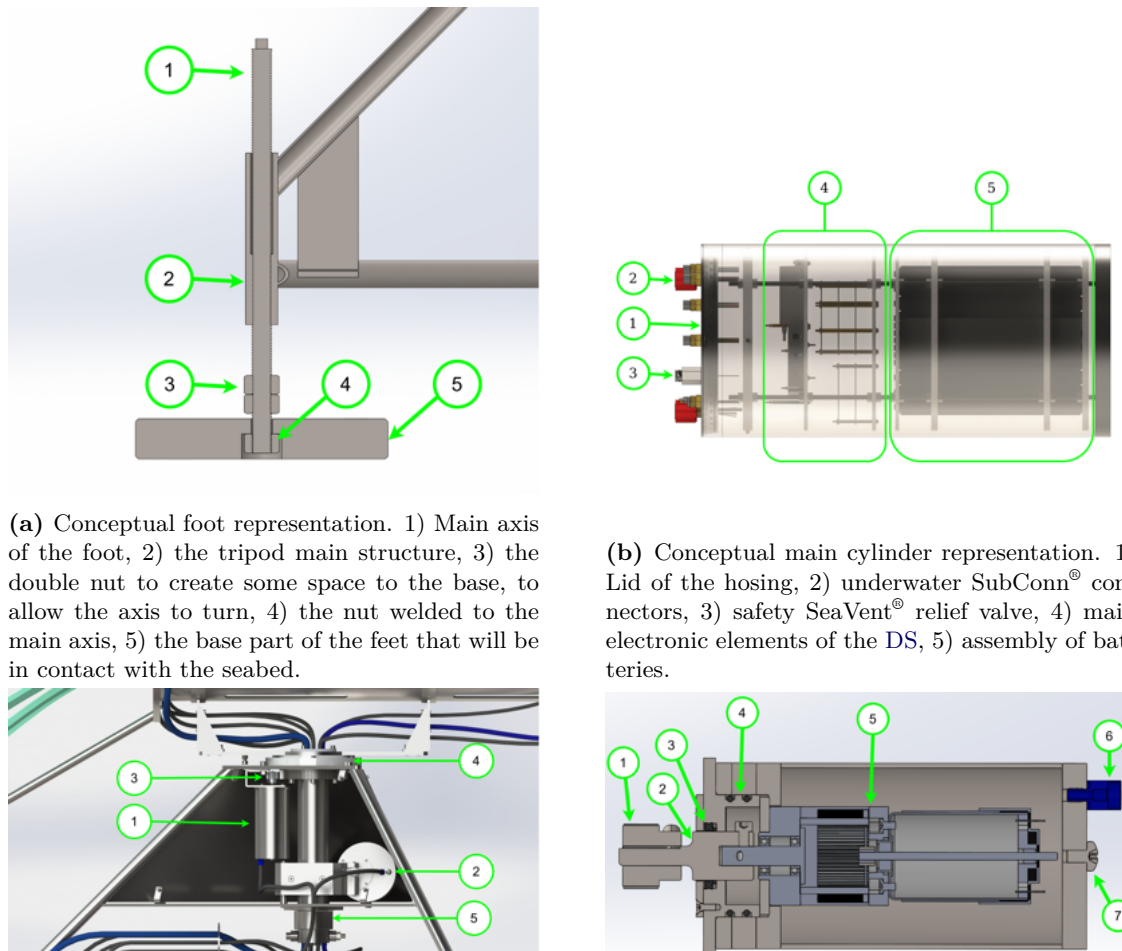
1. A gear is attached to the axis in order to transmit the torque of the motor to the funnel.
2. An external axis was manufactured of 316 stainless steel using CNC late technology with the objective of protecting the motor. It is connected inside the housing with the motor and outside with the gear.
3. The sealing of the axis consists of a combination of a Quad-Ring[®] with a Back-up Ring from Trelleborg [21]. A secondary lid was manufactured in order to be able to mount the sealing rings.
4. The main lid consists of a CNC late manufacturing part with two O-Rings [21], for sealing redundancy.
5. The motor consists of a Mclennan E192 geared DC motor [26], which allows the system to obtain a specific orientation, considering the gear ratio.
6. A 316 stainless steel penetrator was manufactured in order to be able to connect the motor with the main cylinder. The electrical cables pass through the penetrator and are fulfilled with epoxy to ensure the sealing.
7. A standard screw cap was added also, for allowing the air to leave the housing when the system is mounted.

A.2.2 Funnel

The funnel is the assembly where the AUV docks, it contains the main devices of the DS, a soft-collision system, and a balance configurator.

Several devices were implemented in the funnel, see Fig. A.3:

1. An acoustic modem for localization and basic communication with the AUV, the Blueprint Subsea Seatrack X110 [27]. The AUV localize the DS position using the acoustic modem and its USBL, knowing the position in the world from the DS and considering it stationary, the AUV corrects its position (recall Chapter 4).
2. A camera for receiving visual feedback on the operations.
3. A WiFi antenna to allow short-range high bandwidth communication. Allowing the AUV to transmit the data obtained during the mission to the DS.



(c) Conceptual representation of the central part of the DS. 1) Motor to control the funnel DoF, 2) linear actuator to brake the funnel DoF, 3) gear system to transmit the rotation from the motor to the funnel axis, 4) main bearing, 5) secondary bearing.

(d) Representation of the housing of the motor of the DS that controls the DoF of the funnel. 1) Gear to transmit the torque, 2) external axis to protect the motor, 3) sealing of the external axis, 4) lid of the housing, 5) electrical motor, 6) sealed penetrator, 7) housing cap.

Figure A.2: Representation of the main elements of the tripod of the Sparus Docking Station.

4. A latching motor system, to ensure the position of the AUV inside the DS. It consists in a system that clamps the antenna of the AUV to not mechanically allow the AUV to leave the DS.
5. An inductive charger prototype, designed for the ATLANTIS project by INESC TEC.
6. A visual modem, for wireless underwater high bandwidth communication, the Luma X from Hyrdomea [28]. In the future, this device will be used to communicate the DS with other vehicles in order to transmit the data when the DS is deployed in permanent not easy-to-access locations.
7. A DVL in order to monitor the ocean currents close to the DS, the NavQuest LinkQuest 600 Micro [29]. It is used to obtain the information in order to decide the orientation of the funnel DoF.

The collision system consists of a funnel-shaped entrance manufactured using polyethylene M

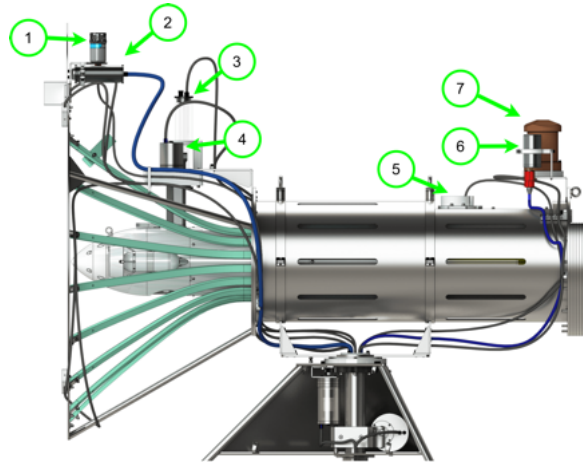


Figure A.3: Sparus Docking Station funnel representation. 1) Acoustic modem from BluePrint Subsea, 2) camera, 3) WiFi antenna, 4) latching motor, 5) inductive charger from INESC TEC, 6) visual modem from Hydromea, 7) DVL from LinkQuest.

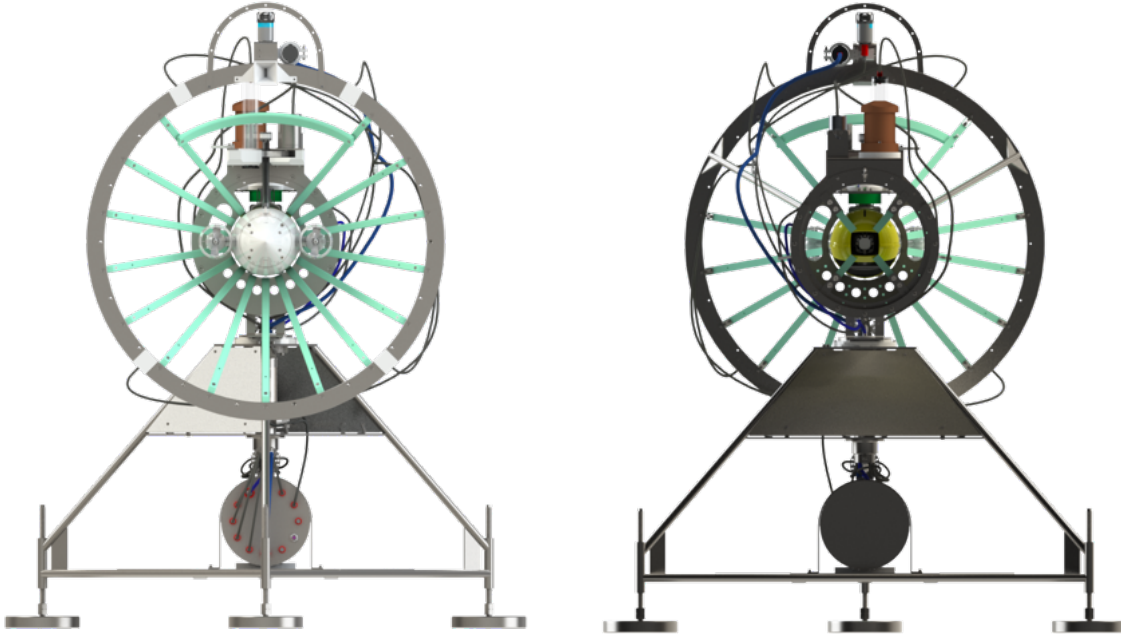


Figure A.4: Sparus Docking Station frontal and back view representation.

AST PE-1000, as can be seen in Fig. A.4 (the polyethylene part is represented in green). This system allows the AUV to collide with the DS without major mechanical problems, thanks to the properties of the polyethylene. To be able to achieve the shape of the entrance of the funnel, a stainless steel structure was prepared, with some laser-cut rings welded with stainless steel pipes (recall Fig. A.3 and Fig. A.4).

In order to have control of the rotation of the funnel, the joint between the funnel and the tripod consists of a main axis with two bearings for the torque compensation (recall Fig. A.2c). Despite having the double bearing system, it is needed to have the center of mass of the funnel approximately in the main axis of the joint. To be able to adjust mechanically the position of the center of mass of the funnel a weight system was designed, see Fig. A.5. This weight

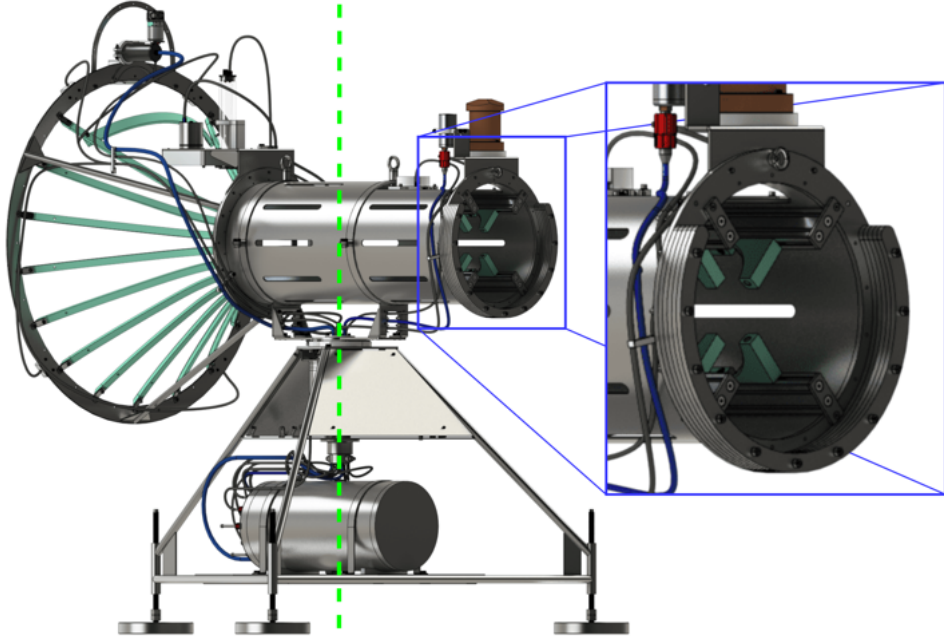


Figure A.5: Representation of the modular center of mass adjustment of the funnel of the DS. In green is represented the main axis of the DS, and zoomed in blue is presented the modular weight system.

compensation system consists of a "C" shape laser-cut parts that can be added to the back part of the funnel in order to move the center of mass to the main axis of the DS.

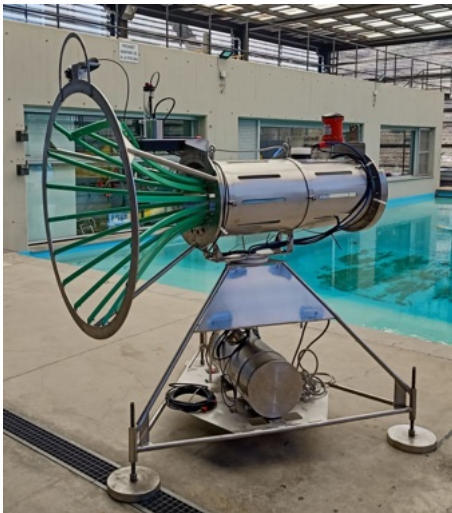
A.3 Experimental experience

The design presented in this section was built and tested as it is explained in Chapter 4. The Sparus Docking Station was deployed in two sea scenarios: in Sant Feliu de Guíxols (Spain) and in Viana do Castelo (Portugal), see Fig. A.6. A video representation of the experimental application of the Sparus Docking Station can be found in [30].

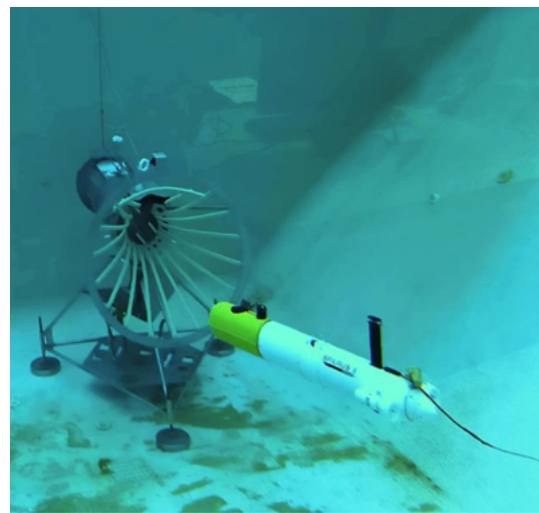
First, it was tested in the test tank of the CIRS to verify the design, showing that the AUV was able to enter the DS if it hits the polyethylene part, only applying surge velocity.

Second, it was deployed for eighteen days in Sant Feliu de Guíxols, where it was developed the first autonomous docking explained in Chapter 4. It was recovered with no major corrosion problems. Only the penetrators of the motor housings that were originally from anodized aluminum were corrupted, replacing them with stainless steel for future tests. The DS was deployed and recovered using a team of divers with no reported problems. It was deployed on a flat sand seabed, requiring no adjustments.

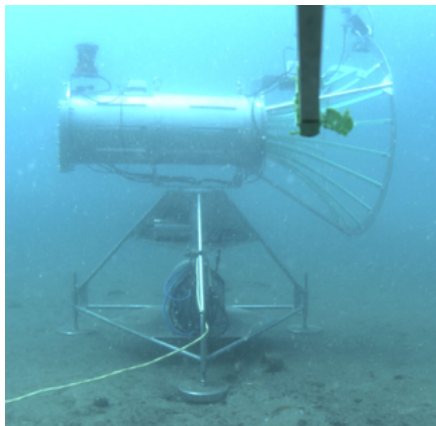
Finally, it was deployed for seven days in Viana do Castelo, reporting no major corrosion, and no deployment and recovery problems. It was also installed using a team of divers, this time in an inclined mud seabed. The feet were modified due to the change on the seabed (from sand to mud), it was added some woods in order to increase the contact surface with the seabed, see Fig. A.7a. Being installed in an inclined plane, the three feet were adjusted by a diver in order to maintain the funnel parallel to the water surface, as can be seen in Fig. A.7b. The diver deployment operation was partially recorded and can be found in [31]. After the docking experiments, the status of the Sparus II AUV was checked, presenting no significant damage, validating the design and the use of the polyethylene parts.



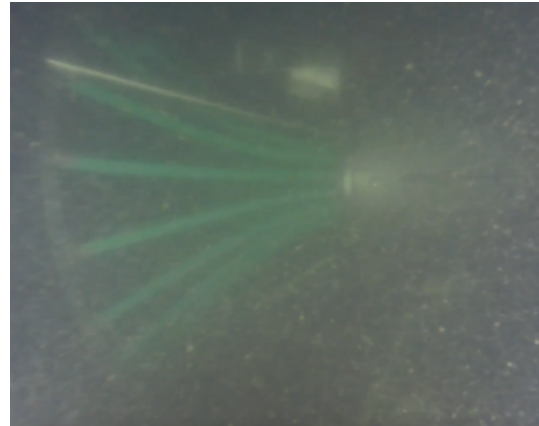
(a) On the CIRS ground.



(b) Inside the CIRS test tank.



(c) At 8 meters depth in Sant Feliu de Guíxols (Spain).



(d) At 8 meters depth in Viana do Castelo (Portugal).

Figure A.6: Photographies of the Sparus Docking Station in different scenarios.

(a) Feet modification due to the mud seabed.



(b) Divers adjusting a foot height.

Figure A.7: Photographies of the Sparus Docking Station deployment in Viana do Castelo.

A proper study of energy autonomy was not developed before the experiments. The **DS** used their battery system but a backup power supply was ready if the batteries had not enough capacity for the tests, using a 40 meter long cable connected onshore. The system is designed to have a sleeping mode to consume less energy that can be activated and deactivated using the acoustic modem, meaning that the **AUV** can wake up the **DS** when it considers, but in the time of the experiments, was not tested. At the moment of writing this thesis, an energy consumption study is being carried out by the **UdG** team, with the final objective to develop an energy consumption optimization solution.

As well as the autonomy of the system, not all the potential applications of the **DS** were tested during the first experiments. It is the case of the **DVL** that being the **DS** deployed in shallow water, it was not able to obtain robust ocean current observations. Also, the inductive charger prototype was not used during the application, as well as the visual modem. With respect to the **DVL**, it will be used in the future when the **DS** will be deployed in a deeper environment for the PLOME research project [10]. Regarding the inductive charger, the prototype was not achieving the requirements of the **AUV**; a new inductive charger will be placed in the future, to be able to charge properly the Sparus II from the **DS**. Finally, the visual modem will be used in future applications when the **DS** will be deployed in less accessible places, to communicate with other vehicles.

B

GIRONA DOCKING STATION

In this section, the novel prototype of DS designed for the Girona AUV is presented, see Fig. B.1.



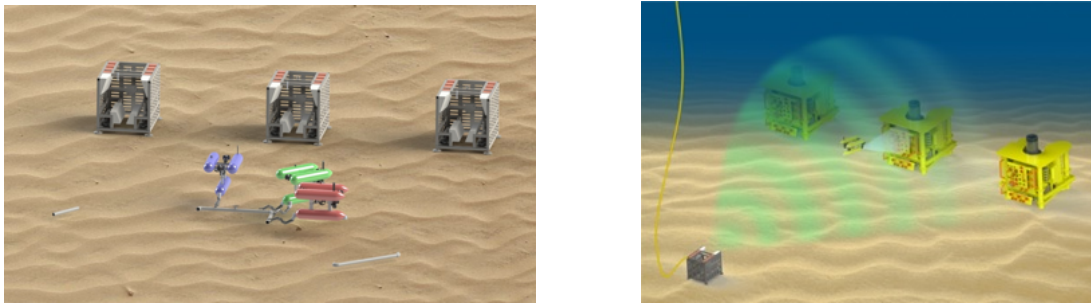
Figure B.1: Girona Docking Station conceptual general view.

B.1 Context

After the success achieved with the Sparus Docking Station, and the potential of the **LTD**, the **UdG** decided to create the novel Girona Docking Station.

The **LTD** is a research line that will lead the future of the **AUV** technology, following this belief, several research projects that involve the **UdG** include development in the **LTD**. Some of them include development related to the Sparus II **LTD**, but specifically, COOPERAMOS [32] and OPTHIROV [9] are focused on the development of the Girona **AUV LTD**.

The COOPERAMOS [32] research project aims to develop a resident multiple **I-AUV** system to perform autonomous intervention tasks. Each vehicle begins its operation from its own **DS**, as can be seen in Fig. B.2a. The OPTHIROV [9] research project is focused on increasing the Technology Readiness Level (**TRL**) of the underwater robotic systems, presenting an underwater platform that can be operated remotely; being one of the key points the **DS**, as can be seen in Fig. B.2b. It is a proof of concept project to demonstrate the shared autonomy concept implemented on a optically linked Hybrid Remotely Operated Vehicle (**HROV**), which is deployed from a **DS**.



(a) Conceptual representation of COOPERAMOS research project.

(b) Conceptual representation of OPTHIROV research project.

Figure B.2: Conceptual representation of two of the **UdG** research projects that involves the Girona Docking Station.

B.2 Concept

The Girona **AUV** is a characteristic design for its triple torpedo structure, it is because of its shape that a new concept of docking was developed, see Fig. B.1. The Girona Docking Station is designed with the objective to simplify the docking maneuver of the **AUV**, with this idea in mind and considering the shape of the Girona, a vertical landing **DS** was developed. Also, the **AUV** does have holonomic control in the plane parallel to the water surface, making the vertical maneuver more suitable than the classical horizontal one.

The Girona Docking Station development consists mainly of three parts: an accessory added to the **AUV** to allow the coupling with the **DS**, a main body that consists in the skeleton of the **DS** itself, and the interface between the **DS** and the **AUV**.

B.2.1 Girona AUV coupling accessory

In order to couple the **AUV** with the **DS** a new assembly was added to the **AUV**. It consists of four legs located in the bottom part of the top torpedos (see Fig. B.3), that will be used to lock the **AUV** inside the **DS**.

Each leg consists of a modular coupling to avoid a permanent modifications to the AUV structure. They are manufactured with 7075 anodized aluminum alloy and end with a cylinder that will be coupled in the DS contact structure.

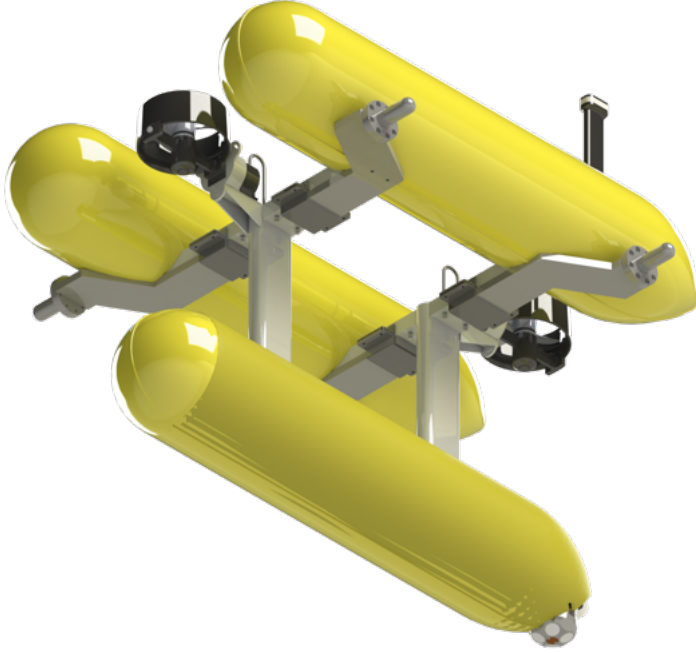


Figure B.3: Conceptual representation of the Girona AUV adaptation for docking, with the coupling accessory assembled.

B.2.2 Body structure

The body structure consists of the skeleton of the DS, see Fig. B.4. It is manufactured mainly with 304 stainless steel square pipes in combination with laser-cut plates. It contains four modular feet, following the concept of the ones presented in section A.2.1. The bottom part contains space for four pressure vessels, also like the one presented in section A.2.1. It also holds a weight compensation system, to adjust the position of the center of mass, and a modular part in the center for adding, in the future, the necessary elements (i.e, visual markers, inductive charger). The central part contains the supports for the interface structure presented in the next subsection. Finally, the top part contains some devices like an optical modem with a pan and tilt system, the USBL, as well as structural handles for the deployment.

B.2.3 Interface structure

This part consists on the assembly that allows the AUV to collide and dock. It has two main components that are represented in Fig. B.5 in different colors. In green is represented the funnel-shaped entrance, with the objective of allowing some tolerance in the entrance, following similar principles of the Sparus Docking Station. In blue is represented the assembly that aligns the AUV inside the DS. The coupling system consists of an electric motor connected to a metallic zip that locks the cylinder of the AUV coupling accessory.

It was manufactured from polyethylene M AST PE-1000 using water jet cutting technology and a CNC milling machine.



Figure B.4: Main structure of the Girona Docking Station representation.

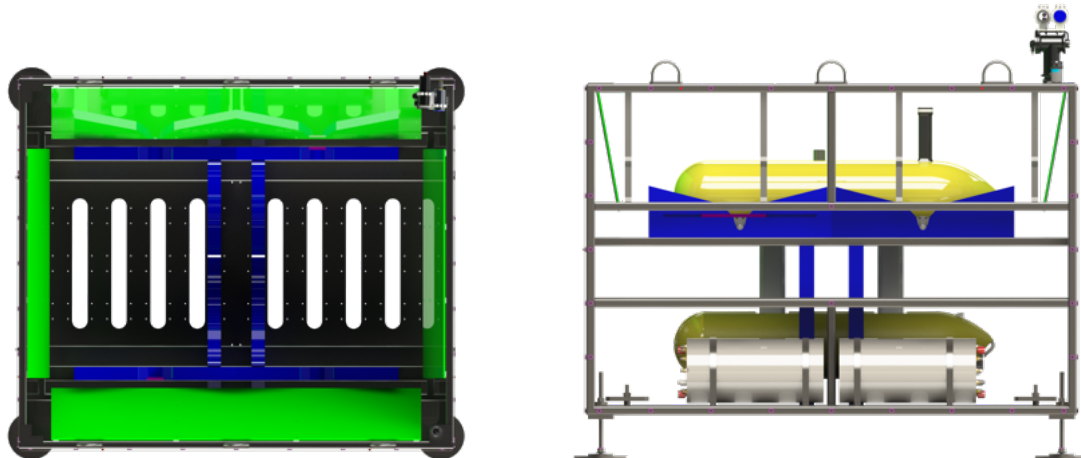


Figure B.5: Conceptual representation of the contact part of the DS with the AUV. On the left is an image from a top view, and on the right is an image from a lateral view. In green is represented the funnel and in blue is the axis alienation.

B.3 Future work

The Girona Docking Station has been already implemented (Fig. B.6). It was designed as an open platform for being able to add of new devices in the future. At the time of this thesis, a Master's Student is working on the development of a visual servoing docking algorithm. The method uses custom-developed markers adapted for their use underwater. Future work

will explore strategies for docking using only acoustic sensors. In parallel, another Master's Student is working on the development of an autonomous launch and recovery system for the deployment of the DS in the sea.



Figure B.6: Photography of the Girona Docking Station.

BIBLIOGRAPHY

- [1] **Joan Esteba**, Patryk Cieslak, Narcis Palomeras, and Pere Ridao. “Docking of Non-holonomic AUVs in Presence of Ocean Currents: a Comparative Survey”. In: *IEEE Access* 9 (2021), pages 86607–86631. DOI: [10.1109/ACCESS.2021.3083883](https://doi.org/10.1109/ACCESS.2021.3083883) (cited on pages ix, 15).
- [2] **Joan Esteba**, Patryk Cieslak, Narcís Palomeras, and Pere Ridao. “Managed Surge Controller : A Docking Algorithm for a Non-Holonomic AUV (Sparus II) in the Presence of Ocean Currents for a Funnel-Shaped Docking Station”. In: *Sensors* 23 (2023). DOI: [10.3390/s23010241](https://doi.org/10.3390/s23010241) (cited on pages ix, 41).
- [3] **Joan Esteba**, Patryk Cieslak, Narcís Palomeras, and Pere Ridao. “Sparus Docking Station: A Current Aware Docking Station For a Non-holonomic AUV”. In: *Journal of Field Robotics* () (cited on pages x, 69).
- [4] *Victor 6000: Design, Utilization And First Improvements*. Volume All Days. International Ocean and Polar Engineering Conference. 2003 (cited on page 8).
- [5] Robert D Ballard. “The MEDEA/JASON remotely operated vehicle system”. In: *Deep Sea Research Part I: Oceanographic Research Papers* 40.8 (1993), pages 1673–1687. DOI: [https://doi.org/10.1016/0967-0637\(93\)90021-T](https://doi.org/10.1016/0967-0637(93)90021-T) (cited on page 8).
- [6] M Carreras, C Candela, D Ribas, A Mallios, L L Magí, E Vidal, N Palomeras, and P Ridao. “Sparus {II}, design of a lightweight hovering {AUV}”. In: *Proceedings of the 5th international workshop on marine technology. Martech'13* (2013), pages 152–155 (cited on page 8).
- [7] Narcís Palomeras, Pere Ridao, David Ribas, Guillem Vallicrosa, and Computer Vision. “Autonomous I-AUV Docking for Fixed-base Manipulation”. In: (2014), pages 12160–12165. DOI: [10.1109/IROS.2014.6942870](https://doi.org/10.1109/IROS.2014.6942870) (cited on page 8).
- [8] Universitat de Girona. *ATLANTIS research project official website*. <https://www.atlantis-h2020.eu/>. [Online; accessed 2022-12-21] (cited on page 8).
- [9] Universitat de Girona. *OPTHIROV research project official website*. <https://optihrov.udg.edu/>. [Online; accessed 2022-12-21] (cited on pages 8, 116).
- [10] Universitat de Girona. *PLOME research project official website*. <https://plomeproject.es/>. [Online; accessed 2022-12-21] (cited on pages 8, 114).
- [11] Mbari. *MARS system from MBARI*. <https://www.mbari.org/technology/monterey-accelerated-research-system-mars/>. [Online; accessed 2023-01-31] (cited on page 8).

- [12] BlueLogic. *BlueLogic Subsea Docking Station*. <https://www.bluelogic.no/news-and-media/subsea-docking-station-sds->. [Online; accessed 2023-01-31] (cited on page 8).
- [13] N. Palomeras, G. Vallicrosa, A. Mallios, J. Bosch, E. Vidal, N. Hurtos, M. Carreras, and P. Ridao. “AUV homing and docking for remote operations”. In: *Ocean Engineering* 154.May 2017 (2018), pages 106–120. DOI: [10.1016/j.oceaneng.2018.01.114](https://doi.org/10.1016/j.oceaneng.2018.01.114) (cited on pages 10, 108).
- [14] Andry Maykol Pinto, Joao V. Amorim Marques, Daniel Filipe Campos, Nuno Abreu, Anibal Matos, Martio Jussi, Robin Berglund, Jari Halme, Petri Tikka, Joao Formiga, Christian Verrecchia, Serena Langiano, Clara Santos, Nuno Sa, Jaap Jan Stoker, Fabrice Calderoni, Shashank Govindaraj, Alexandru But, Leslie Gale, David Ribas, Natalia Hurtos, Eduard Vidal, Pere Ridao, Patryk Chieslak, Narcis Palomeras, Stefano Barberis, and Luca Aceto. “ATLANTIS - The Atlantic Testing Platform for Maritime Robotics”. In: *Oceans Conference Record (IEEE)* 2021-Septe (2021), pages 1–5. DOI: [10.23919/OCEANS44145.2021.9706059](https://doi.org/10.23919/OCEANS44145.2021.9706059) (cited on pages 11, 98).
- [15] Patryk Cieslak. “Stonefish: An Advanced Open-Source Simulation Tool Designed for Marine Robotics, With a ROS Interface”. In: *OCEANS 2019 - Marseille* (2019), pages 1–6. DOI: [10.1109/oceanse.2019.8867434](https://doi.org/10.1109/oceanse.2019.8867434) (cited on pages 11, 13).
- [16] Marc Carreras, Juan David Hernandez, Eduard Vidal, Narcis Palomeras, David Ribas, and Pere Ridao. “Sparus II AUV - A Hovering Vehicle for Seabed Inspection”. In: *IEEE Journal of Oceanic Engineering* 43.2 (2018), pages 344–355. DOI: [10.1109/JOE.2018.2792278](https://doi.org/10.1109/JOE.2018.2792278) (cited on page 11).
- [17] David Ribas, Narcís Palomeras, Pere Ridao, Marc Carreras, and Angelos Mallios. “Girona 500 AUV: From survey to intervention”. In: *IEEE/ASME Transactions on Mechatronics* 17.1 (2012), pages 46–53. DOI: [10.1109/TMECH.2011.2174065](https://doi.org/10.1109/TMECH.2011.2174065) (cited on page 11).
- [18] Blueprint Design Engineering Ltd. *Blueprint subsea Oculus imaging sonar*. <https://www.blueprintsubsea.com/oculus/oculus-m-series>. [Online; accessed 2022-09-21] (cited on page 98).
- [19] Iqua Robotics. *SoundTiles website*. <https://iquareobotics.com/soundtiles>. [Online; accessed 2023-01-31] (cited on pages 98, 100).
- [20] Charles Caristan and Air Liquide. *Laser Cutting Guide for Manufacturing*. *Laser Cutting Guide for Manufacturing*. July. SME, 2017 (cited on page 108).
- [21] Trelleborg. *Oring technical document*. https://www.trelleborg.com/seals/-/media/tss-media-repository/tss_website/pdf-and-other-literature/catalogs/o_ring_gb_en.pdf?rev=-1&openpdf=1. [Online; accessed 2023-01-31] (cited on pages 108, 109).
- [22] Macartney. *Subconn section inside the Macartney website*. <https://www.macartney.com/what-we-offer/systems-and-products/connectors/subconn/>. [Online; accessed 2023-01-31] (cited on page 108).
- [23] DeepSea Inc. *DeepSea Seavent relieve valve website*. <https://www.deepsea.com/seavent-relief-valves/>. [Online; accessed 2023-01-31] (cited on page 108).
- [24] Raspberry Pi. *Raspberry Pi official website*. <https://www.raspberrypi.com/products/raspberry-pi-3-model-a-plus/>. [Online; accessed 2023-01-31] (cited on page 108).

- [25] Morgan Quigley, Brian Gerkey, Ken Conley, Josh Faust, Tully Foote, Jeremy Leibs, Eric Berger, Rob Wheeler, and Andrew Ng. "ROS: an open-source Robot Operating System". In: *ICRA workshop on open source software* (2009) (cited on page 108).
- [26] Mclennan Servo Supplies. *Mclennan motor E192 website*. <https://www.mclennan.co.uk/product/e192-gearied-dc-motor>. [Online; accessed 2023-01-31] (cited on page 109).
- [27] Blueprint Design Engineering Ltd. *Blueprint subsea SeaTrac X150 USBL beacon*. <https://www.blueprintsubsea.com/seatrac/>. [Online; accessed 2022-09-21] (cited on page 109).
- [28] Hydromea. *Luma X website*. <https://www.hydromea.com/underwater-wireless-communication>. [Online; accessed 2022-09-21] (cited on page 110).
- [29] LinkQuest Inc. *NavQuest Micro DVL 600 website*. https://www.link-quest.com/html/intro_nq.htm. [Online; accessed 2022-09-21] (cited on page 110).
- [30] Universitat de Girona. *Video that shows the Sparus Docking Station application*. https://drive.google.com/drive/folders/156XWRRVy8R47qkTzDrrMHCJvhyPnD2zI?usp=share_link. [Online; accessed 2023-01-31] (cited on page 112).
- [31] University of Girona. *Sparus Docking Station underwater deployment in Viana do Castelo*. https://drive.google.com/drive/folders/115U2X5KBrF_1AqaFB00-xgM559V9dU3D?usp=share_link. [Online; accessed 2023-01-31] (cited on page 112).
- [32] Universitat de Girona. *COOPERAMOS research project official website*. https://vicorob.udg.edu/portfolio_page/per2iauv/. [Online; accessed 2022-12-21] (cited on page 116).

